INFORMATION TO USERS

This manuscript has been reproduced from the microfilm master. UMI films the text directly from the original or copy submitted. Thus, some thesis and dissertation copies are in typewriter face, while others may be from any type of computer printer.

The quality of this reproduction is dependent upon the quality of the copy submitted. Broken or indistinct print, colored or poor quality illustrations and photographs, print bleedthrough, substandard margins, and improper alignment can adversely affect reproduction.

In the unlikely event that the author did not send UMI a complete manuscript and there are missing pages, these will be noted. Also, if unauthorized copyright material had to be removed, a note will indicate the deletion.

Oversize materials (e.g., maps, drawings, charts) are reproduced by sectioning the original, beginning at the upper left-hand corner and continuing from left to right in equal sections with small overlaps.

ProQuest Information and Learning
300 North Zeeb Road, Ann Arbor, MI 48106-1346 USA
800-521-0600

University of Alberta

Depositional facies and reservoir-enhancing dolomitization surrounding monadnocks in the Slave Point Formation, Dawson Field, Alberta, Canada

by

Ross Andrew Keilly 

A thesis submitted to the Faculty of Graduate Studies and Research in partial fulfillment of the requirements for the degree of Master of Science

Department of Earth and Atmospheric Sciences

Edmonton, Alberta

Spring 2005

"I worked on monadnocks on the making – and I didn't even know it"

E.A. Shinn (pers. comm, 2003)

ABSTRACT

The Dawson field is a prolific dolomitized oil reservoir located in northwestern Alberta, Canada, in the Devonian Slave Point Formation. These Devonian shallow marine carbonates backstepped onto antecedent topography of the block-faulted Precambrian Peace River Arch. Monadnocks formed as the result of faulting augmented by fluvial (Granite Wash) erosion, which created a series of relatively small, isolated land masses of the Precambrian arch. These land masses acted as nuclei for localized reef and patch reef growth surrounding monadnocks. Six major environmental facies can be recognized within the Slave Point: the shallow shelf, back reef, reef, forereef, off reef, and basinal facies. Oil production is commonly associated with upper forereef, reef, and back reef facies. Geochemical and petrographic evidence, and facies associations suggest that the dolomitizing fluid(s) responsible for the formation of matrix and saddle dolomites, was seawater that had traveled through the porous sands and gravels of the underlying Granite Wash.

ACKNOWLEDGEMENTS

This thesis was funded by Anadarko Canada Corporation, and by a National Sciences and Engineering Research Council grant awarded to Dr. H.G. Machel.

The author would like to thank Dr. H.G. Machel and Jeff Lonnee for their critical reviews, guidance, and support. Thanks to Dr. K. Muehlenbachs for assistance in the stable isotope laboratory and Dr. R.A. Creaser for radiogenic isotope analysis.

I would like to thanks Hans Machel for accepting me as a graduate student and providing excellent scientific support and always providing an alternate view to most things considered 'popular' culture. Additionally, thanks for agreeing to send me the Bathurst 2003 in Durham, England. It was world class, once in a lifetime conference and the experience was amazing, again, thanks! Numerous people have made my time in Edmonton enjoyable and memorable. I would like to thank Jeff Lonnee, Michael Hearn, Hilary Corlett, Markus Loegering, Rabin Thanju, Ben Crutchfield, and John Jamieson for their friendship and numerous barstool discussions during my time at the University of Alberta.

I would like to thank my wife Nicole, for her constant love, support and encouragement. Additionally, I would also like to thank my family for their love and support throughout the years.

TABLE OF CONTENTS

CHAPTER ONE 1

1 INTRODUCTION 1

1.1 Introduction and previous studies 1

1.2 Objectives of research 2

1.3 Study Area 3

1.4 Sample Collection and Methods of Investigation 3

CHAPTER TWO 9

2 REGIONAL GEOLOGICAL SETTING AND PLAY TYPE 9

2.1 Western Canada Sedimentary Basin 9

2.2 The Peace River Arch 10

2.3 Devonian stratigraphy in the PRA region 11

2.3.1 Granite Wash Lithozone 13

2.3.2 Beaverhill Lake Group 14

2.4 Play types and monadnocks 15

2.4.1 Backstepping carbonate ramp 16

2.4.2 3D Seismic – Constraining exploration 18

CHAPTER THREE 26

3 FACIES, STRATIGRAPHY, AND PALEOTOPOGRAPHY OF THE SLAVE POINT 26

3.1 Introduction 26

3.2 Previous work 26

3.2.1 Slave Field 27

3.2.2 Golden Field 28
3.3 New data and facies analysis from Dawson 34
3.3.1 Zone Ib – Intertidal mudstones and wackestones 36
3.3.2 Zone IIb – Fossiliferous packstones and wackestones 36
3.3.3 Zone IIIb – *Amphipora* floatstones and grainstones 38
3.3.4 Zone IVb – Stromatoporoid rudstones and bafflestones 40
3.3.5 Zone IV/V – Reef core bindstones and rudstones 42
3.3.6 Zone IVf – Forereef bafflestones and rudstones 44
3.3.7 Zone IIIf – Crinoidal-stromatoporoid floatstones and rudstones 46
3.3.8 Zone IIf /If – Crinoidal floatstones to sparsely fossiliferous mudstones 46
3.3.9 Other lithofacies at Dawson 48
3.4 Paleotopography at Dawson 50
3.4.1 Monadnock effect 55
3.5 Depositional evolution 55
CHAPTER FOUR 60
4 DIAGENESIS AND PETROGRAPHY 61
4.1 Introduction 61
4.2 Diagenetic Processes at Dawson 65
4.2.1 Biogenic Alteration/Micritization 65
4.2.2 Dissolution 67
4.2.3 Compaction 68
4.2.4 Cementation 70
4.2.5 Recrystallization 71

4.3 Dolomitization 73
4.3.1 Matrix Dolomite 75
4.3.2 Saddle Dolomite 76
4.4 Evaporite minerals 78
4.5 Porosity 78
4.5.1 Primary porosity 81
4.5.2 Secondary porosity 83
4.5.3 Fracture porosity 83
4.6 Granite Wash 84
4.7 Paragenetic sequence of diagenetic events 84
CHAPTER FIVE 87
5 ISOTOPE GEOCHEMISTRY 87
5.1 Introduction 87
5.2 Stable Isotopes – theoretical concepts 87
5.2.1 Stable isotope application to carbonate diagenesis 89
5.2.1.1 Oxygen 89
5.2.1.2 Carbon 93
5.2.1.3 Dolomite 94
5.2.2 Analytical Methods 96
5.2.3 Carbon and Oxygen Isotope Results 98
5.3 Radiogenic (Sr) isotopes – theoretical concepts 100
5.3.1 Radiogenic Isotope Methods 104
5.3.2 Strontium Isotope Results 104

CHAPTER SIX **106**

6 DISCUSSION AND INTERPRETATION OF DIAGENESIS **106**

6.1 Introduction 106

6.2 Cementation 106

6.2.1 Early marine cementation 106

6.2.2 Dogtooth calcite spar cement 108

6.2.3 Late-stage calcite cement 108

6.2.4 Anhydrite cementation 109

6.3 Dolomitization 109

6.3.1 Models of Dolomitization 109

6.3.2 Matrix dolomitization at Dawson 110

6.3.3 Saddle Dolomite 114

6.3.4 Conduit for dolomitizing fluids 115

6.4 Dissolution 118

6.5 Porosity evolution during diagenesis 120

6.6 Diagenetic evolution of the Slave Point Formation 121

CHAPTER SEVEN **123**

7 SUMMARY AND CONCLUSIONS **123**

REFERENCES **129**

APPENDIX A **138**

CURRICULUM VITAE **141**

LIST OF TABLES

TABLE		PAGE
3.1	Summary of lithologic descriptions of facies A to G	31
3.2	Summary of substages at Golden	32

LIST OF FIGURES

CHAPTER ONE **PAGE**

1.1 Regional map and location of Alberta....4

1.2 Location of the Western Canada Sedimentary Basin....5

1.3 Major structural elements of the Western Canada Basin....6

1.4 Location of Dawson and analogous pools....7

CHAPTER TWO

2.1 Stratigraphic column and nomenclature....12

2.2 Backstepping Slave Point Formation....17

2.3 Monadnock development at Dawson....19

2.4 Schematic cross-section of monadnock and Slave Point Formation....20

2.5 Slave Point isochron map....21

2.6 Edge detection map with bank margin....22

2.7 Waterways Formation to Slave Point Formation isopach map....25

CHAPTER THREE

3.1 West-east cross section....33

3.2 Facies model used in core logging of Slave Point Formation....35

3.3 Structure map on top of Slave Point Formation....51

3.4 Stratigraphic cross-section....52

3.5 Structural cross-section....53

3.6 Interval geometry isopach map of Dawson....54

3.7 Depositional evolution of the Slave Point Formation....57

3.8 Depositional model for the Slave Point Formation.....58

3.9 Devonian sea level curve.....61

CHAPTER FOUR

4.1 Classification of diagenetic settings.....63

4.2 Schematic illustration of significant recrystallization.....75

4.3 Schematic illustration of Granite Wash channels.....80

4.4 Porosity vs. permeability cross-plot.....83

4.5 Paragenetic sequence.....87

CHAPTER FIVE

5.1 Meteoric Water Line.....92

5.2 Diagenetic CO_2 within different diagenetic zones.....96

5.3 Reaction rates of calcite and dolomite.....98

5.4 Isotope cross-plots.....100

5.5 $^{87}Sr/^{86}Sr$ for the Phanerozoic.....103

5.6 Radiogenic isotope plot of carbonate phases.....104

CHAPTER SIX

6.1 Paragenetic sequence with burial depths.....108

6.2 Temperature determination plot of dolomite phases.....113

6.3 Modified startigraphic column.....118

LIST OF PLATES

PLATE		PAGE
A	Core photographs of facies Ib and IIb	38
B	Core photographs of facies IIIb	40
C	Core photographs of facies IVb	42
D	Core photograph of facies IV/V	44
E	Core photographs of facies IVf	46
F	Core photographs of facies IIIf, IIf, and If	48
G	Core photographs of Calmut member, Waterways, and Precambrian	50
H	Photomicrographs of micrite envelopes and early-diagenetic fabrics	67
I	Photomicrographs of diagenetic fabrics	70
J	Photomicrographs of dolomites and dolomite textures	78
K	Photomicrographs of void-filling cements and porosity	81
L	Photomicrographs of the Granite Wash	86

CHAPTER ONE

1 INTRODUCTION

1.1 Introduction and previous studies

This study attempts to determine the depositional facies of the Middle Devonian Slave Point Formation and its relationship to reservoir-enhancing dolomitization processes in the Dawson field of Alberta, Canada. Dolomitization is important because it affected the development of porosity and permeability and, therefore, the oil-bearing potential of the host rocks. Understanding the controls and processes of dolomitization at Dawson will benefit reservoir development and subsequent exploration in the field.

Stratigraphic and lithologic descriptions of Middle Devonian strata, including the Slave Point Formation, from the Western Canada Sedimentary Basin are numerous. Depositional environments, stratigraphy, and faunal assemblages of the Slave Point have been previously documented by Belyea and Norris (1962), Cameron (1968), Crawford (1972), Craig (1987), Gosselin (1990), and Mossop and Shetsen (1994). However, no previous studies have been dedicated to determining the timing and phases of dolomitization at Dawson. Though this limits the scope of a significant literature review/critique and data comparison, there are several other locations which serve as analogues to the Dawson field, including the Golden and Evi pools nearby. In this study, the timing of dolomitization and interpretation of the fluid sources affecting the carbonates at the Dawson field are addressed, as well as whether or not depositional facies and/or fabrics were controls on the dolomitization process.

Several studies have been conducted on Slave Point reservoirs of the Devonian system proximal to the Dawson field. Dunham et al. (1983) studied the Slave field in Township 84, Range 14W5 about 30 km northwest of Dawson. Gosselin et al. (1989) studied the Golden and Evi Slave Point field bounded by Township 86 and 87. and Ranges 11 through 15W5, about 65 km northwest of Dawson. Finally, Tooth and Davies (1989) studied the Slave Point Formation at Gift Lake, in Townships 78 and 79, ranges 10 and 11W5, about 40 km east southeast of Dawson. These studies have contributed to the understanding of the Slave Point geologic setting and stratigraphic relationships in northern Alberta, and also addressed the controls and constraints on dolomitization of the formation. In addition, these studies have contributed to a better understanding of the Peace River Arch – a basement-controlled, periodically active rift that was an exposed granitic island during the Devonian - and its importance to the overall geometry and play type of the Slave Point Formation. The Peace River Arch exerted a major control on the reservoir geology at Dawson.

1.2 Objectives of research

The major objective of this study is to understand the relationship between dolomitization and reservoir development of the Slave Point Formation at the Dawson field. To this end, the following aspects will be addressed:

1) to establish whether or not depositional facies and/or fabric were controls on the dolomitization process;
2) to identify type(s) of porosity in the Slave Point and their genesis at Dawson;
3) to identify type(s) of dolomite in the Slave Point at Dawson;

4) characterize diagenetic fluids responsible for limestone diagenesis and dolomitization with the aid of isotope data; and

5) to create a paragenetic sequence of diagenesis.

In addition, a brief overview of the regional geology, sedimentology and stratigraphy of the Slave Point at Dawson will be presented, as they also are important controls on dolomitization.

1.3 Study Area

The Dawson field is located in northwestern Alberta about 300 km from the City of Edmonton (Figures 1.1, 1.2, 1.3, 1.4). The 600-km^2 study area is bound in its NW corner at 07-81-17W5M and in its SE corner at 26-78-15W5M, and is about 100 km from the Peace River Arch, which represents the zero edge of Slave Point deposition (Figure 1.4).

1.4 Sample Collection and Methods of Investigation

During the summer of 2002, thirty-two (32) cored wells from the Slave Point Formation at Dawson were logged and sampled at the AEUB Core Research Centre in Calgary, Alberta. The cores were examined to identify vertical facies variations as well as the distributions of dolomite and porosity. About 170 core samples were taken, 54 of which were thin sectioned and stained with a mixture of Alizarin Red-S and potassium ferricyanide according to Dickson (1965). The thin sections were examined using a standard petrographic microscope in order to supplement core descriptions, investigate diagenetic fabrics, and establish a paragenetic sequence of diagenetic phases.

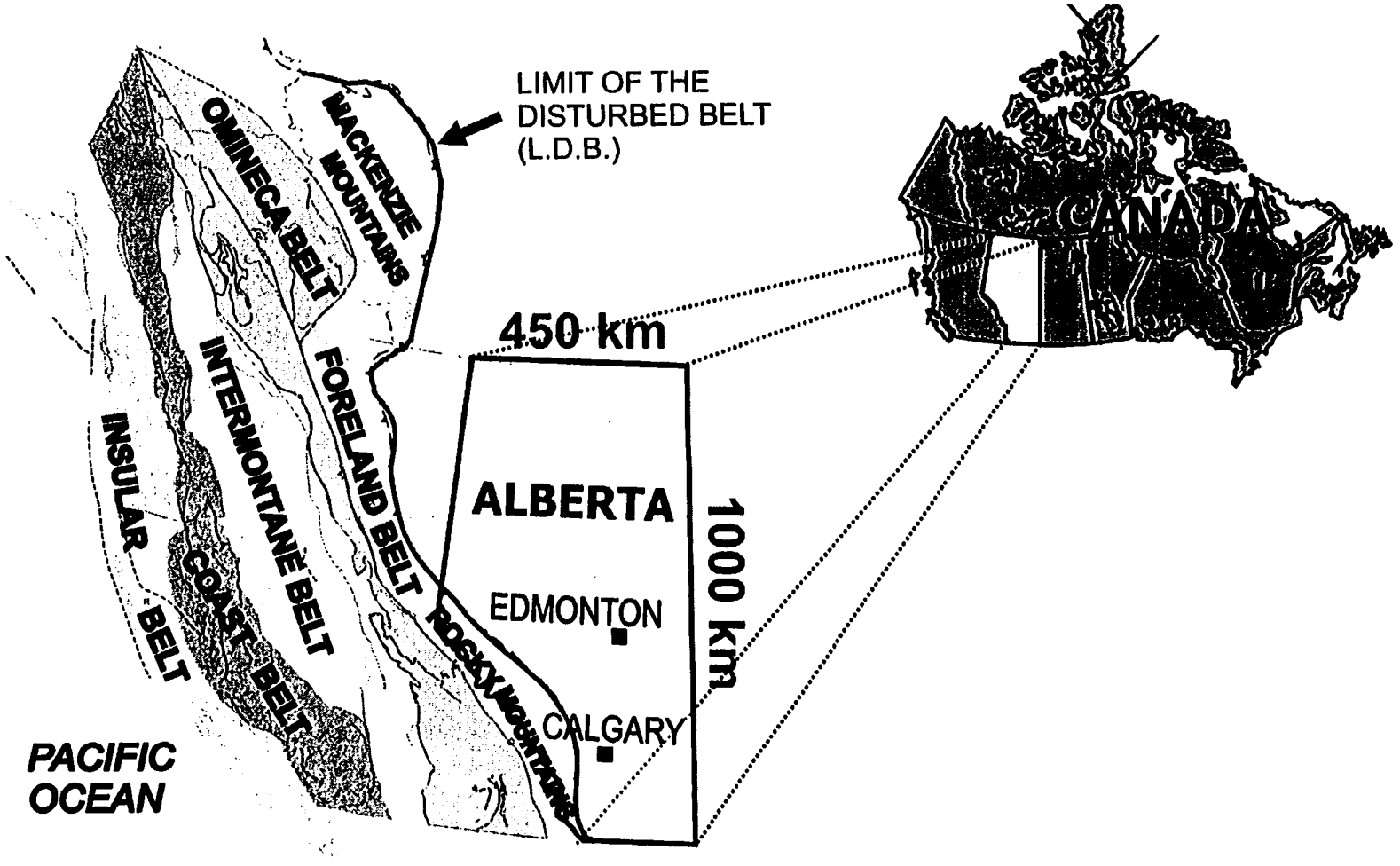

Figure 1.1 Regional map and the location of Alberta and British Columbia in Canada (modified from Mossop and Shetsen, 1994)

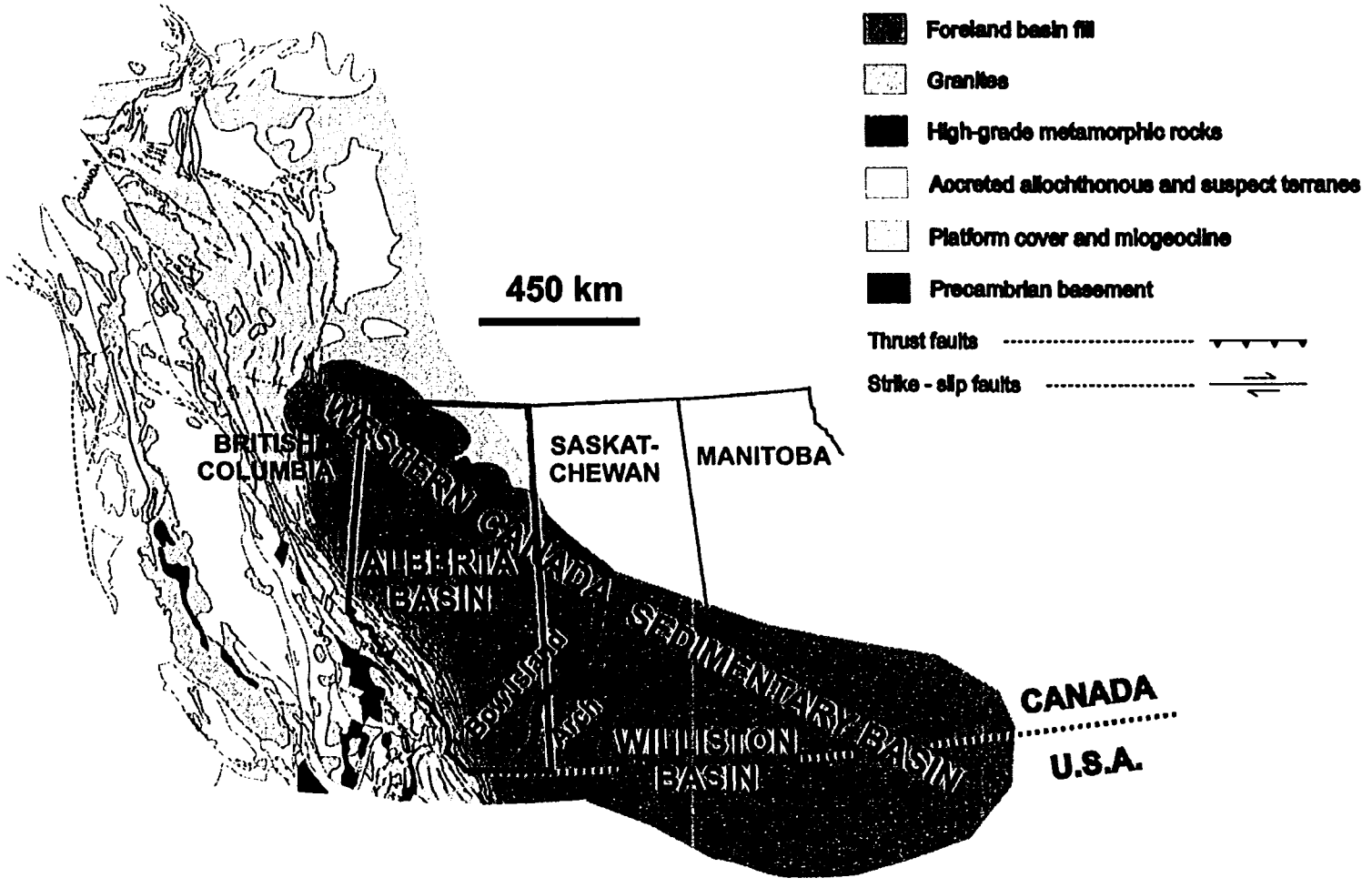

Figure 1.2 Location of the Western Canada Sedimentary Basin (WCSB) and Williston and Alberta sub-basins (modified from Mossop and Shetsen, 1994).

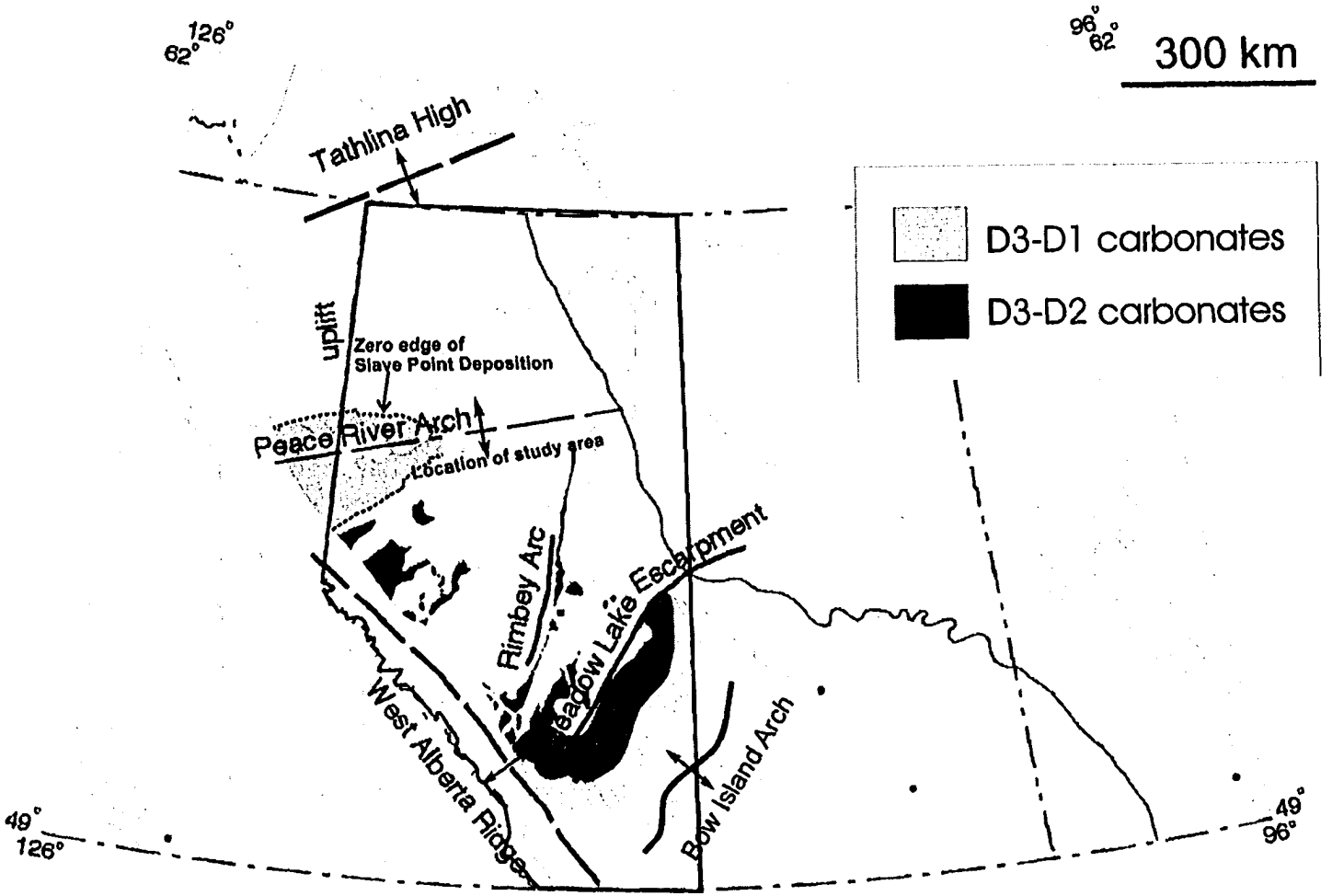

Figure 1.3 Major structural elements of the WCSB and location of study area (yellow box). Note the 'zero' edge of Slave Point deposition (black dashed line) around the Peace River Arch (modified from Mossop and Shetsen, 1994).

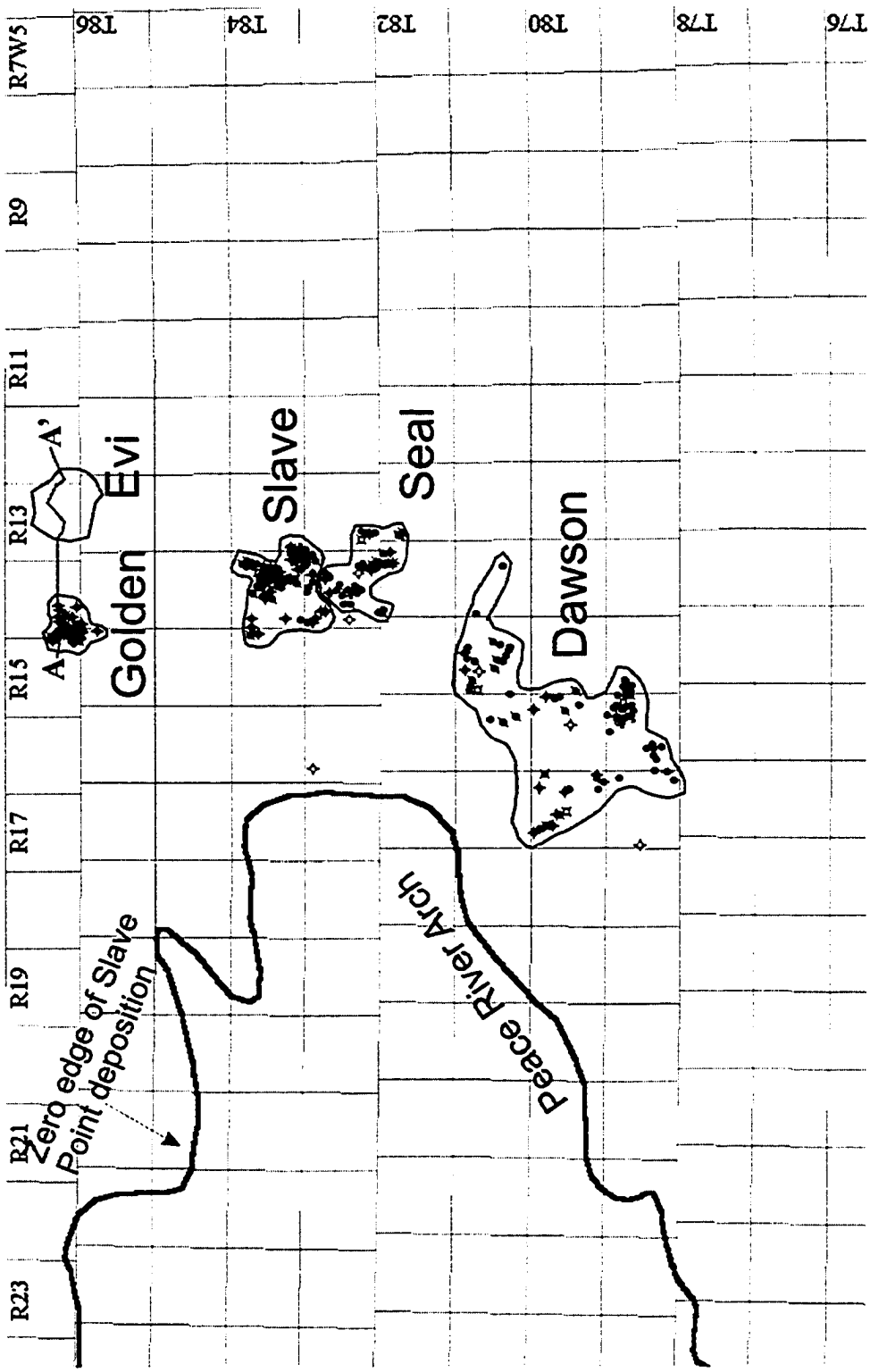

Figure 1.4 Location of Dawson and analogous pools. For section A-A', see Figure 3.1

Carbon and oxygen stable isotope analyses were conducted at the University of Alberta's stable isotope research laboratory. Calcite and dolomite samples were analyzed for carbon (C) and oxygen (O) and are reported against the PeeDeeBee (PDB) belemnite standard. Calcite and dolomite samples were reacted with 100% pure phosphoric acid (H_3PO_4) at 25^0C and 50^0C, respectively, and the produced carbon dioxide gas, was analyzed on a Finnegan_Mat 252 Mass Spectrometer. Carbon and oxygen isotope ratios have an analytical precision of $\pm$ 0.05 ‰.

Strontium (Sr) was extracted with a dental drill from calcite and dolomite phases. All samples were analyzed on a VG 354 multi-collector Thermal Ionization Mass Spectrometer (TIMS). The samples were loaded as a phosho-tantalate gel on a single Re ribbon bead assembly. Values for $^{87}Sr/^{86}Sr$ were corrected to N.B.S SRM-987 for which repeated analytical runs during the course of this study gave a value of 0.7102651. Analytical precision on individual runs was better than 0.000024 (2σ).

CHAPTER TWO

2 REGIONAL GEOLOGICAL SETTING AND PLAY TYPE

2.1 Western Canada Sedimentary Basin

The Western Canada Sedimentary Basin (WCSB; Figure 1.2 and 1.3) is the name given to the westerly thickening wedge of sedimentary units originating from its zero-edge along the exposed margin of the Precambrian Shield in Manitoba and Saskatchewan to greater then 6 km thickness near the Cordilleran foreland thrust belt (Ricketts, 1989). The WCSB is bound to the north by the Tathlina High in the Northwest Territories and extends with its southernmost margins into the northern United States. The western limit of the basin is defined by exposed, deformed sediments coincident with the eastern limit of allochthonous terranes in British Columbia, i.e., near the boundary between the Omineca and the Intermontane belts of the Cordillera (Figures 1.1, 1.2, 1.3; Wright et al. 1994).

The WSCB is thickest, and stratigraphically most complete, within the eastern parts of the Rocky Mountain foreland fold and thrust belt and the Omineca belt. The WCSB consists of two sub-basins: the Alberta basin, a northwest-trending trough in front of the Cordilleran fold and thrust belt, and the intracratonic Williston Basin, centered in North Dakota and extending into southeastern Saskatchewan and southwestern Manitoba, separated from the Alberta Basin by the Bow Island Arch (Figure 1.2, 1.3).

The evolution of the WCSB was governed by several tectonic phases, i.e., a rift and passive margin in the Precambrian and Cambrian, to foreland basin in the Middle

Jurassic to Early Cretaceous, and again from Late Cretaceous to Paleocene. The western tilting and structural loading during these phases of evolution resulted in the deep burial of Devonian strata along the western margin of the WCSB. This burial led to the maturation of organic-rich Devonian source rocks and subsequent migration of hydrocarbons updip to the east and northeast (Wendte, 1992).

2.2 The Peace River Arch

The Alberta Basin contains several large structural features (Figure 1.3) that controlled its sedimentary development. One of these features is the Peace River Arch (PRA) in northwestern Alberta and northeastern British Columbia, a cratonic uplift that formed during the Late Proterozoic at a high angle to the passive margin of ancestral North America (O'Connell et al. 1990). It is a major crustal anomaly that resulted in the uplift of granitic Precambrian rocks about 1000m above their regional position in the basement (Cant and O'Connell, 1990). The Arch is elongated in an east-northeast to west-southwest direction and extends from the passive Paleozoic continental margin for about 400 km across northern Alberta and British Columbia (Figure 1.3). Precambrian rocks of the Arch are onlapped by the entire Devonian section of Western Canada (Figure 2.1)

The PRA has existed in three different phases: 1) a Late Proterozoic and early Paleozoic Arch; 2) a Late Paleozoic to earliest Mesozoic embayment; and, 3) a deep basin component of a Mesozoic foreland basin (O'Connell et al. 1990). This study deals with the relationship of the Arch to the Devonian of the WCSB surrounding the PRA, specifically the Slave Point Formation during the first phase. The younger units and their

relation to the Arch will not be discussed. The structure of the basement, topographic relief of the Arch (about 800 to 1000 m), and the existence of small structures interpreted as structurally controlled horsts and grabens, or fault blocks, parallel the axis of the Peace River Arch (Cant and O'Connell, 1990). The grabens are filled by the Granite Wash, which is composed of material shed into the grabens from the exposed Precambrian rocks of the Arch.

2.3 Devonian stratigraphy in the PRA region

The Arch was formed in the Late Proterozoic and remained topographically elevated until the Middle to Late Devonian when it was onlapped by siliciclastic, evaporite, and carbonate strata. By the beginning of the Mississippian, the Arch had been buried and embayments formed close to, and overlying the position of, the PRA (O'Connell et al. 1990). The initial sediments that onlapped the Peace River Arch were the evaporites, carbonates, and clastics of the Elk Point Group (Figure 2.1). Younger Devonian strata comprise four successive shallow marine carbonate units that onlap the Arch from the middle Givetian to the Famennian; these are in ascending order: 1) Beaverhill Lake Group; 2) Woodbend Group; 3) Winterburn Group; and, 4) Wabamun Group (O'Connell et al. 1990). The Slave Point Formation is contained within the Beaverhill Lake Group (Figure 2.1). In addition to the above-mentioned units, the Granite Wash forms a diachronous siliciclastic unit that backsteps onto the Arch and forms terrestrial and nearshore equivalent facies to each of the above units (O'Connell et al. 1990).

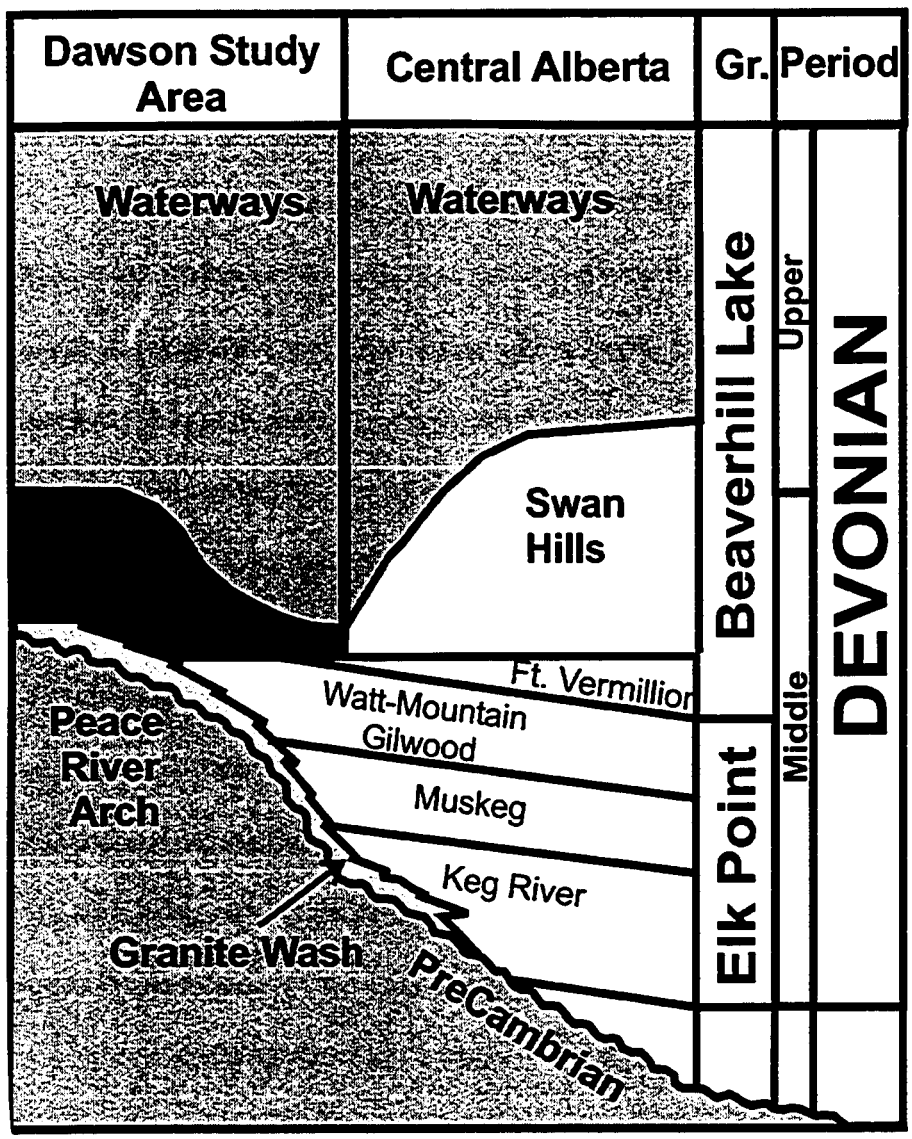

Figure 2.1 Stratigraphic column and nomenclature (modified from Gosselin et al. 1989) S.P Platform = Slave Point Platform.

2.3.1 Granite Wash Lithozone

The Granite Wash is coarse-to medium-grained siliciclastics composed mainly of weathered granite derived from the exposed landmass of the PRA. Shallow-marine carbonate deposition was partly synchronous with Granite Wash deposition around the Arch during the Middle – Late Devonian. The Granite Wash is designated a lithozone, which is a body of strata defined by distinct lithological features, but for which there is insufficient information or need to justify its designation as a formal stratigraphic unit (North American Stratigraphic Code, 1983). The Granite Wash, over the crest of the Arch, is between 0 and 100 m thick and is confined within graben structures. The graben-filling units are interpreted as braided stream and alluvial fan deposits (Trotter and Hein, 1988). To the north and south of the Arch, the Granite Wash forms blanket deposits up to 60 m thick in the south and 100 m in the north. Trotter and Hein (1988) interpreted these facies as belonging to fluvial, shoreline, and shallow marine complexes.

With the exception of Granite Wash sediments that interfinger with Middle to Upper Devonian strata, the exact stratigraphic age of the Granite Wash sediments in unknown. Where, the Granite Wash underlies the Middle Devonian (Slave Point) sediments and infills the grabens along the Arch crest it is undated (O'Connell et al. 1990). Cant (1998) suggested that it is possible that most of the Granite Wash accumulated over a long time period between the late Precambrian and the Middle Devonian.

2.3.2 Beaverhill Lake Group

The middle Givetian to early Frasnian Beaverhill Lake Group thickens rapidly and seaward from the Arch landmass, and reaches a thickness of about 180m to the northeast and southeast of the Arch. Three major stratigraphic units comprise this group: 1) the Slave Point Formation, fossiliferous carbonates; 2) carbonate buildups equivalent to the reefs of the Swan Hills Formation of central Alberta; and, 3) basinal shales, argillaceous limestones, and limestones of the Waterways Formation (Figure 2.1) (O'Connell et al. 1990). Local movement along fault-bounded Precambrian highs that controlled deposition of carbonate buildups, together with increased rates of subsidence in the basin away from the Arch during early Waterways time, were two important controls on sedimentation during Beaverhill Lake time (O'Connell et al. 1990).

The Slave Point Formation is a carbonate unit that extends from its type/outcrop location near Great Slave Lake, NWT, to just south of the Peace River Arch, where it is buried to an average depth of about 2100 m. The formation is thickest at Great Slave Lake and in northern British Columbia and progressively thins southwards to the Arch, pinching out against its flanks. To the south of the Arch, the Slave Point forms the basal platform from which the Swan Hills reefs grew. Along the west side of the basin, shallow-water lithofacies are included in both the Swan Hills and Slave Point Formations; however, the distinction in nomenclature corresponds purely to geography. For example, shallow-water carbonates flanking and to the north of the Peace River Arch comprise, the Slave Point Formation. On the other hand, shallow-water facies in the Swan Hills area comprise the Swan Hills Formation (Campbell, 1992).

The Slave Point is abruptly overlain by argillaceous limestones and shales of the Waterways Formation (Figure 2.1). The contact is often found to be a submarine hardground surface that is commonly pyritic and bored by organisms. These hardground surfaces are thought to be caused by a rapid rise in sea level followed by submarine cementation and/or non-deposition (Craig, 1987).

2.4 Play types and monadnocks

The Peace River Arch has greatly influenced the overall geometry, facies distribution, and exploration of the Slave Point Formation at Dawson. Specifically, the locations of the Slave Point carbonate buildups are controlled by the pre-depositional topographic relief of the underlying Precambrian. Stoakes (1987) noted that there are various well-understood play types within the Beaverhill Lake Group and, hence, the Slave Point Formation: 1) reefs; 2) the platform margin; and, 3) backstepping carbonate ramps.

Reef exploration plays produce from isolated limestone reef complexes like those found in the Swan Hills reef complex and show variety in both size and morphology. No significant biohermal reef buildups are found at Dawson. At best, reef plays produce only from a few small, isolated patch reefs. The platform margin play type occurs via stratigraphic closure along the updip margins of the platform where limestones and/or dolostones of the reef margin, upper foreslope, and foreslope facies are productive (Stoakes, 1987). The best developed play type in the Slave Point is around the 'nose' of the Peace River Arch and Dawson where several large pools are located (Figure1.4). These pools belong to the third play type, backstepping carbonate ramps.

2.4.1 Backstepping carbonate ramp

Well-documented examples of backstepping reef deposition have been described from the Middle and Upper Devonian of Canada (Bassett and Stout, 1967; Stoakes, 1987) and from the Australian Canning Basin (Playford, 1980). Backstepping reefs are common and typically associated with platform onlap during transgression. As is the case at Dawson, the rate of sea-level rise was "pulsed" (i.e. transgression-standstill-transgression) and recolonization occurred on antecedent Precambrian topography into progressively shallower waters. Essentially, reef deposition transgressed in stages, moving to shallower, higher positions on the platform margin with time (Tucker and Wright, 1990; Figure 2.2).

At Dawson, the Slave Point Formation backsteps onto the antecedent Precambrian topography of the PRA. As sea level continued to rise, the Slave Point Formation stepped farther back onto the Peace River Arch but without ever completely covering the Arch. Furthermore, the surface of the PRA was differentiated into "highs" and "lows". The highs were bald as the result of the Precambrian topographic relief being too high for the Slave Point to fully colonize before transgression and drowning by the Waterways Formation. Thus, smaller erosional remnants of the PRA, acted as nuclei for localized patch reef growth. This phenomenon was first described in the carbonate literature by Shinn (1973). Such erosional remnants, now commonly referred to as monadnocks, formed relatively small hills or mountains of circumdenudation rising conspicuously above the general level of the peneplain. The monadnocks at Dawson are not only erosional but partly structural, as they appear to be the erosional remnants of

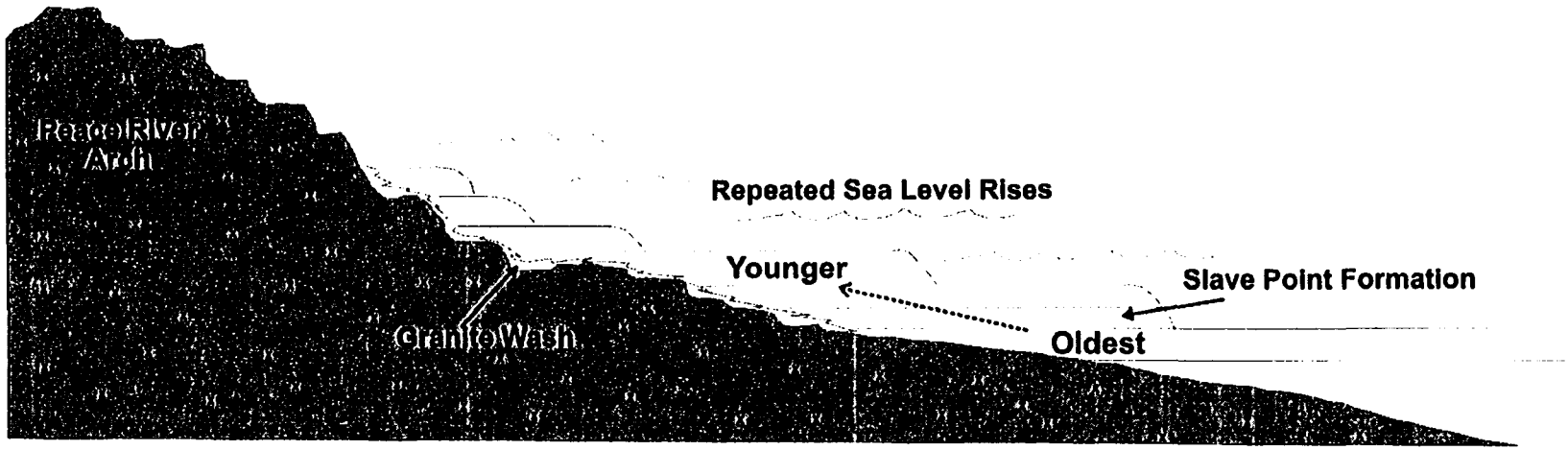

Figure 2.2 Backstepping Slave Point Formation onlapping the Granite Wash, and Precambrian Peace River Arch (Modified from Stoakes, 1987)

fault blocks in a general block-and-graben regime. In other words, these monadnocks are the result of faulting

augmented by fluvial erosion, which created a series of relatively small, isolated land masses of the Precambrian arch that the Slave Point colonized (Figure 2.3 and 2.4).

2.4.2 3D Seismic – Constraining exploration

Definition of the bank margin, which is critical for exploration and defining the overall field geometry, is a combination of: 1) isochron mapping techniques, 2) edge detection maps; and 3) traditional isopach mapping. Three-dimensional (3D) seismic data has allowed for detailed definition of the underlying Precambrian highs. This allows the explorationist to avoid the 'bald highs' (i.e., no Slave Point), and focus on exploring their flanks, where reefs are common. 3D seismic coverage at Dawson is extensive. However, for proprietary reasons, figures that use 3D seismic to aid in interpretation (Figures 2.5, 2.6) that can be included in this discussion have no geographic reference points. The Dawson study area, however, is located within the maps shown.

In order to constrain exploration at Dawson is it important to identify the bank margin, or in lithologic terms, the boundary between the shales of the Waterways Formation and the porous Slave Point Formation carbonates. An isochron map uses known seismic horizons and converts them to a travel time in milliseconds between two picks, which results in images similar to conventional isopach maps, as travel times can be converted to thickness. Isochron maps can be used to illustrate and define the bank margin.

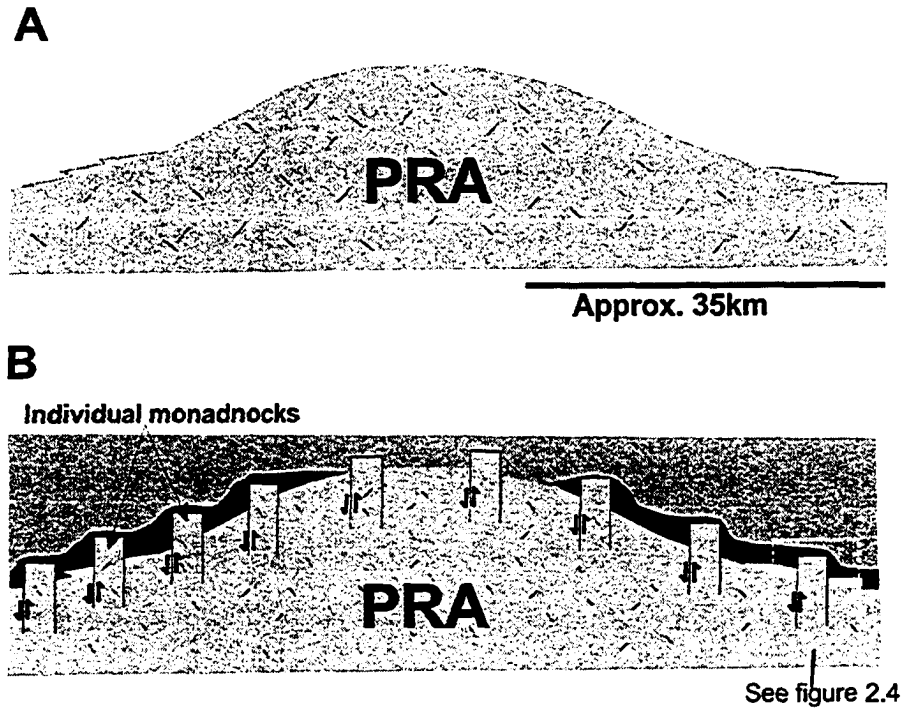

Figure 2.3 Schematic development of monadnocks at Dawson. A) Initial uplift of the Peace River Arch, Granite Wash sands in yellow. B) Block faulting of the Peace River Arch. Erosion isolating fault blocks. Backstepping Slave Point Formation in blue and Waterways Formation in green. C) Monadnocks (yellow highlights) near the south rim of the Grand Canyon, Arizona; recent analogues to those at Dawson. Figure 2.4 shows schematic enlargment of the facies relationship around a single monadnock

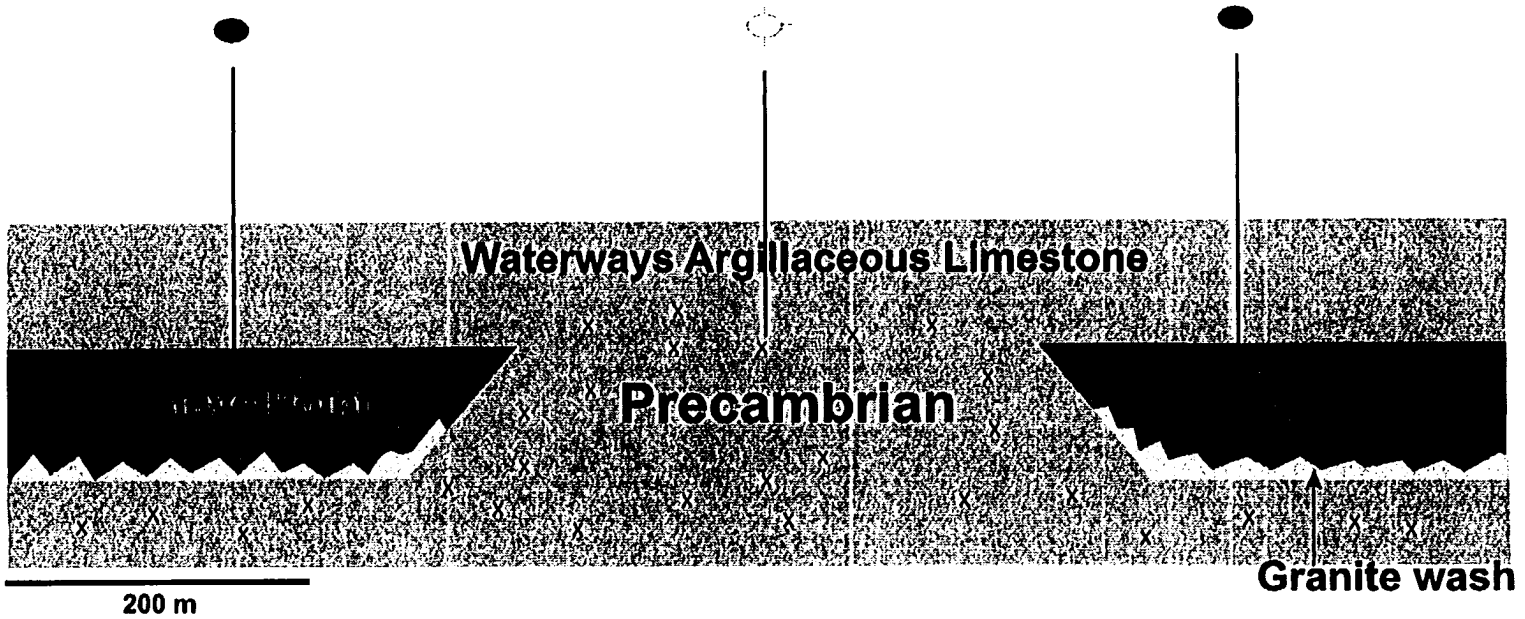

Figure 2.4 Schematic cross-section illustrating the spatial and stratigraphic relationship between the Slave Point Formation and a single monadnock (from highlighted box on Figure 2.3) located along the flank of the PRA. The arch proper would be located to the back or front of this picture. In this example, the Slave Point was unable to colonize on the topographically high Precambrian monadnock before being drowned by the argillaceous shales and limestones of the Waterways Formation. Exploration is focused on the flanks of such highs were favourable facies are found, indicated in orange on the diagram.

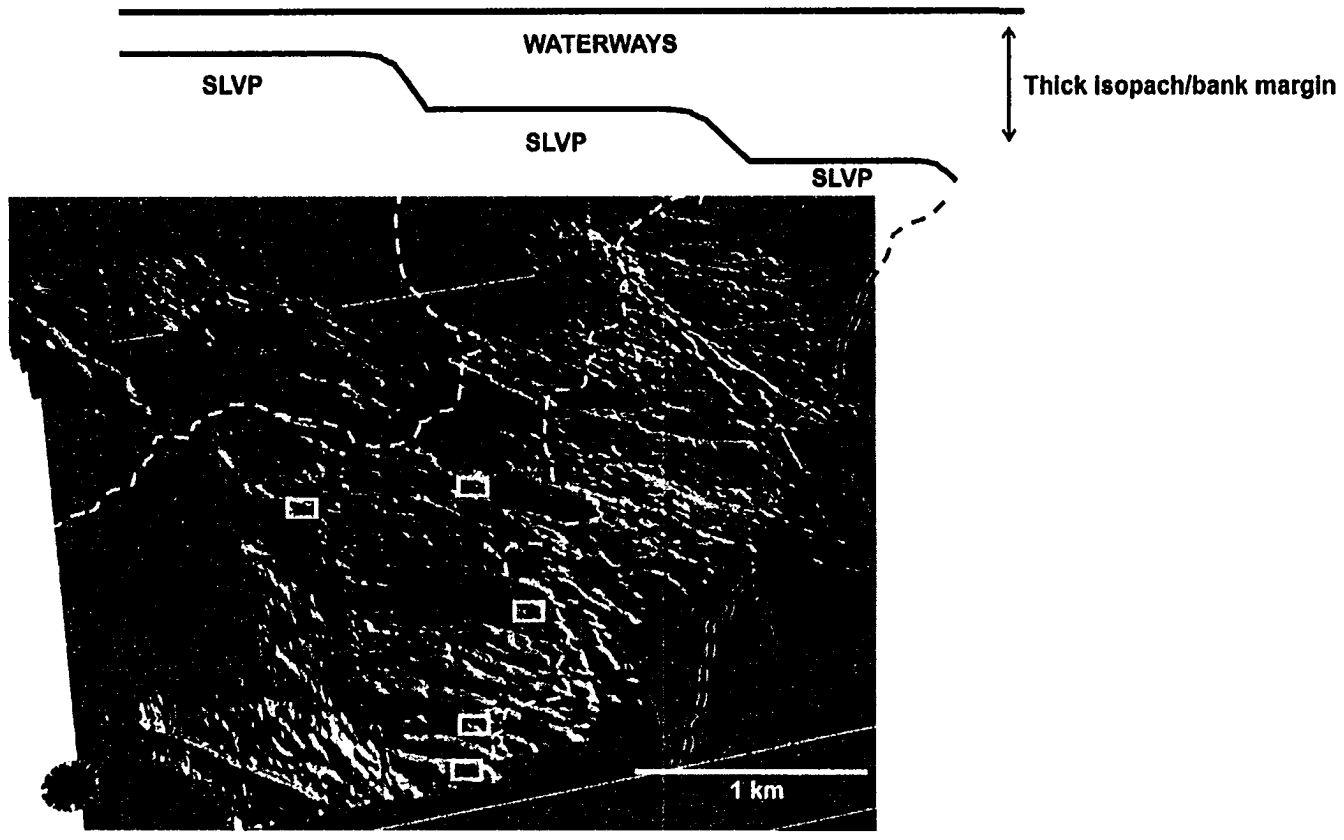

Figure 2.5 Beaverhill Lake (Waterways Formation) to Slave Point isochron map. Dashed lines represents interpreted backstepping edges. Dashed red line indicates the break from the basinal muds to the productive Slave Point. Hotter colours (reds and deep greens) indicate smaller isochrons. Cooler colours (baby blues and purples) represent larger isochrons and greater thickness between the Waterways and Slave Point. Upper diagram is a schematic cross-section of the interpreted backstepping edges.

Figure 2.6 Edge detection map with bank margin in red, this map view is to the same scale as Figure 2.5. This figure illustrates steep dipping edges (yellow, greens, and reds) and the shallower dipping basinsediments (blues and purples). Stippled pattern indicates were 3D seisimic is available but not included since it is not 100% owned by project sponsor (Anadarko Canada Corporation). The dashed red line is equivalent to the red dashed line figure 2.5.

For example, figure 2.5 is an isochron map from the Waterways Formation to the Slave Point Formation where dashed lines represents interpreted backstepping edges. The dashed red line indicates the break between the basinal muds of the Waterways Formation from the porous carbonates of the Slave Point Formation. Hotter colours (reds and deep greens) indicate smaller isochrons; whereas, cooler colours (baby blues and purples) represent larger isochrons and great thickness between the Waterways and Slave Point. The upper diagram on Figure 2.5 is a schematic cross-section of the interpreted backstepping edges.

In conjunction with traditional isopach mapping and isochron maps, an edge detection map has been used to define the aforementioned bank margin. The edge detection map highlights sharp changes in dip, like reef edges, faults, or steep horizon dips, such as changes in slope or a sharp change in topographic relief. Steep dip changes expected at a bank margin/reef edge are exaggerated, allowing for better definition of the bank margin (Figure 2.6).

Figure 2.6 illustrates the aforementioned reef edges and dip changes. This figure exaggerates steep dip changes (hot colours, yellows and reds) along the flanks of the Precambrian high structures and/or reef edges. Exploratory drilling is focused along the edges of these highs and targets Slave Point Formation reef growth along these flanks. Additionally, using figure 2.6, the bank margin (red dashed line) separates the productive Slave Point carbonates from the tight shales of the Waterways Formation. The bank margin is defined using numerous geological techniques, including seismic isochron mapping and traditional isopach mapping. However, the most useful way of defining the bank margin, in conjunction with isochron and isopach maps, is using drill core/facies

analysis. Essentially, all facies to the northwest side of the margin are productive reef core or 'reefal' facies, whereas, those facies to the southeast of the bank margin are shales and argillaceous limestones of the Waterways Formation.

The bank margin has also been defined using drill core taken in the area. Wells drilled to the basinward side (southeast) of the bank margin encounter little, if any, Slave Point. Where the Slave Point is encountered basinward, it is < 2m thick and unproductive. The dominant lithologies of wells drilled south of the bank margin are the argillaceous carbonates and shales of the Waterways Formation. Furthermore, this margin also corresponds to an isopach cut off of 60 m from the top of the Waterways to the Slave Point, therefore, a greater than 60 metre Waterways isopach corresponds to no Slave Point production. The 60m contour provides a valuable exploration tool on the platform side of the play at Dawson (Figure 2.7).

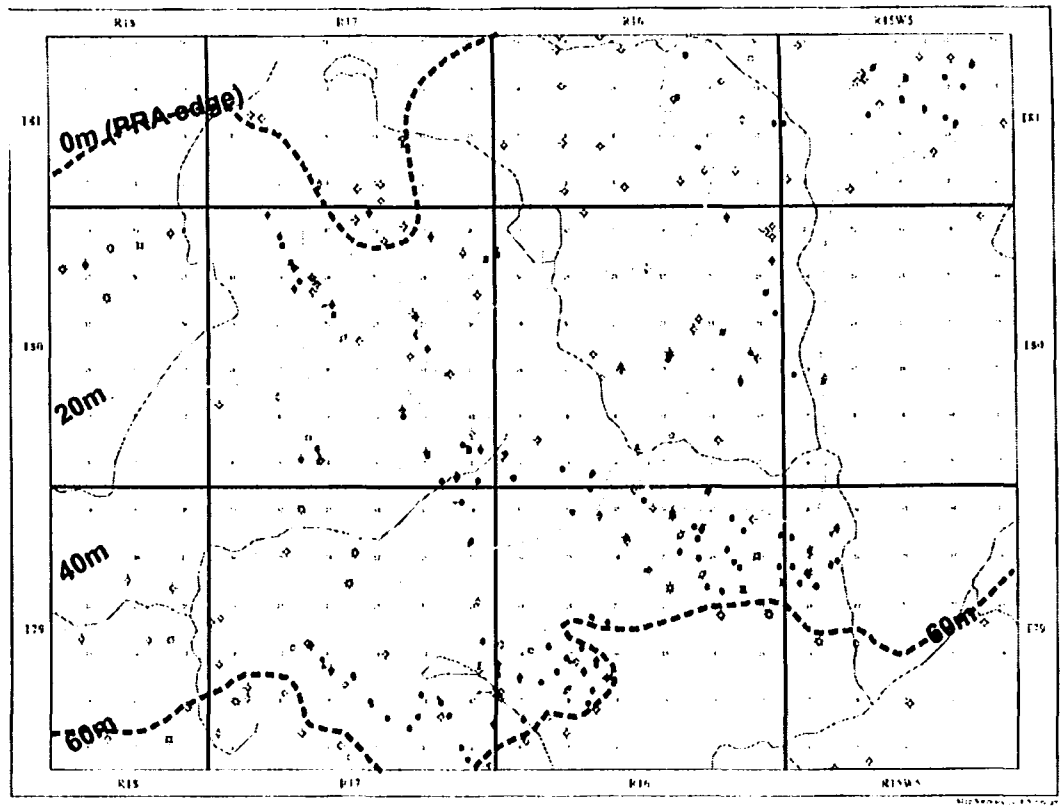

Figure 2.7 Isopach map from the Waterways Formation to the top of the Slave Point. The 60m contour separates the productive Slave Point toward the NW from the basinal limestones and mudstones of the Waterways towards the SE. The 60m contour correlates to the red line on figures 2.6 and 2.7. The 0m contour is correlative to the Peace River Arch edge - the zero mark of Slave Point deposition.

CHAPTER THREE

3 FACIES, STRATIGRAPHY, AND PALEOTOPOGRAPHY OF THE SLAVE POINT

3.1 Introduction

The Slave Point Formation at Dawson consists mainly of clean, fossiliferous, shallow marine carbonates deposited on a structurally controlled carbonate platform that is overlain by the argillaceous limestones and shales of the Waterways Formation. Vertical facies variations within the Slave Point can be correlated regionally and represent episodic rises in sea level followed by standstills. Within the Slave Point, six major environmental facies can be recognized, i.e., the shallow shelf, back reef, reef, forereef, off reef, and basinal facies.

3.2 Previous work

There are no previously published facies or stratigraphic analyses of the Slave Point at Dawson. However, there are studies of adjacent fields that serve as analogues for the facies at Dawson, most notably the Slave and the Golden fields (Figure 1.4). These studies document similar facies and facies relationships seen at Dawson, and the relationship of these facies to the underlying Precambrian basement.

3.2.1 Slave Field

Dunham et al. (1983) provided a general facies overview of the Slave Point at the Slave field, Alberta, around Township 84 and Range 14W5 (Figure 1.4). Although the carbonates of the Slave field have been replaced by dolomite, original depositional textures, structures, and fossil assemblages are still recognizable. Dunham et al. (1983) were able to distinguish four distinct facies types within the Slave Point Formation. In addition, variable thicknesses of the Granite Wash sands and gravels are present in the lower portions of some cores.

Facies Type 1 – CARBONATE MUDSTONE AND FLOATSTONE WITH MARINE FAUNA

Facies Type 1 consists of a matrix of dark-brown argillaceous carbonate mud containing scattered crinoids and brachiopods, and isolated stromatoporoids. Dunham et al. (1983) suggested that fauna in this facies represents normal marine salinity, while the abundance of mud indicates quiet-water sedimentation. They interpreted this facies to represent sedimentation on an open shelf at water depths below fair weather wave base.

Facies Type 2 – STROMATOPOROID BOUNDSTONE

Dunham et al. (1983) defined Facies Type 2 based solely on the presence of sediment-binding to baffling tabular and bulbous stromatoporoids. The authors interpreted this facies to represent semi-turbulent to turbulent, normal-marine conditions, as encountered at the seaward edge of a shallow-water carbonate bank.

Facies Type 3 - AMPHIPORA FLOATSTONE TO RUDSTONE

Facies Type 3 is defined by the presence of *Amphipora* in excess of 10% of the total rock volume. Additionally, small nodular stromatoporoids may be present. Dunham et al. (1983) interpreted this facies as shallow, quiet water, restricted-marine conditions.

Facies Type 4 - DOLOMITE MUDSTONE:

Dunham et al. (1983) defined Facies Type 4 by the near absence of macroscopic fossils. They noted that scattered *Amphipora* and gastropods are present but represent less then 10% of the rock volume in mudstones that are laminated or featureless, or, in some intervals, contain fenestral pores. This facies is interpreted to represent restricted-marine carbonate conditions relatively close to the paleoshoreline.

Using well log correlations, Dunham et al. (1983) also noted the importance of the Precambrian basement controlling the thickness of the Slave Point. Specifically, Dunham et al. (1983) found that topographic highs of the basement localized deposition of the Slave Point shallow-water carbonate facies. Rise in sea level apparently resulted in the upward growth of the Slave Point carbonate bank composed of shallow-water facies fringing pre-existing basement highs. Laterally, away from the basement structures, the carbonate facies changes to a crinoid-brachiopod mudstone, recording deeper-water open shelf deposition (Dunham et al. 1983).

3.2.2 Golden Field

Gosselin et al. (1989) documented the facies and stratigraphy of the Golden Field located north of Dawson between Townships 86 and 87, and Ranges 15W5 and 14W5 (Figure 1.4). The Slave Point at Golden attains a maximum thickness of 20 m and pinches out against a granitic Precambrian high at its centre. A reef complex comprises

10 m of thickness, reflecting a single stage of reef growth, while the remainder is composed of underlying and overlying open marine off-reef units (Gosselin et al. 1989). The margin of the reef complex can be traced for about 15 km as a fringe around the granitic island, separating a lagoon from an open marine area, similar to the facies and physiographic zonation of Pacific atolls today.

Gosselin et al. (1989) also noted that reef facies of the Golden Field rest unconformably on granitic Precambrian basement, where the Precambrian protrudes through the Slave Point Formation, producing a 'bald high' synonymous to what is documented at Dawson. This is similar to what Dunham et al. (1983) documented for the Slave Field. The facies at Golden have been divided into three main types: (1) an open marine facies; (2) a platform margin facies; and, (3) a platform interior facies (Tables 3.1 and 3.2), which are further divided into 7 facies types.

1) The open marine facies consists of off-reef, mud-dominated sediments that lack framework-building organisms. This facies (A in table 3.1) is a dark brown, nodular, skeletal wackestone containing abundant crinoids and brachiopods.

2) The platform margin facies comprises the true reef rim and contiguous back reef and foreslope, and forms a narrow belt that separates the platform interior from the open marine facies. The platform margin was further divided into four subfacies (subfacies B to E; Table 3.1) consisting of framework building, binding, and baffling organisms and their debris. The lithologies are *Stachyodes*, *Thamnopora* or stromatoporoid rudstone/floatstones and boundstones.

3) The platform interior facies comprises the portion of the reef complex that is sheltered from the sea by the reef rim. The dominant fauna in this facies realm are

	Facies	Description
OPEN MARINE	A	Open marine facies lacking frame-building organisms. Dark brown, nodular, skeletal-pelodial wackestone containing abundant crinoids and brachiopods
PLATFORM MARGIN	B	Stachyodes-Thamnopora rudstone/floatstone is composed of abundant Stachyodes and Thamnopora together with crinoids and brachiopods, interpreted to occur in a foreslope position and commonly containing reef derived debris
	C	Laminar stromatoporoid boundstone is composed of tabular/sheet-form stromatoporoids, with minor Stachyodes, Thamnopora, gastropods, brachiopods, and crinoids scattered in the matrix. This subfacies forms an extensive reef barrier
	D	Massive hemispherical stromatoporoid framestone/rudstone composed of broken and abraded massive stromatoporoids. Stachyodes, brachiopods, crinoids, and laminar stromatoporoids are a minor component of the facies. Abundant quartz and feldspar grains reflect the close proximity to the granitic basement. In addition, this facies represents a true reef rim
	E	Massive hemispherical stromatoporoid-Amphipora rudstone/floatstone composed primarily of reef debris with a mixture of Amphipora, Stachyodes, and small bulbous stromatoporoids. Gosselin et al., (1989) attributed this facies to a narrow back reef zone behind the reef rim of Subfacies D
PLATFORM INTERIOR	F	Amphipora floatstone/rudstone that is composed of Amphipora, small bulbous stromatoporoids, and minor amounts of gastropods
	G	Laminite, consists of light to dark brown layers of pelleted mudstone; on occasion these mudstones display microbial lamination and fenestral fabric

Table 3.1 Summary of lithologic descriptions of Facies A to G (Gosselin et al. 1989).

Substage	Description
IA	Basal stage. Comprised of subfacies A and B, largely open marine, and is the lowest interval of the Slave Point; maximum thickness of 5m and pinches out again a Precambrian high
IB	Comprised of subfacies B and C; forms a reef-rimmed promontory that is part of a more extensive carbonate platform to the south
IIA	IIA is an open marine facies and comprises subfacies A; this substage attains a maximum thickness of 8m, but thins as it onlaps the reef margin of substage IB
IIB	This substage attains a maximum thickness of 10m at Golden and represents the only stage of reef growth fringing the Precambrian high/island and is represented by subfacies B, D, and E
IIIA	Composed primarily of subfacies A and is uncomformably overlain by calcareous shales and argillaceous limestones of the Waterways Formation; this substage overlies the reef lithologies of substage IIB
IIIB	Thinnest reef stage obtaining a maximum thickness of 5m. Gosselin et al. (1989) noted that facies correlations are difficult within this stage due to a lack of core, but a platform margin is inferred because of the relief this units displays.

Table 3.2 Summary of stratigraphic substages at Golden. 'A' denotes basinal deposition; whereas, 'B' is reef growth stage (Gosselin et al. 1989).

organisms that are adapted to low energy and moderate sedimentation rates. Contained within this realm are two facies (facies F and G; Table 3.1), *Amphipora* floatstone and a dark, pelleted mudstone.

Stratigraphically, Gosselin et al. (1989) subdivided the Slave Point Formation into three distinct, informal members (Table 3.2), each representing a period of growth responding to a transgression and subsequent standstill. Within each of these stages sedimentation includes basinal deposition (A) and associated reef growth (B).

It should be noted that not all substages in Table 3.2 are present in the Golden Field. The Evi Field to the east represents all of the above-mentioned stages. However, Evi was omitted from this review because it has been determined by this author that Golden serves as a better analogue to Dawson. Nevertheless, Figure 3.1 shows the stratigraphic and facies relationship between Golden and Evi, as well as the basement control on carbonate deposition.

Gosselin et al. (1989) concluded that at Golden the reef complex was localized and initiated by a fault-controlled basement high, forming an island during Slave Point time. In comparison to the Evi Field, the reef complex at Golden is thinner and contains a less diverse fossil assemblage that apparently lacks corals. Gosselin et al. (1989) hypothesized that this low fossil diversity may have been caused by a lesser nutrient supply due to the 'shadowing' effect of the Evi reef complex to the east, assuming the prevailing wind and ocean currents were from the north and northeast, which is consistent with paleowind and current directions established for the Middle Devonian (Gosselin et al. 1989). Additionally, block faulting along the Peace River Arch to the southwest of the

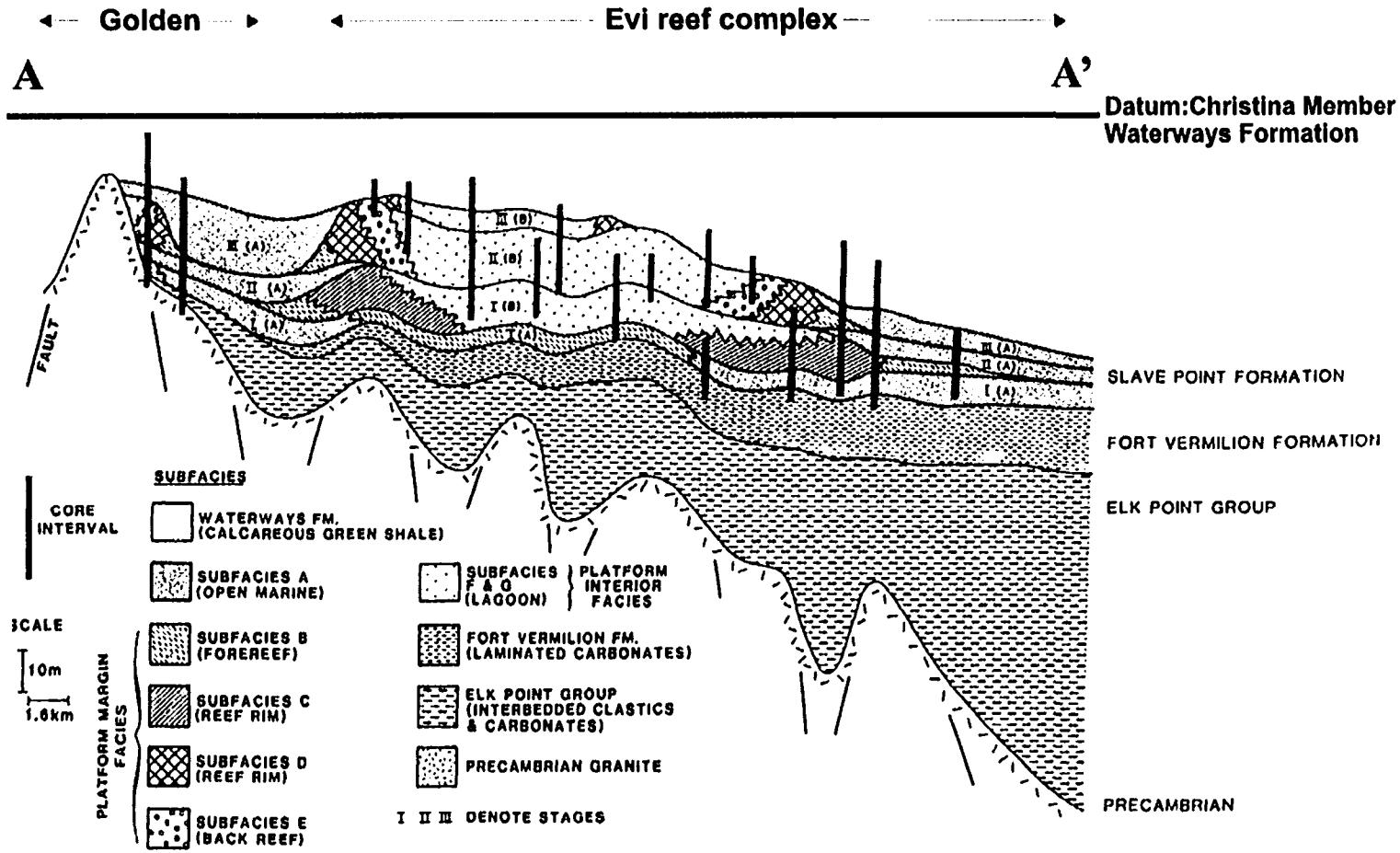

Figure 3.1 West-east cross section(modified from Gosselin et al. 1989) through Golden and Evi fields; see Figure 1.4 for line of cross-section

Golden reef complex may have periodically shed terrigenous clastics, affecting reef growth and therefore, the absence of reef development (Gosselin et al. 1989).

3.3 New data and facies analysis from the Dawson Field

A facies is a body of rock defined by the association of sedimentary characteristics such as lithology, texture, composition, sedimentary structures, fossil content, and colour (Tucker and Wright, 1990). In this study of the Slave Point and associated formations, thirty-two individual cores were logged to document changes in facies, porosity distribution, the presence of matrix and saddle dolomites, and other diagenetic features.

Devonian reef facies models have been studied for many years and a large body of literature have been published including several models to aid in facies analysis. However, most of these models have been developed for specific reefs or reef complexes in relatively small areas. For example, Murray (1966), Fischbush 1968), and Jenik and Lerbekmo (1968) developed a models for individual Swan Hills reefs; Klovan (1964) developed a model for the Redwater reef. Core logging and facies analysis was based on Machel and Hunter (1994) who established a facies model for Middle to Late Devonian shallow-marine carbonates, for several reasons: 1) it integrates most important studies of Devonian reefs on three continents (Canada, Europe, Australia), 2) it provides a quick guide for accurate facies analysis in core and outcrop, 3) presents facies zonations in shallow marine ramp carbonates from below wave base to supratidal faces.

The Machel and Hunter (1994) model (Figure 3.2) is composed of five water energy zones, with increasing energy from I to IV (IV/V, the reef proper) and are

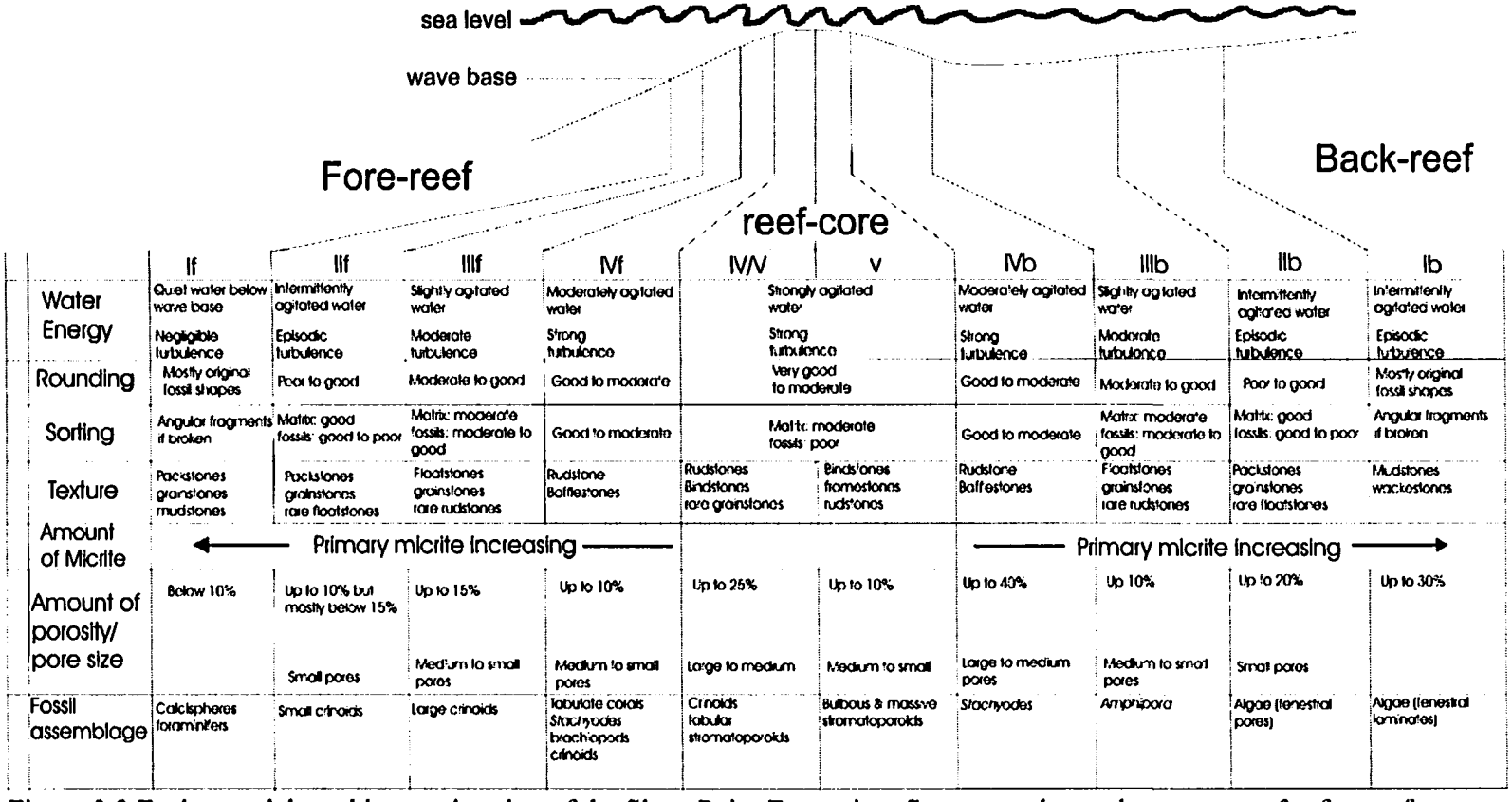

Figure 3.2 Facies model used in core logging of the Slave Point Formation. Stages are denoted on top row; **f** = forereef **b** = backreef (Modified from Machel and Hunter, 1994).

designated as either **f** = forereef or **b** = backreef. In this model, the forereef zones are narrower than the backreef zones of comparable water energy, because the forereef slope is steeper. The reef core - the highest energy zone – is divided using biofacies (see Machel and Hunter, 1994 for discussion). Most facies types of Machel and Hunter's (1994) model classification are identifiable at Dawson.

3.3.1 Zone Ib – Intertidal mudstones and wackestones

Zone Ib is dominated by laminated, generally non-porous mudstones and wackestones with some fenestral pores (Plate A/1-3). This facies usually contains few, if any, macrofossils. Where present, fossils are usually small (< 1 cm) fragments of *Amphipora*. Disseminated detrital grains of quartz and feldspar suggest proximity to a Precambrian high. Zone Ib is interpreted to represent shallow, intermittently agitated waters of episodic turbulence (storms). The depositional fabrics suggest that this facies was deposited in an intertidal setting and that some wells were close to Precambrian highs shedding episodic pulses of detrital material.

3.3.2 Zone IIb – Fossiliferous packstones and wackestones

Zone IIb facies is comprised of slightly macrofossiliferous, generally non-porous packstones and wackestones with scattered amounts of *Amphipora*, and abraded fragments of other, larger stromatoporoids (Plate A/4-6), and some gastropods. Calcite spar fills intra- and interparticle pores of *Amphipora* and other stromatoporoid fragments. Stylolitization is common and dolomitization of the matrix ranges from minor to complete replacement (Plate A/ 6).

PLATE A

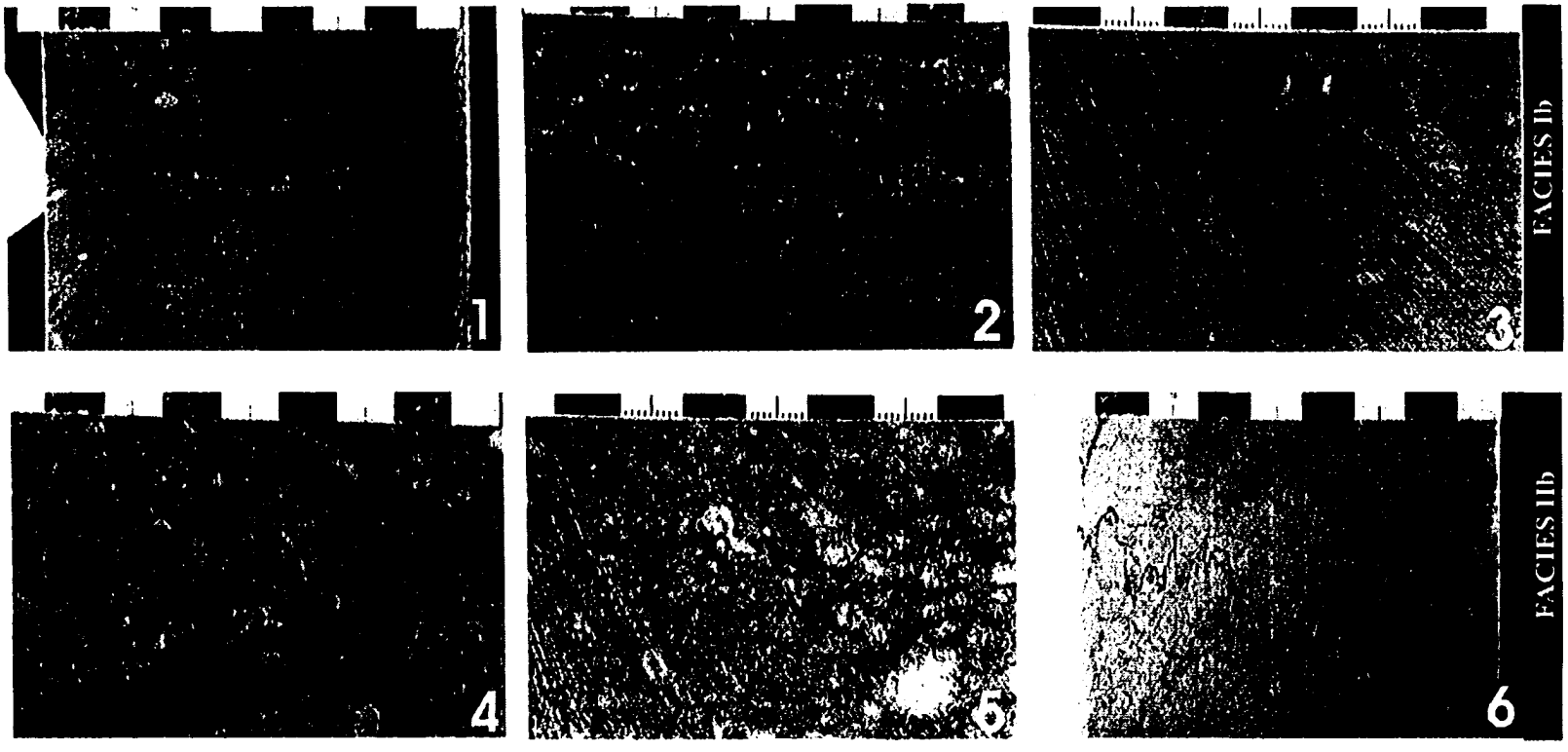

1) Core photograph of facies Ib; note development of diagenetic nodules and wispy stylolite seams. Location 5-19-79-15W5, 2053 metres. 2) Core photograph of facies Ib; note laminations as well as siliciclastics from the Granite Wash facies. Location 2-32-80-17W5, 2116.5 metres. 3) Core photograph of facies Ib typical mudstone/wackestone texture; note well developed low amplitude stylolites. Location 13-16-80-16W5, 2075 metres. 4) Core photograph of facies IIb; note cement filling pores of *Amphipora* molds. Location 2-23-80-17W5, 2111.3 metres 5) Core photograph of facies IIb; note large calcite void-filling cement, blueish anhydrite cement and stylolites in this wackestone/packstone. Location 13-16-80-16W5, 2083.5 metres. 6) Core photograph of facies IIb; note high amplitude stylolite in this wackestone. Location 5-19-79-15W5, 2056 metres. Scale divisions are in centimetres at stratigraphic tops.

Zone IIb is interpreted to be deposited in shallow, intermittently agitated waters of episodic turbulence. The fossil assemblage and depositional fabrics suggest an environment somewhat more turbulent then Ib, as it contains some larger fossil fragments derived from the reef core. However, this derivation was episodic at best, as evidenced by the partially laminated nature of this facies.

3.3.3 Zone IIIb – *Amphipora* floatstones and grainstones

Zone IIIb facies is dominated by 5 to 35 cm thick layers variably-porous *Amphipora* floatstones and grainstones, though *Amphipora* is scattered and disseminated throughout this facies (Plate B). Other macrofossils, such as bulbous and tabular stromatoporoids, *Stachyodes*, and gastropods, occur as fragments and detritus in this facies.

The matrix is generally lime mud or fine carbonate sand. Porosity in this facies is the result of leaching of fossils resulting in biomoldic porosity, which is as high as 30-35% in places (Plate B/ 2 and 5). This facies contains calcite spar and/or saddle dolomite filling intra- and interparticle pores of *Amphipora* (Plate B/ 1, 3, 4, 5, and 6). Replacive dolomitization of the matrix ranges from minor to complete. Complete matrix replacement resulted in an increase in the permeability connecting the larger fossil molds to the high permeability matrix.

The ubiquitous presence of *Amphipora* suggests this facies was deposited in a slightly restricted, back reef lagoonal environment in slightly agitated waters. Additionally, the presence of sporadic, small, well-rounded stromatoporoid fragments also suggests transport into and deposition in the back reef environment.

PLATE B

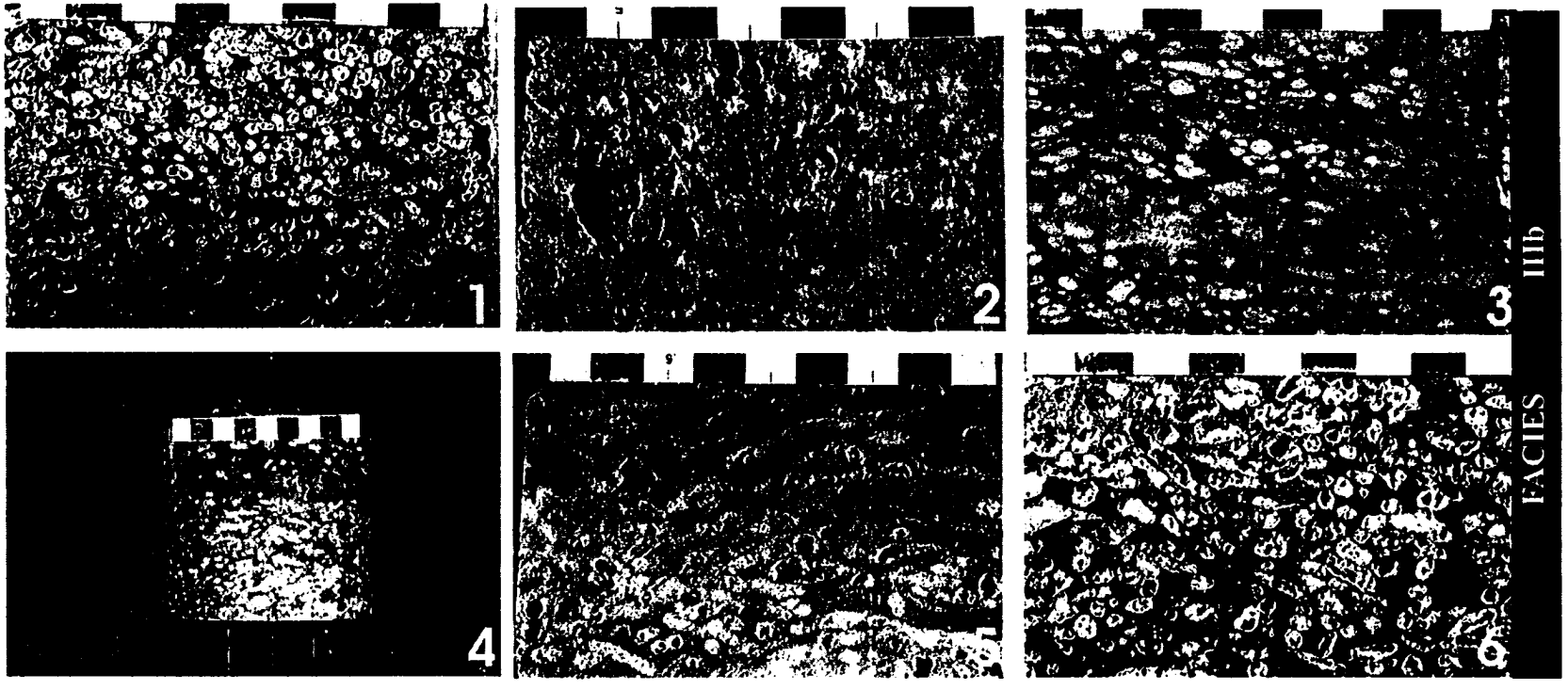

1) Core photograph of facies IIIb; note the dark mud matrix and the calcite and/or saddle dolomite cementing pore spaces. Location 11-34-79-16W5, 2093 metres. 2) Core photograph of facies IIIb; note the fine-grained sandy matrix and leaching of pre-existing macrofossils. Location 4-35-79-16W5, 2075.5 metres. 3) Core photograph of facies IIIb; note the sub-parallel alignment of the *Amphipora* and muddy matrix, and cemented pores. Location 12-18-79-16W5, 2138.2 metres. 4) Core photograph of facies IIIb with muddy matrix and cemented *Amphipora*. Location 15-15- 80-16W5,2075.6 metres. 5) Core photograph of facies IIIb; note less muddy matrix than in previous pictures, and leached *Amphipora*; white patches are late calcite void-filling cements. Location 11-34-79-16W5, 2091 metres. 6) Core photograph of facies IIIb; note leached *Amphipora* in a muddy matrix; saddle dolomite (cream color) and late calcite cement line and fill open voids partially, respectively. Location 11-34- 79-16W5, 2092 metres. Scale divisions are in centimeters at stratigraphic tops.

3.3.4 Zone IVb – Stromatoporoid rudstones and bafflestones

Zone IVb facies is dominated by large (>2 cm), subrounded to angular, porous and non-porous stromatoporoid rudstones and bafflestones (Plate C), though it is common for *Amphipora* to be scattered throughout the matrix of this facies zone. The macrofossil content of this facies ranges from 20 to 80%. Most skeletal fragments are detritus of tabular and bulbous stromatoporoids, *Stachyodes*, and *Thamnopora*. Other skeletal fragments also include small, disarticulated brachiopods, gastropods, and crinoids.

The matrix is composed of lime mud or carbonate sand, however, carbonate sand is more common. Porosity is up to 30%, averaging 15%, mostly developed by dissolution of framework stromatoporoids producing large vugs (Plate C/1 and 2). Dissolution occurred mainly where the matrix was composed of fine sand, allowing for fluids to permeate the rocks to leave large vugs and a porous and permeable matrix. Dissolution porosity is restricted to core intervals with matrix dolomitization, which suggest that dissolution was a by-product of dolomitization, as found elsewhere in the Western Canada Sedimentary Basin (e.g., Amthor et al. 1993). This facies is partially cemented by calcite spar, filling large vugs left by the dissolution of precursor stromatoporoids (Place C/ 3,4, and 5). In addition, gypsum and/or anhydrite are common as cements in the large voids. Matrix dolomitization ranges from minor to pervasive in this facies, and stylolitization is common.

Zone IVb was deposited in a back reef environment between the reef core and the previous IIIb facies (Figure 3.2) in relatively agitated, and at least episodically turbulent

PLATE C

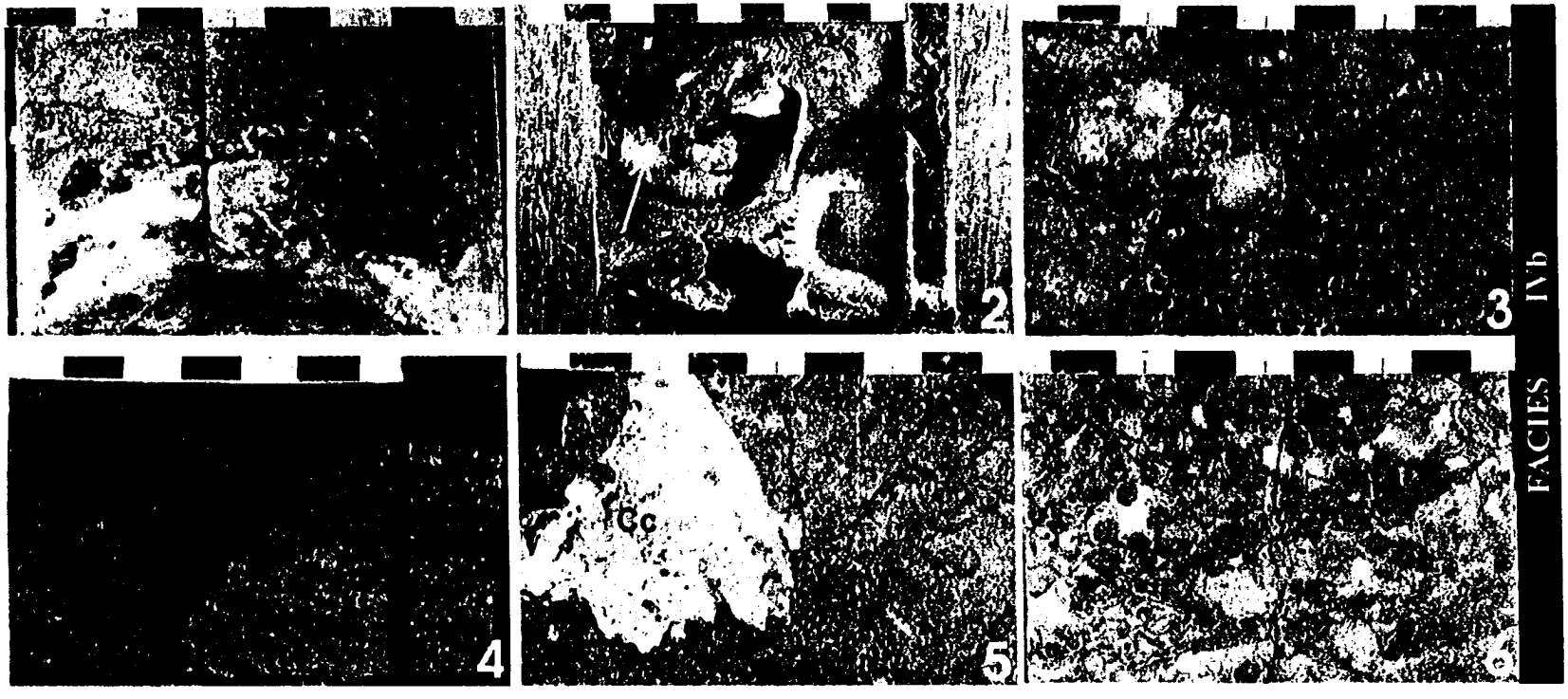

1) Core photograph of facies IVb; note large vuggy porosity and late calcite cement partially filling the void. Location 1-29-80-17W5, 2122.9 metres. 2) Core photograph of facies IVb; large vuggy porosity developed after dissolution of bulbous stromatoporoid partially filled with late calcite spar (yellow arrow). Location 14-34-79-16W5, 6831.5 ft 3) Core photograph of facies IVb; note calcite spar filling large vugs left by dissolution of stromatoporoid. Location 2-32-80-17W5, 2110.3 metres. 4) Core photograph of facies IVb; note calcite spar filling intraparticle porosity of stromatoporoid. Location 5-23-80-16W5, 6847.5 ft 5) Core photograph of facies IVb; note calcite cement (Cc) filling pore space, and stylolites. Location 2-32-80-17W5, 2110.8 metres 6) Core photograph of facies IVb; small milky white patches are anhydrite cementing mainly primary porosity. Location 8-25-79-16W5, 2043 metres. Scale divisions are in cenitmetres and stratigraphic tops.

waters. The presence of large, angular to subrounded stromatoporoids suggests transport from the reef core. Additionally, fossils found in the matrix, in particular *Amphipora*, and in places the muddy composition of the matrix in this facies (Plate C/ 2 and 4), suggest deposition on the back reef side on the slope of the reef core.

3.3.5 Zone IV/V – Reef core bindstones and rudstones

Zone IV/V is mainly bulbous and massive stromatoporoids, 3 to 10 cm in diameter, as framework-building organisms in variably porous bindstones and rudstones. Porosity ranges up to 70% by volume (Plate D). *Thamnopora* and *Stachyodes* are also common in this facies, and comprise about 20-25% of the megafossil content.

Generally, the matrix of the reef core facies is quite muddy at least in the Slave Point Formation in most of Northern Alberta and British Columbia. Hence, the reference (by the author) to the reef core facies as a "non-conventional" reef, as this type of reef does not consist of a major biohermal structure. At best, this type of reef is small muddy patch reefs ranging in thickness from 1-3 m, with associated lagoonal (IIIb and IVb) and foreslope facies (IVf). The matrix of this facies consists of well-sorted debris of crinoid ossicles, fragments of small (<3cm) branching stromatoporoids, solitary rugose corals, and brachiopod fragments (Plate D/ 5 and 6). Dissolution of large stromatoporoids has led to large vuggy porosity development in some core intervals (Plate D/ 2). However, matrix dolomitization is minor, thus, the effective porosity and permeability of the rocks is moderate. Calcite spar cements voids left by dissolution of stromatoporoids, while saddle dolomite fills the interstices within the matrix and in some of the smaller voids (Plate D/ 1, 3, and 4).

PLATE D

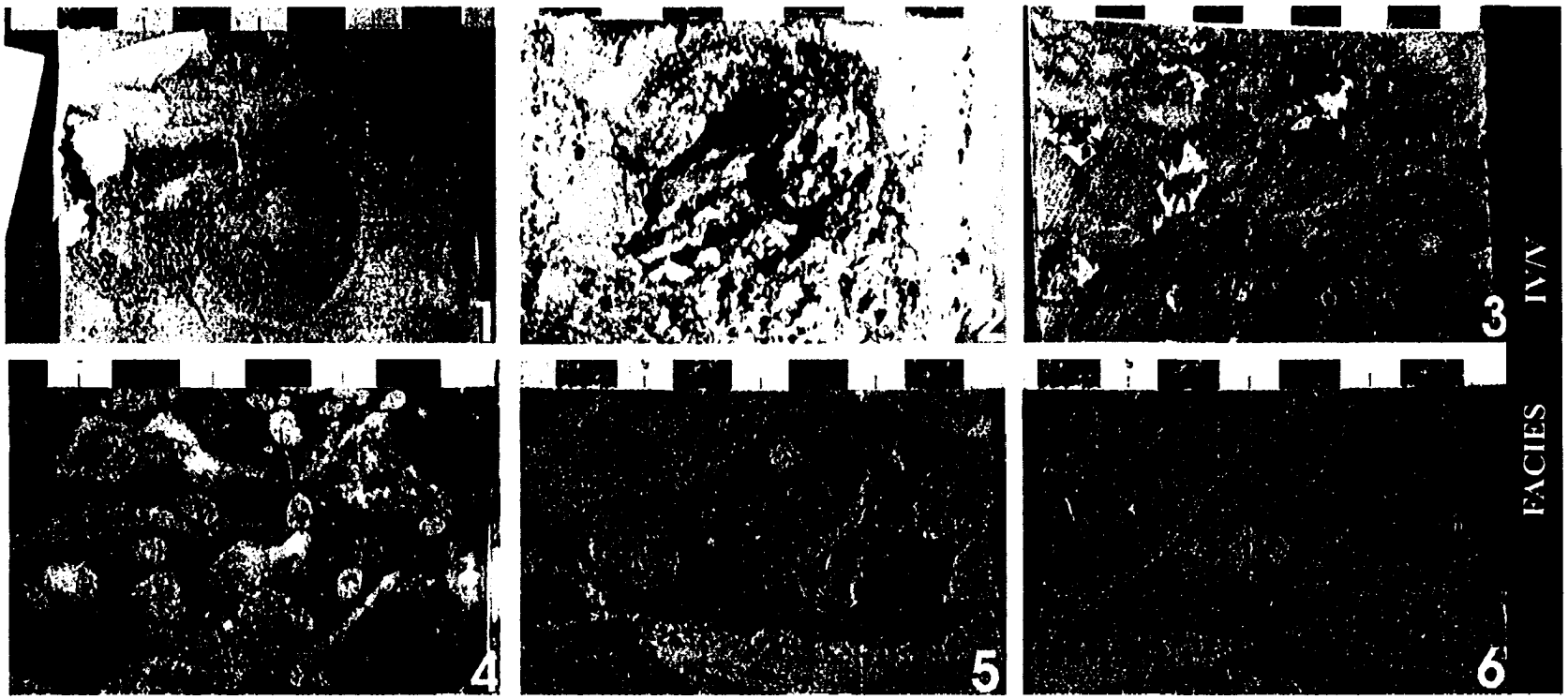

1) Core photograph of facies IV/V; note calcite spar cementing void left by dissolution of bulbous stromatoporoid. Location 1-29-80-17W5, 2021 metres. 2) Core photograph of facies IV/V; large vug left by partial dissolution of stromatoporoid. Location 14-19-80-16W5, 2037.5 metres. 3) Core photograph of facies IV/V; large tabular stromatoporoid rudstone with saddle dolomite (white) cementing some pores between framework building stromatoporoids. Location 4-13-80-16W5, 2048 metres. 4) Core photograph of facies IV/V; note the muddy matrix of this tabular stromatoporoid rudstone and saddle dolomite (white) filling pores. Location 4-35-79-16W5, 2086.5 metres. 5) Core photograph of facies IV/V; stromatoporoid rudstone with solitary rugose coral in the matrix; note the brown coloration of the matrix due to oil staining. Location 5-29-79-15W5, 2066 metres. 6) Core photograph of facies IV/V; tabular stromatoporoid rudstone, brown coloration of matrix is due to oil staining. Location 5-29-79-15W5, 2062.2 metres. Scale divisions are in centimeters at stratigraphic tops.

Facies IV/V is interpreted as being the reef core facies of the Slave Point Formation, although as mentioned previously, it is more of a muddy reef facies than the conventional biohermal reef buildup facies developed in other reef carbonates of the WCSB.

3.3.6 Zone IVf – Forereef bafflestones and rudstones

Zone IVf facies contains transported and abraded bulbous stromatoporoids and *Stachyodes* as the dominant fossil constituents in porous, poorly sorted bafflestones and rudstones (Plate E). These constituents occur as detritus ranging in size from 1.0 to 4.0 cm. Small (<2cm) solitary rugose corals and tabular stromatoporoids comprise a minor component of the framework organisms.

The matrix is composed of fine-to medium-grained carbonate sand and contains abundant biogenic detritus, mainly, brachiopods, crinoids, gastropods, and fragmented rugose corals. Porosity is high, commonly primary (interparticle) and ranges from 15-30%. However, some of this porosity is filled with calcite spar (Plate E/ 1) and/or saddle dolomite. Dolomitization ranges from minor to pervasive in this facies.

Zone IVf is interpreted to be part of the forereef zone of the Slave Point reefs. Megafossil components are broken, abraded, poorly sorted, and have a matrix component consisting of fine-to medium-grained bioclastic sand. These features are consistent with strongly turbulent and highly agitated waters of the forereef environment, where lime mud would not be able to settle out of suspension to form a considerable matrix component.

PLATE E

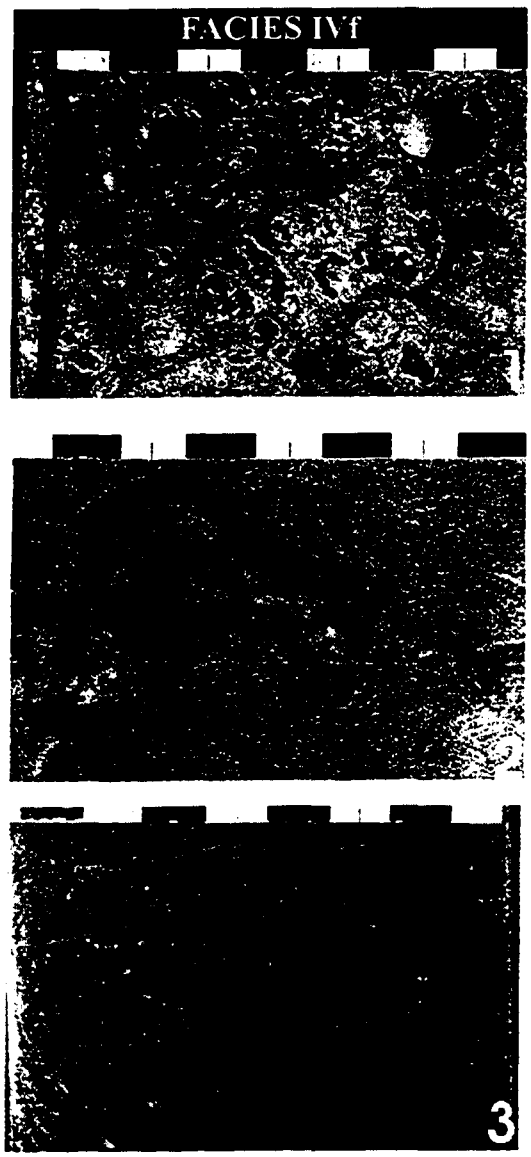

1) Core photograph of facies IVf; typical fore reef rudstone; note vuggy porosity and calcite spar in voids. Location 4-35-79-16W5, 2092 metres. 2) Core photograph of facies IVf; note sandy matrix, transported and subrounded bulbous stromatoporoid. Location 4-36-79-16W5, 2052.3 metres. 3) Core photograph of facies IVf; note broken and abraded stromatoporoid in a sandy matrix composed of solitary corals, small *Thamnopora*, and crinoid fragments. Location 5-19-79-17W5, 2061.5 metres. Scale divisions are in centimetres at stratigraphic tops.

3.3.7 Zone IIIf – Crinoidal-stromatoporoid floatstones and rudstones

Zone IIIf facies consists mainly of small (commonly <0.5 cm diameter) crinoids and scattered fragments of bulbous and tabular, rounded stromatoporoids with an average size of 2 cm (Plate F/ 1-3). The crinoids are the main bioclastic component in the facies.

The matrix is composed of lime mud and fine sand, with small fragments of crinoid ossicles, rare solitary rugose corals, and brachiopods fragments (Plate F/ 1-3). Porosity is low in this facies, generally <10%. Dolomitization is less pervasive than in the other facies. However, some megafossil components have been dolomitized. Dolomitization of the matrix is incomplete.

Zone IIIf is interpreted to be deposited in the lower fore reef environment below fair-weather wave base. The ubiquitous occurrence of crinoid ossicles, fragmented and rounded stromatoporoids, and muddy nature of the matrix suggest deposition in a relatively quite water environment where lime mud was able to settle out of suspension and would not be winnowed out regularly.

3.3.8 Zone IIf /If – Crinoidal floatstones to sparsely fossiliferous mudstones

Zone IIf/If facies have been grouped together because of the difficulty of distinguishing these two facies in core examination (Plate F/ 4-6). These zones represent the off-reef/basinal units of the Slave Point Formation. The dominant macrofossils are small (<1 cm), in places articulated crinoids ossicles and small fragments of brachiopod shells, which are more abundant in zone IIf than If, generally less the 5-10%.

PLATE F

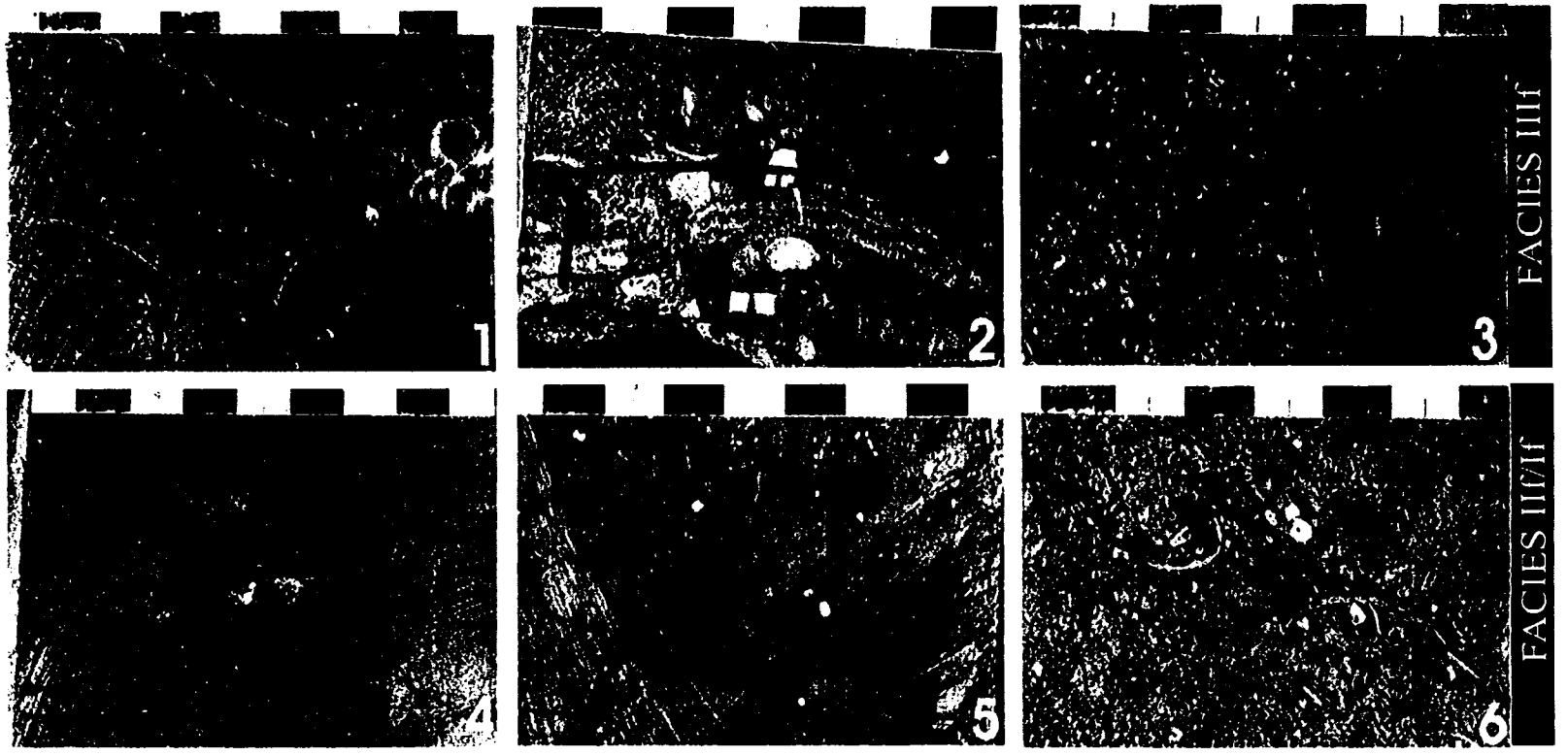

1) Core photograph of facies IIIf floatstone; note muddy matrix, scattered crinoids in the matrix, and solitary rugose corals. Location 5-19-79-17W5, 2052.2 metres. 2) Core photograph of facies IIIf; rare rudstone with tabular stromatoporoids, crinoids in a mud matrix. Location 4-35-79-16W5, 2088.2 metres. 3) Core photograph of facies IIIf; crinoidal floatstone with a bulbous stromatoporoid. Location 5-29-79-17W5, 2058.1 metres. 4) Core photograph of facies IIf/If; nodular mudstone, note brachiopod with geopetal fillof mud and calcite cement. Location 11-34-79-16W5, 2088 metres. 5) Core photograph of facies IIf/If; nodular crinoidal mudstone. Location 8-36-80-16W5, 2014.8 metres. 6) Core photograph of facies IIf/If; note large fragments of brachiopod shells and crinoids scattered throughout the matrix. Location 5-29-79-15W5, 2059.8 metres. Scale divisions are in centimetres at stratigraphic tops.

The matrix of these floatstones to mudstones is lime mud and is essentially devoid of any macrofossil or fossil fragments, rare exceptions are thin-shelled brachiopods and isolated rugose corals. Porosity in this facies is below 10%. Dolomitization in this facies is absent or minimal.

This facies represents sedimentation in "basinal" environments, at water depth below fair-weather wave base. The lack of framework building organisms suggests this facies was deposited in an off-reef marine environment far from the site where reef organisms were actively growing.

3.3.9 Other lithofacies at Dawson

Although the Slave Point Formation is the major focus of this study, two other formations, and the Precambrian basement, play an important role in trapping of hydrocarbons, secondary oil production, and the overall geometry of the Dawson field these formations are: 1) the Waterways Formation; and, 2) the Granite Wash.

The Calmut Member of the Waterways Formation overlying the Slave Point is a sequence of greenish-grey to light grey argillaceous limestones and shales with a stylonodular texture that represents a basin-fill lithofacies (Craig, 1987). The Calmut Member contains mainly open marine fauna such as crinoids, brachiopods, and gastropods (Plate G/ 1 and 2). Hardgrounds are also present within this lithofacies. The Waterways Formation onlapped and drowned the carbonates of the Slave Point Formation, essentially filling the basin with argillaceous limestones and shales that now form a seal for hydrocarbons in the Slave Point.

The Granite Wash lithozone lies between the Slave Point Formation and the Precambrian basement (Figure 2.1). At Dawson, the Granite Wash is a mix of clastic

PLATE G

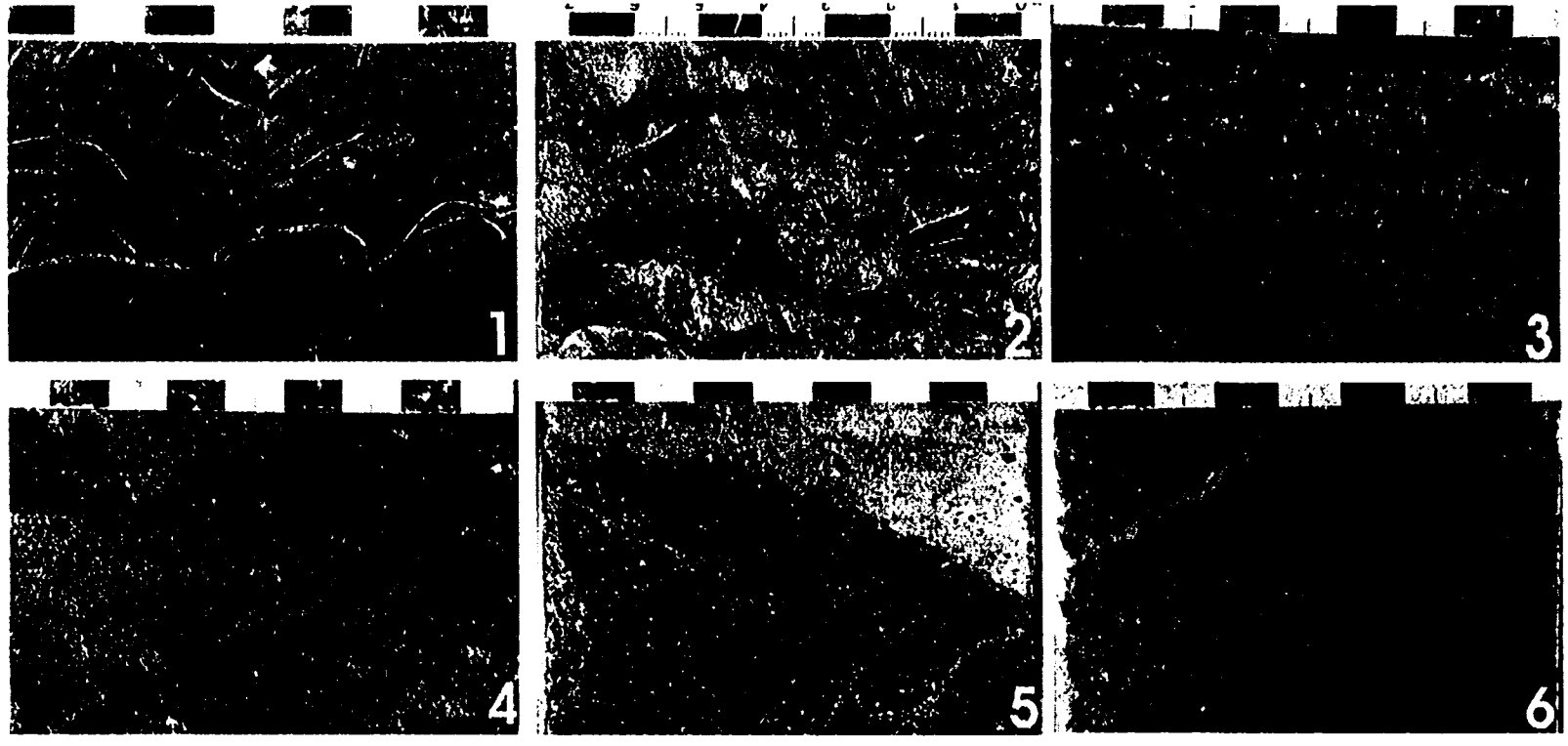

1) Core photograph of the Calmut Member, Waterways Formation; note the abundant brachiopod fragments and muddy matrix of this facies. Location 5-18-80-15W5, 1977.8 metres. 2) Core photograph of Calmut Member with stylonodular texture and brachiopod fragments. Location 13-16-80-16W5, 2074 metres. 3) Core photograph of the Granite Wash lithozone dominated by angular fragments of quartz and feldspar. Location 2-32-80-17W5, 2116.5. 4) Core photograph of oil-stained Granite Wash lithozone. Location 2-32-80-17W5, 2117.2 metres. 5) Core photograph of sharp contact between red, granite basement and overlying carbonates of the Slave Point Formation. Location 8-25-79 -16W5, 2044.6 metres. 6) Core photograph of Precambrian syenite cut by a calcite-filled fracture. Location 5-19-79-17W5, 2163.4 metres. Scale divisions are in centimetres at stratigraphic tops.

material, dominantly quartz and feldspar (Plate G/ 3 and 4), derived from the weathering of the Precambrian basement after tectonic uplift, prior to and partially coincident with deposition of the Slave Point Formation. Trotter and Hein (1988) interpreted the Granite Wash facies as fluvial, shoreline, and shallow marine deposits. This lithofacies occurs mainly along the flanks of the Precambrian. In places, the Granite Wash is porous, permeable, and oil-stained in core (Plate G/ 4). It is common to have production from both the Slave Point and Granite Wash. The Precambrian basement rocks mainly are syenitic granites, rich in potassium feldspar with minor amounts of quartz, mafic, and accessory minerals (Plate G/ 6; Craig, 1987). Where the Granite Wash is missing, the Slave Point is deposited directly on top of these Precambrian igneous rocks (Plate G/ 5).

3.4 Paleotopography at Dawson

The depositional facies and overall geometry of the field at Dawson were controlled to a large extent by the antecedent topography of the Precambrian basement, as discussed in Section 2.4. Figures 3.3, 3.4 and 3.5 illustrate in more detail the thickening and thinning of the Slave Point in relation to the basement, as well as the relationship between the basement and the Granite Wash.

Granite Wash clastics were shed from the highs and accumulated in depressions (Figures 3.4 and 3.5) as well as channels (Figure 3.6). In figure 3.5 the Slave Point drapes over the Precambrian high (monadnock; well 10-21-80-17W5), though it is not common for the Slave Point to be absent, or pinch out again the sides of such highs.

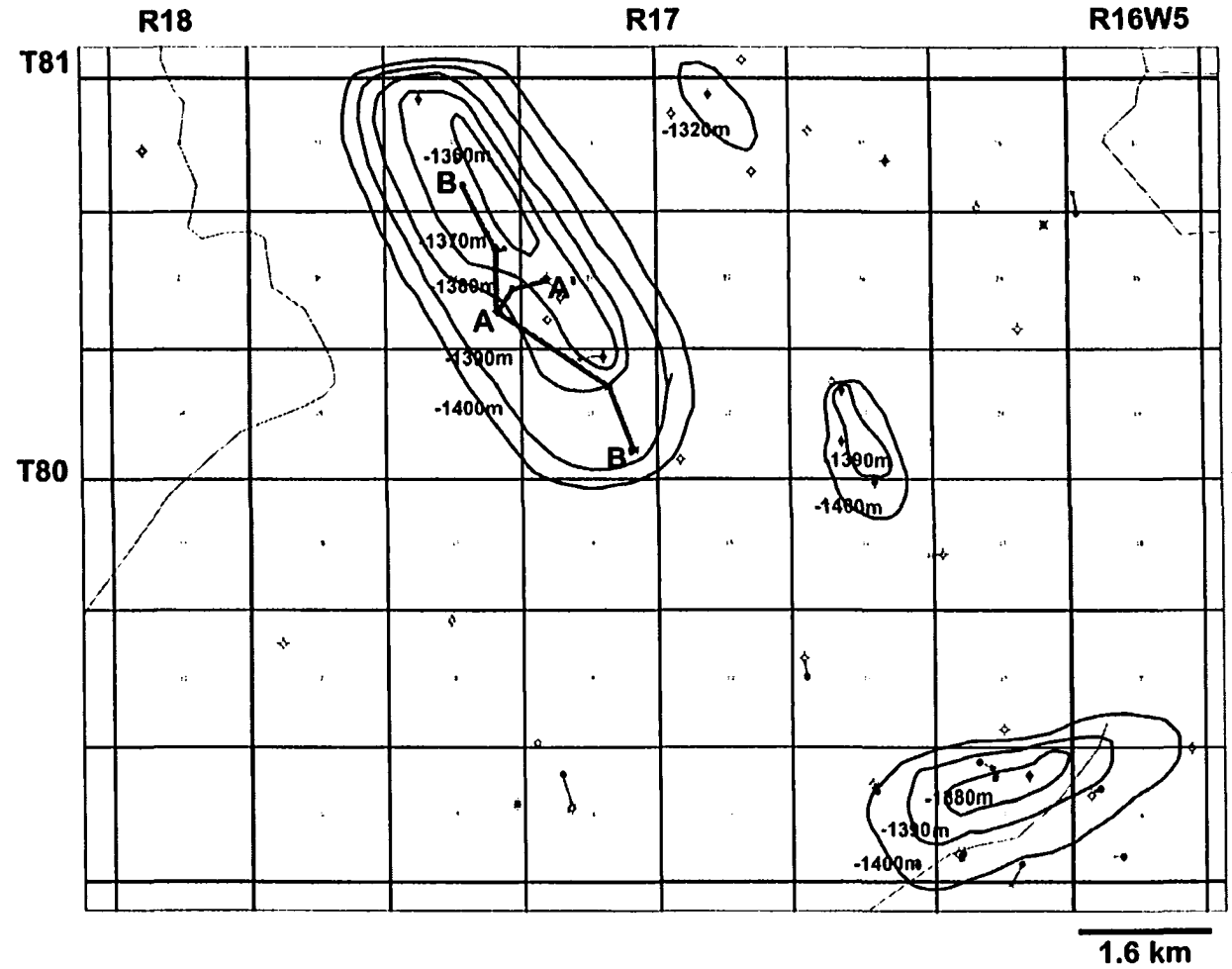

Figure 3.3 Structure map on top of the Slave Point Formation in the northwest corner of the Dawson field and cross section lines; 10 metre contour interval. For cross section A-A' and B-B': see figures 3.4 and 3.5

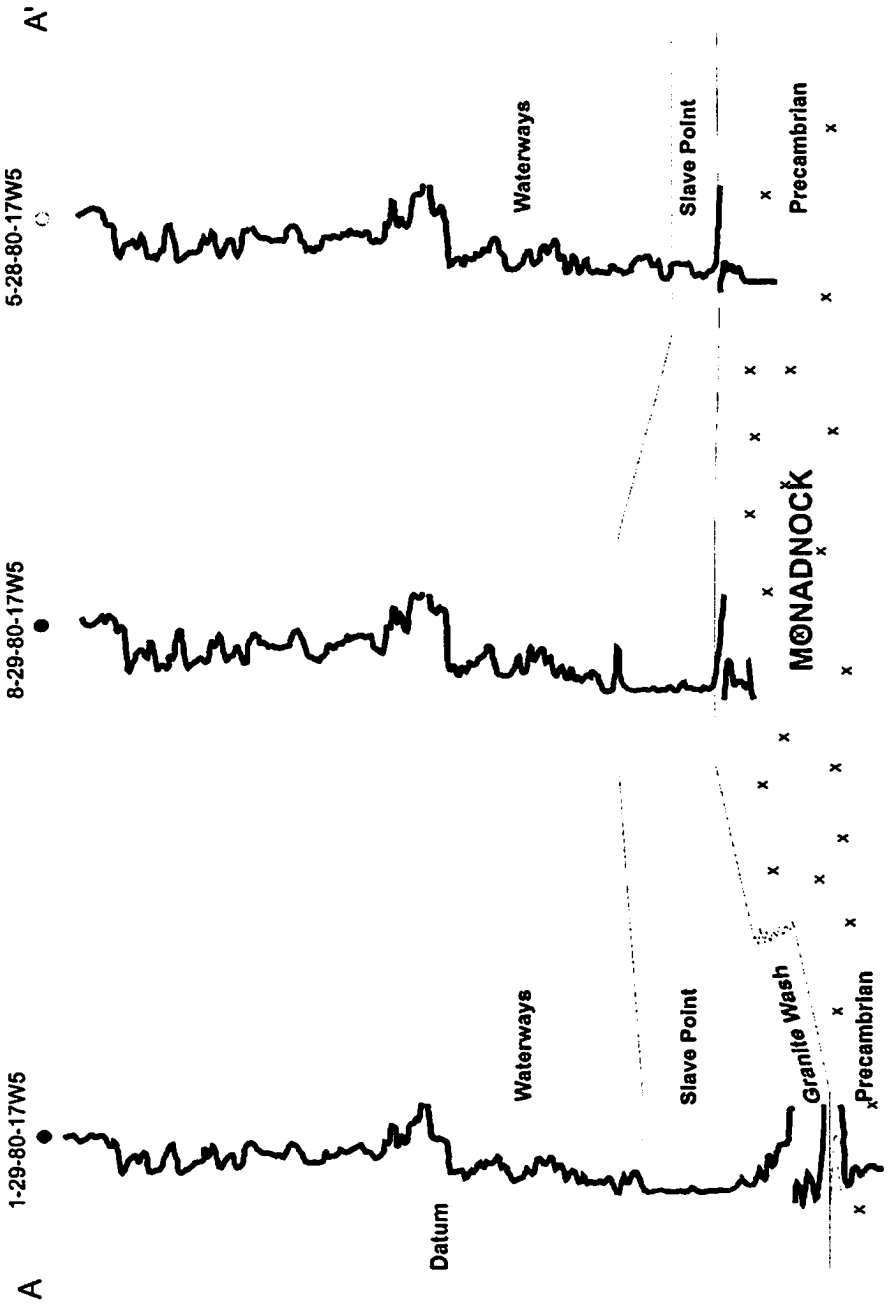

Figure 3.4 Stratigraphic cross section A-A' using gamma ray logs. Note the thinning of the Slave Point on top of the Precambrian basement. Datum is the top of the Calmut member, Waterways Formation. Blue lines trace Slave Point porosity through the wells. Line of cross-section located on Figure 3.3.

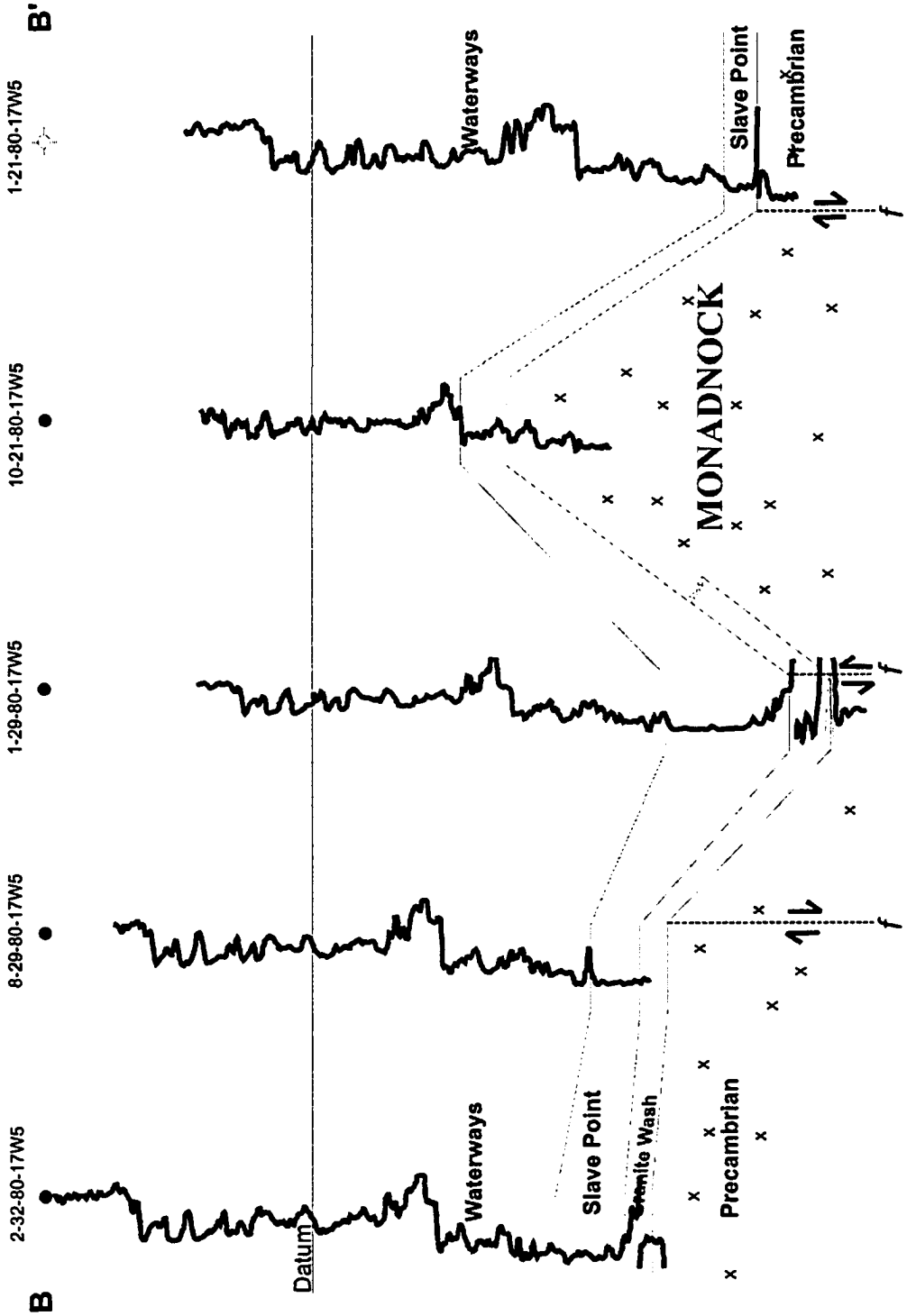

Figure 3.5 Structural cross section B-B'using gamma ray logs. Note the accumulation of Granite Wash clastics at the base of the Precambrian highs, sea level datum, f = fault. Line of cross-section located on Figure 3.3.

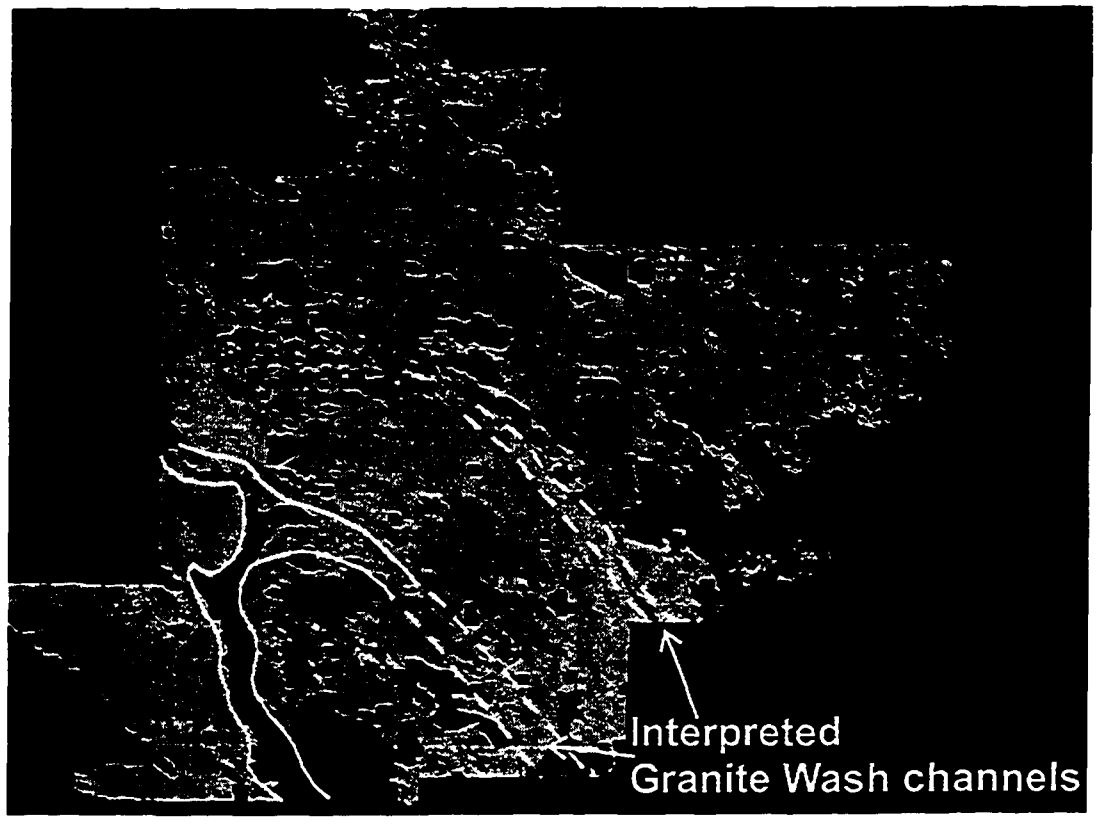

Figure 3.6 Interval geometry isopach map of Dawson area; this figure is a 'time slice' picked on the Granite Wash horizon. The interpreted Granite Wash channels, the deep blue colour on the figure - are outlined in yellow. The outlined area represents areas of thickest Granite Wash deposition and are interpreted to be fluvial channels sourced from the north/north west by the exposed Precambrian Peace River Arch.

3.4.1 Monadnock effect

As already discussed in the more regional overview of the play type, the Slave Point Formation nucleated around structurally controlled monadnocks (Figure 2.4). Where the Slave Point Formation was exposed to relatively strong current and wave action, its matrix is grainy or porous. However, in areas without pervasive and constant wave action, such as behind a barrier such as a monadnock, the matrix is muddier (Plate B/3-4). Generally, the Slave Point is more porous on the eastern sides of monadnocks (windward) compared to the western sides (leeward), which might be a helpful insight when deciding on where to drill.

More specifically, facies IIIb (*Amphipora* floatstone) exhibits both muddy and sandy matrix characteristics. Where this facies is dominated by a mud matrix (Plate B/ 3-4), it was deposited behind a wave barrier allowing mud to settle out of suspension to make up a significant portion of the matrix. Conversely, where facies IIIb exhibits a grainy and porous matrix (Plate B/ 2), it was deposited where wave and current action were much stronger, either on the flank of a monadnock/high, or deposited behind a high but with a connection to the open ocean, allowing for the reworking of sediment and deposition of a grainy matrix. The grain size and composition of the matrix is also important to consider when trying to understand diagenesis/ dolomitization.

3.5 Depositional evolution

The depositional evolution of the Slave Point Formation is schematically illustrated in Figures 3.7 and 3.8. The initial stage (A in Figure 3.7) represents the

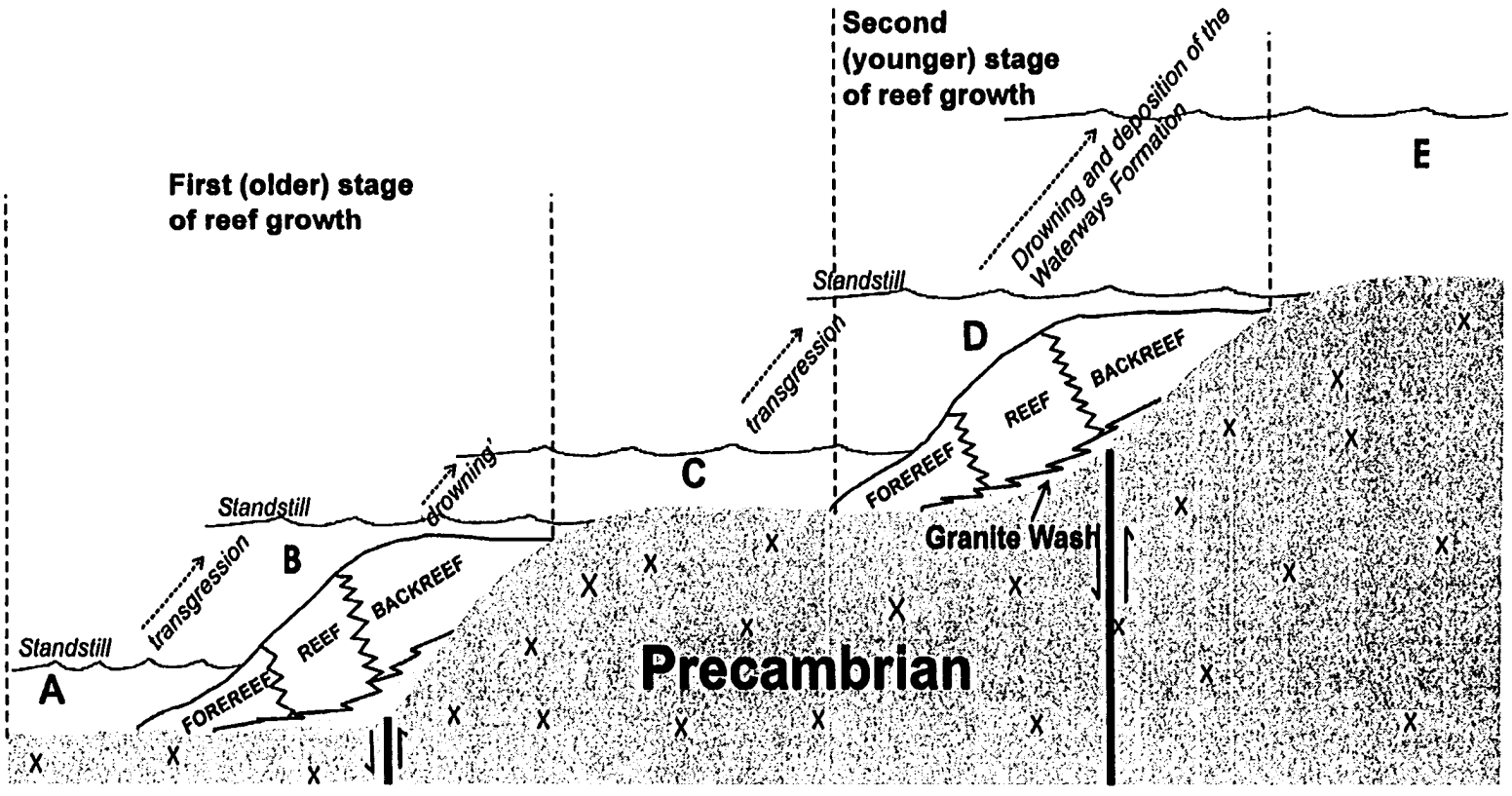

Figure 3.7 Depositional evolution of the Slave Point Formation, northern Alberta. Stage A represents initial deposition of non-reefal, predominately muddy Slave Point sediments. Stage B represent transgression and subsequent standstill of sea level allowing for the deposition of shallow marine carbonates and reef zonation. These shallow marine carbonates were drowned by transgression during Stage C and a subsequent standstill. Stage D is similar to Stage B and represents transgression and standstill allowing once again for the deposition of shallow marine carbonate and reefal zonation. Finally, the Slave Point transgressed to Stage E where the carbonates were drowned and the Waterways Formation was deposited.

Figure 3.8 Depositional model for the Slave Point Formation. 'Backreef' includes facies IVb to Ib; 'Forereef' includes facies IVf and IIIf.

deposition of the non-reefal, predominately muddy Slave Point on the previously uplifted and block faulted Precambrian basement and/or Granite Wash detritus.

A rapid rise in sea level resulted in deposition of facies If/IIf. These muddy sediments act as a platform for shallow water carbonate deposition. *Thamnopora* and other small bulbous stromatoporoids colonized this muddy platform and served as foundations for later reef growth.

After the initial stage of deposition (A), sea level transgressed to stage B (Figure 3.7). At stage B, there is a standstill of the transgressing waters allowing the 'reefal' facies to grow in relatively shallow marine, highly agitated waters along the flanks of the Precambrian highs. A standstill in sea level allowed for development of the zonation of the reef complex. Overall, this stage represents an overall shallowing upward sequence.

After deposition of stage B, sea level rose rapidly again (C) which inhibited the reefal carbonates to keep up with sea level rise (Figure 3.7). At this point, the first stages reef growth (stages A to B, Figure 3.7) were unable to keep up with sea level rise and deposition was terminated. A second phase of deposition occurred, on a higher, shallower portion of the PRA. In other words, there are at least two reef systems of different ages, with the second stage of reef development representing a younger reef development stage than stages A to B (Figure 3.7 and 3.8).

As the Slave Point backstepped onto the exposed Precambrian high, transgression increased sea level to point D (Figure 3.7). Hence, this stage is similar to stage B, in that reefal carbonate deposition and reef zonation now form an overall shallowing upward sequence. Finally, the entire sequence transgressed to stage E (Figure 3.7). At this time no more Slave Point was deposited, however. This may be the result of one of the

following processes, or a combination thereof: (1) the sea level rise was too rapid for reef organisms to keep up (unlikely as the sole reason); (2) increase in terrigenous input, which the environment intolerable for reef organism. Eventually the terrigenous input clearly overwhelmed reef growth, covering the entire paleogeography with the Waterways Formation. This overall transgression, backstepping of the Slave Point, and deposition of the Waterways is consistent with global Middle to Late Devonian sea level (Figure 3.9)

These interpretations, based on facies, stratigraphic, and structural analysis can be generalized to a depositional model (Figure 3.8). This model predicts the distribution of porous Slave Point carbonates around all monadnocks in the area. It also shows that the Slave Point did not colonize on the highest portion of the Precambrian, essentially creating a "bald high". However, in some areas where the relief of the Precambrian was not as pronounced hence, when the Precambrian did not form a distinct monadnock, the Slave Point was deposited right across the low Precambrian high, to be covered later by the Waterways Formation.

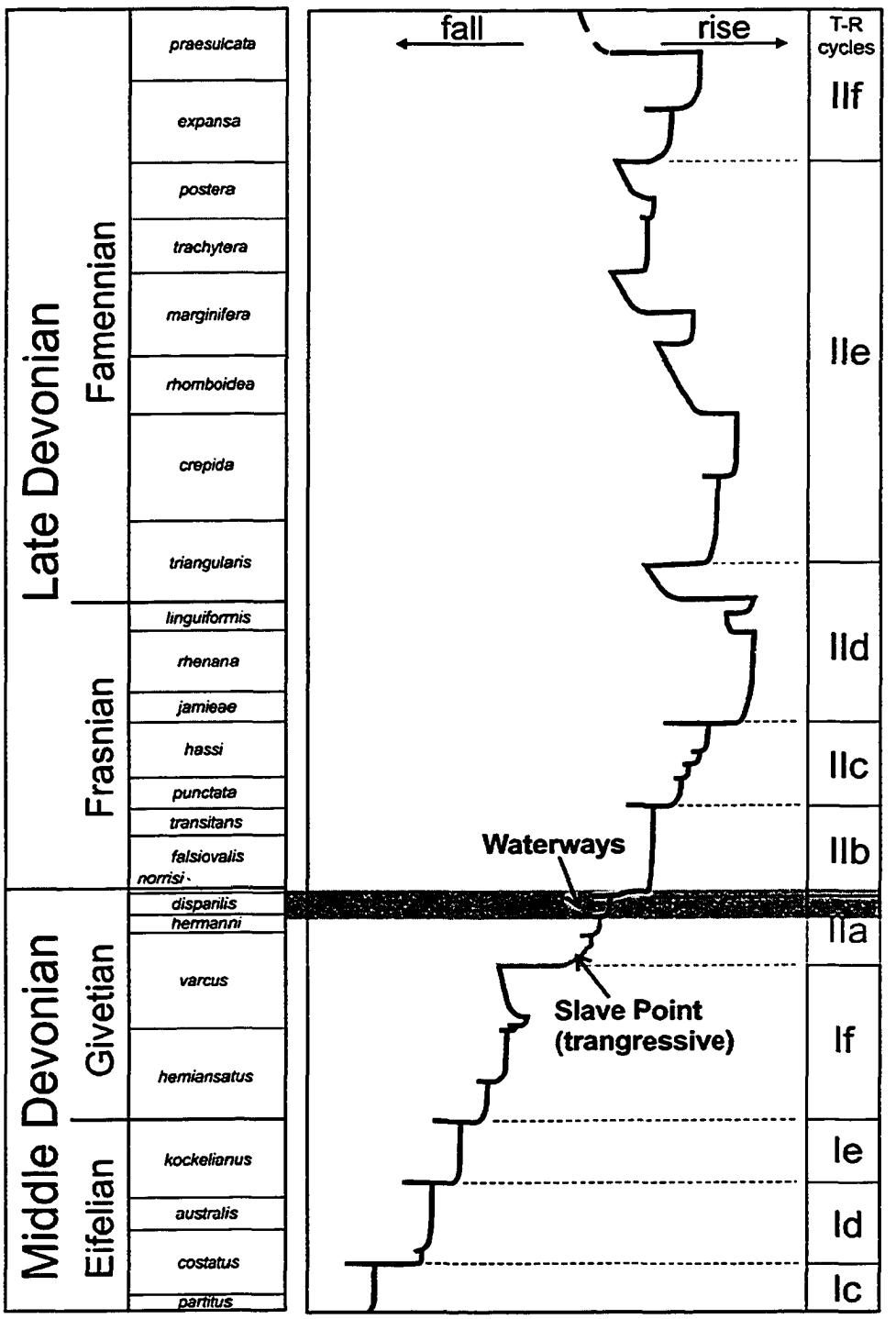

Figure 3.9 Devonian sea level curve (modified from Johnson et al. 1985) showing overall sea level rise throughout Slave Point time (yellow) and increased sea level rise at the end of Slave Point time, defining the Waterways transgression (green). Geologic time scale and conodont zone (modified from Joachimski et al. 2004).

CHAPTER FOUR

4 DIAGENESIS AND PETROGRAPHY

4.1 Introduction

Diagenesis encompasses all the processes that affect sediments after deposition until the realms of incipient metamorphism at elevated temperatures and pressures. After deposition, carbonate sediments are subjected to a variety of distinctive diagenetic processes that bring about changes in porosity, mineralogy, and chemistry. Diagenetic changes may also destroy or modify original depositional textures. Additionally, porosity of carbonate sediments may be either reduced by compaction and cementation or enhanced by dissolution (Boggs, 1992).

Diagenetic settings are commonly divided into 'shallow', 'intermediate', and 'deep' burial (Choquette and James, 1990), yet these terms are ill defined. Machel (1999) combined mineralogic, geochemical (Bustin et al. 1985), and hydrologic (Galloway and Hobday, 1983) criteria from clastics and carbonates, the occurrence of hydrocarbons, and fractures, in a comprehensive classification of diagenetic settings (Figure 4.1). The Machel (1999) classification includes near-surface, shallow-, intermediate-, and deep-burial settings and fractures.

Near-surface diagenetic settings are defined as those within the first few metres of burial, where the pore fluids are surface derived and essentially unaltered meteoric, brackish, marine, or evaporitic (Figure 4.1). Shallow-burial diagenetic settings are similar to the near-surface diagenetic settings, however, differences include added physical

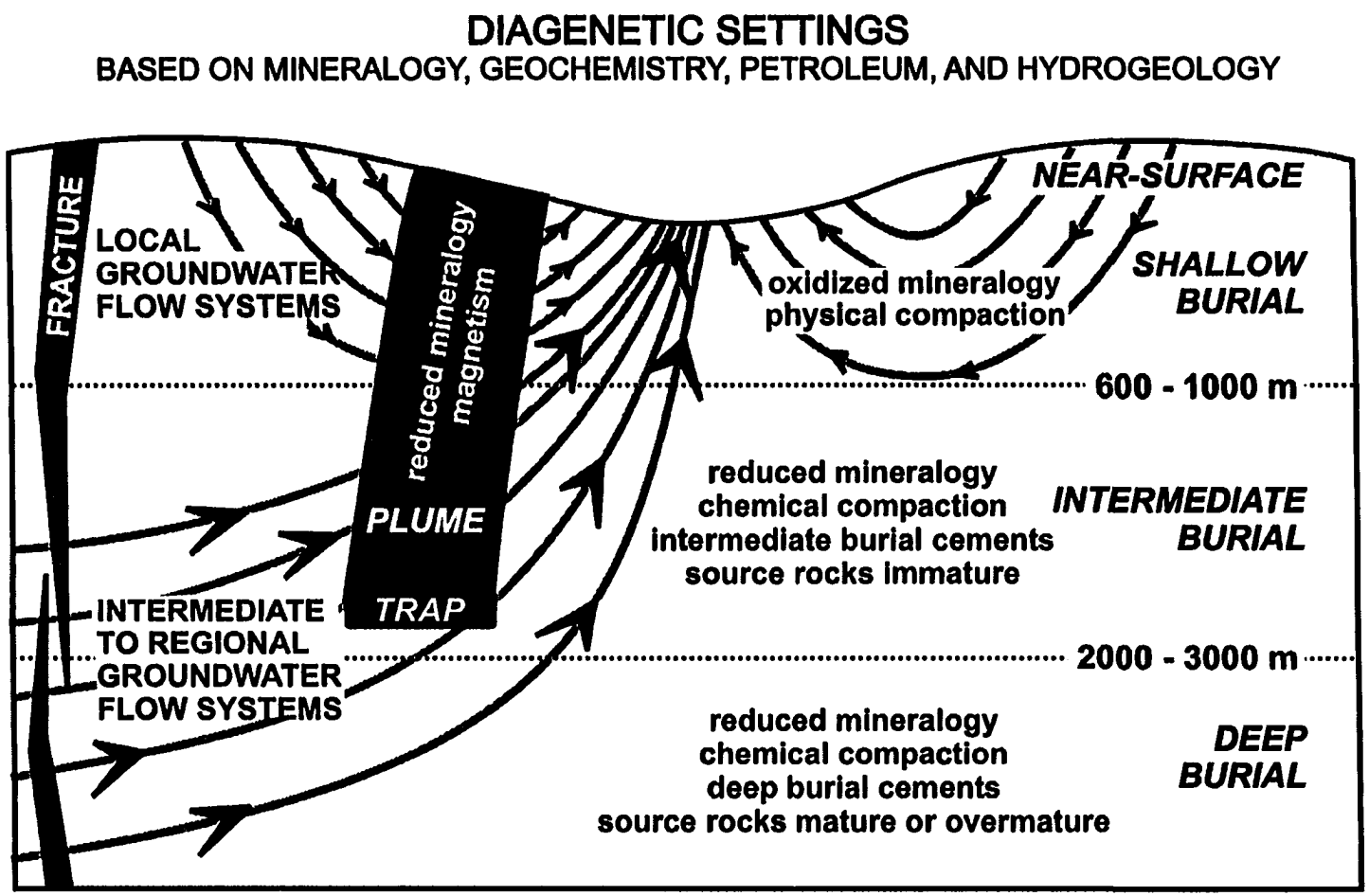

Figure 4.1 Classification of diagenetic settings on the basis of mineralogy, petroleum, hydrogeochemistry, and hydrogeology. Lines represent idealized groundwater flow lines. Depth limits separating the burial diagenetic settings are based on geologic phenomena that are easily recognized. Near-surface settings may be meteoric, brackish, marine, or hypersaline (modified from Machel, 1999).

compaction and hydrologic conditions that may vary from place to place. Common textures generated by physical compaction in carbonates include thinning of laminae; flattened to squashed burrows, and grains; conversion of grain-poor to grain-supported textures and changes from planar to curviplanar grain contacts (Machel, 1999). In carbonates, 300-600m is the interval where chemical compaction (pressure solution) commonly commences with recognizable stylolites developing at depths below 600 m. As a result of stylolite formation, the lower boundary of shallow-burial settings is located at depths of approximately 600-1000 m (Figure 4.1; Machel, 1999). Therefore, where carbonates display evidence of physical compaction but no, or poorly developed stylolites, they are defined to have undergone shallow-burial diagenesis (Machel, 1999).

Intermediate- and deep-burial diagenetic settings are located below shallow burial settings (Figure 4.1). Rocks in this setting experience chemical compaction, subsurface cementation, and dissolution. Pressure solution textures in carbonates are diverse and include stylolites and other types of sutured seams (Machel, 1999). In carbonate rocks of these diagenetic settings, most burial cements are calcite, dolomite, and anhydrite. These burials cements have various characteristics, including: 1) crystals crosscut stylolites and pressure solution seams terminate at cement crystals; 2) crystals occur in fractures that cross-cut near-surface cements and compaction features; 3) crystals have relatively large size; 4) crystals are blocky, form equant mosaics, increase in mean diameter toward pore centers, or are poikilotopic, 5) crystals are not recrystallized; and 6) crystals show well-defined cathodoluminescence zonation from bright towards quenched (dull) luminescence, or they are dull-luminescent throughout, commonly caused by ferroan composition (Machel, 1999). The intermediate burial realm also contains the liquid oil

window.

The lower limit of intermediate-burial diagenetic settings and the upper limit of deep-burial diagenetic settings is defined relative to the top of the liquid oil window in hydrocarbon source rocks (Machel, 1999). In petroleum geology, this depth has been used to define the boundary between "diagenesis" and "catagenesis" (Hunt, 1996). In mineral diagenesis, this boundary is useful because the introduction of oil into pores spaces commonly arrests diagenesis (Machel, 1999). Unfortunately, the depth to the top of the oil window varies widely, depending on kerogen type and geothermal history, with a distribution maximum of about 2000-3000 metres (Hunt, 1996). Therefore, this depth interval is taken as the bottom of the intermediate-burial diagenetic settings.

Deep-burial diagenetic settings merge into the metamorphic realm at temperatures around 200^{0}C and commensurate depths and pressure that depend on the geothermal gradient (Machel, 1999). Most sedimentary rocks spend most of their existence in the intermediate- and deep-burial realms, where porosity and permeability are often altered significantly, and where hydrocarbon maturation, migration, and most trapping occurs (Machel, 1999).

Patterns of diagenesis may change greatly from one carbonate sequence to another, and often there are frequent variations both laterally and vertically within one carbonate sequence. Major controls on diagenesis are the composition and mineralogy of the original sediment, the pore-fluid chemistry and flow rates, geological history of the sediment, influx of different pore-fluids, and prevailing climate (Tucker and Wright, 1990). Studies of carbonate diagenesis often involve identifying the original mineralogy of various cements, their significance in terms of pore-fluid chemistry and the relative

timing of precipitation and recrystallization (Tucker and Wright, 1990). Descriptions of diagenetic modifications in this study are based mainly on hand specimen examination and thin sections.

The Slave Point Formation carbonates at Dawson have undergone a complex diagenetic history from early marine diagenesis to deep burial environments, with distinct and varying fluid compositions. A complete description summarizing the paragenetic sequence of events at Dawson is presented in section 4.7. Dolomitization is extensive and significant at Dawson, therefore, it will be discussed in a separate section of this chapter

4.2 Diagenetic Processes at Dawson

4.2.1 Biogenic Alteration/Micritization

Micritization is a process whereby bioclasts are altered while on the seafloor or just below, by many kinds of microorganisms, such as fungi, bacteria, and algae, by the boring, burrowing, or sediment-ingesting activities of these organisms (Tucker and Wright, 1990; Boggs, 1992). Fine-grained (micritic) aragonite or high-magnesian calcite may then precipitate into these borings. Boring and micrite-precipitation may be so intense that carbonate grains are converted completely to micrite. If boring is less intensive, a thin micrite rim or envelope may be produced around the grains (Boggs, 1992).

At Dawson, micritization of the Slave Point Formation is pervasive in facies that are rich in macroskeletal material such as stromatoporoids, crinoids, brachiopods, and other shell fragments. Micrite envelopes commonly rim stromatoporoid and other fossil fragments (Plate H/1). Additionally, larger borings are common among stromatoporoid

PLATE H

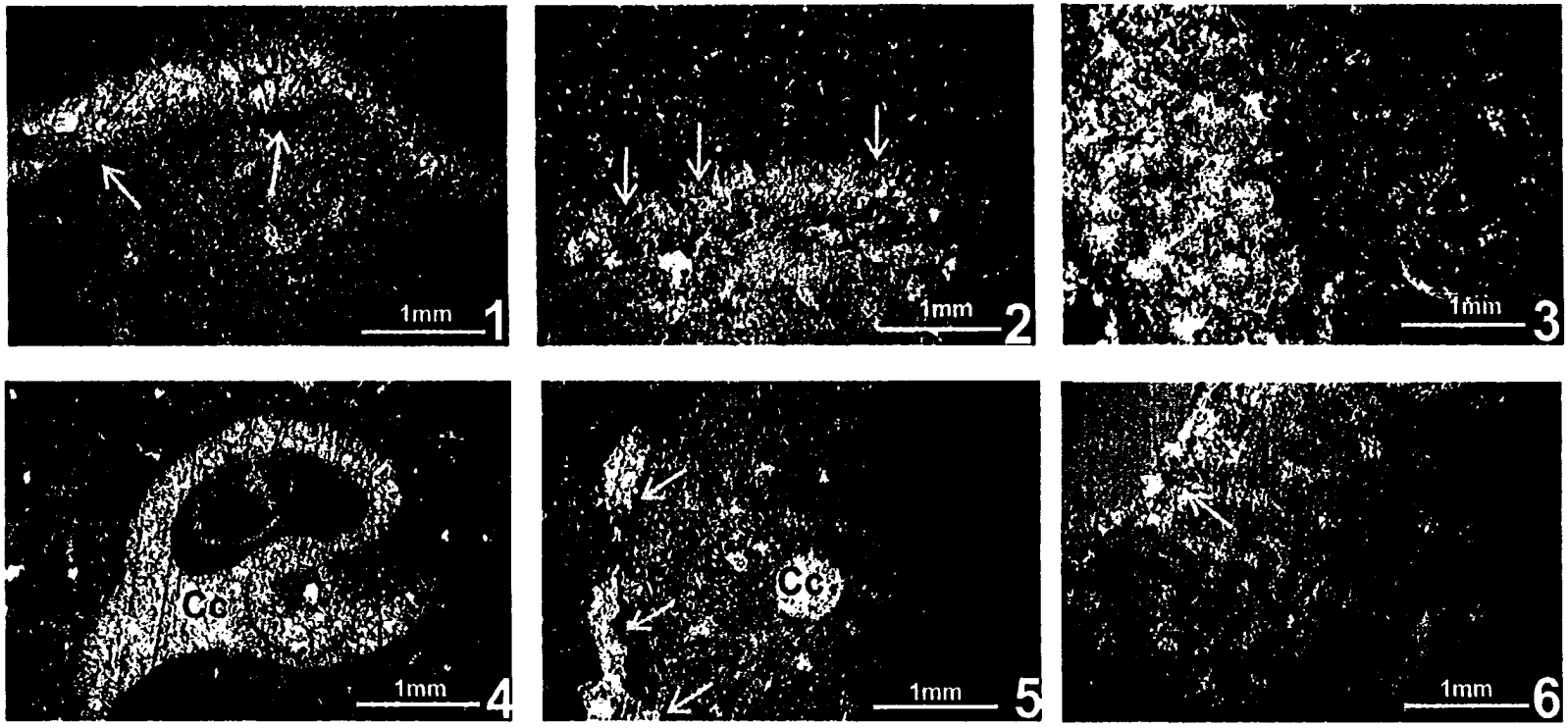

1) Photomicrograph of dark micrite envelope (arrows) developed around a stromatoporoid. 5-18-79-16W5, 1979.1 metres. 2) Borings (arrows) into stromatoporoid fragment, filled with micrite indicating that micritization occurred after the organism was bored. 8-36-80-16W5, 2022.4 metres. 3) Fossiliferous wackestone matrix; note early marine cement (arrow) filling primary porosity in stromatoporoid fragment. 9-24-80-16W5, 1995.8 metres. 4) Photomicrograph of calcite spar (Cc) filling void left by dissolution of gastropod. 8-36-80-16W5, 2021.5 metres. 5) Micrite envelope developed around stromatoporoid (arrows); note preservation of original fossils structure and intrakeletal porosity filled with calcite cement (Cc). 5-19-79-16W5, 1979.1 metres. 6) Primary porosity in stromatoporoid; note early-diagenetic cements filling intraskeletal pores (arrow). 5-19-79-16W5, 1980.7 metres.

fragments and are filled with micrite, indicating that micritization occurred after these organisms were bored (Plate H/2). Micrite is also common at Dawson as matrix (plate H/3).

4.2.2 Dissolution

Lime mud or lithified limestones may undergo dissolution of unstable mineralogy (i.e., aragonite or high-magnesian calcite) favoured by cool temperatures, and/or relatively low-pH pore waters. Though dissolution is relatively unimportant on the seafloor, it is prevalent in the meteoric realm where chemically aggressive waters percolate through the vadose zone into the phreatic zone (Tucker and Wright, 1990). Extensive dissolution of aragonite and high-magnesian calcite takes place in such environments, often concentrated along the water table, which accounts for the presence of many caves in carbonate rocks at the level of the water table. Dissolution, however, is not as intense or rare in the deep-burial/subsurface realm for two reasons: 1) aragonite and high-Mg calcite are commonly converted to more stable low-Mg calcite in the meteoric realm; and, 2) increasing temperature at depth decreases the solubility of all carbonate minerals (Boggs, 1992; Tucker and Wright, 1990).

At Dawson, the Slave Point Formation has undergone both early-digenetic (shallow) and late-diagenetic (deeper burial) dissolution. Late-diagenetic calcite spar fills voids left by the dissolution of fossils originally composed of aragonite and high-Mg calcite, i.e., mainly stromatoporoids, mollusks, and gastropods (Plate H/4). Where a micritic envelope had developed around some grains, the original structure of a fossil is preserved, whereby the interior of the shell may be open or filled with calcite cement

(Plate H/5 and 6). Some fossils, most notably crinoids, have not been affected by dissolution, reflecting their stable primary mineralogy.

4.2.3 Compaction

During burial overburden pressures increase, which leads to a reduction in sediment thickness and the development of compactional textures. Compaction processes are classified as either mechanical (physical) or chemical (pressure-solution) (Choquette and James, 1987), and distinctions between them are made on the basis of features that each produce.

Mechanical compaction occurs when loose or poorly lithified carbonate sediments are buried. Grain fracture, reduction in porosity and permeability, dewatering, fracturing, re-orientation, and breakage of allochems takes place (Tucker and Wright, 1990). Mechanical compaction affects sediments at shallow depths, i.e., with a few tens to hundreds of metres. Choquette and James (1987) noted that particle re-orientation and sediment dewatering begin at depths of about 1 metre below the sediment-water interface.

At Dawson, there is only minor evidence for mechanical compaction in the Slave Point Formation, commonly in facies with a mud-supported matrix. Indicators of mechanical compaction at Dawson are fossils re-oriented from their original depositional positions to horizontal and rotated geopetal indicators away from their original stratigraphic top (Plate I/1).

Chemical compaction develops under increasing pressures during and after lithification, such as in intermediate to deep burial environments, where grains begin to

PLATE I

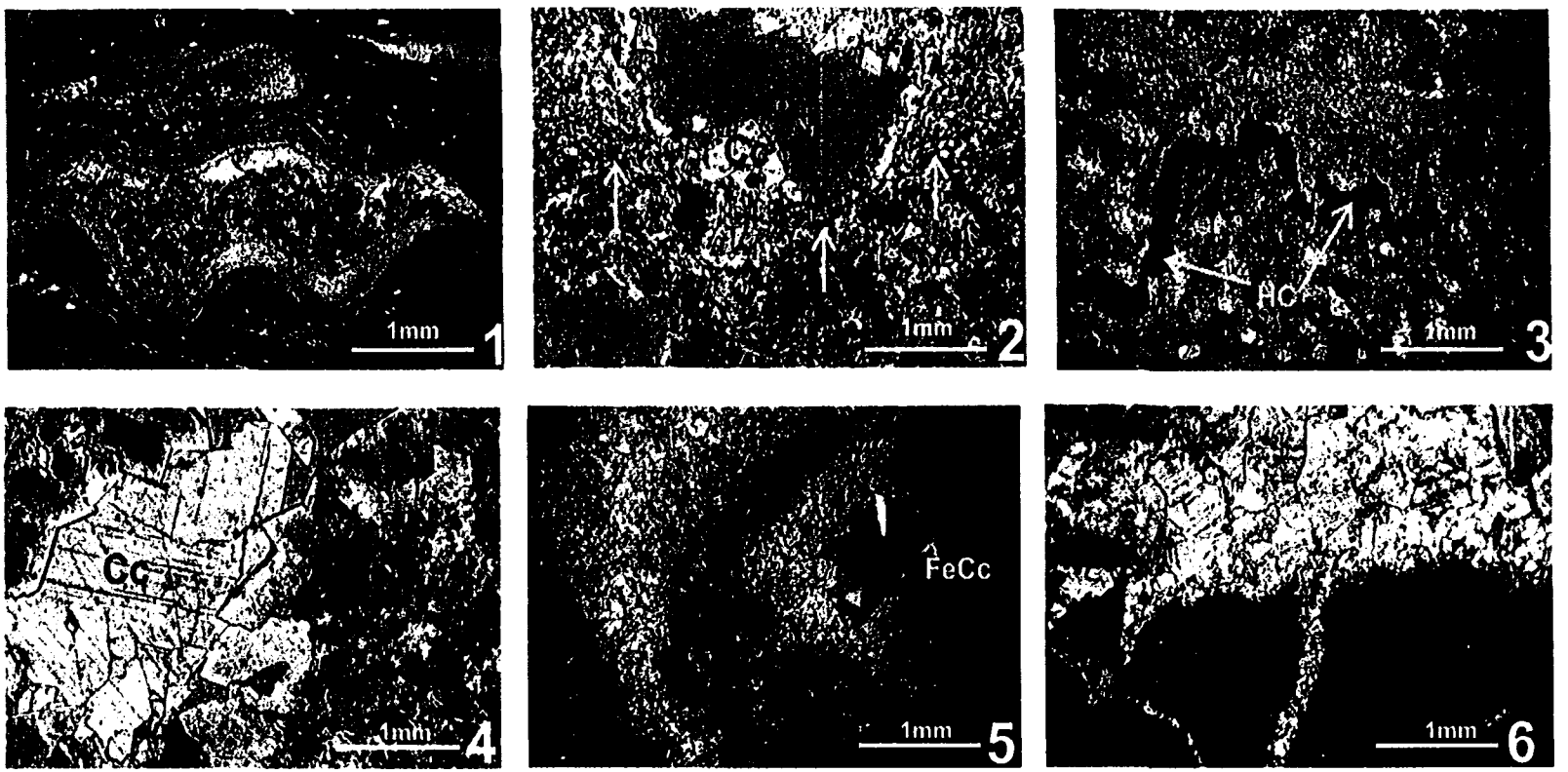

1) Photomicrograph of brachiopod geopetal; note intenal mud sediment overlain by calcite cement (Cc), indicating stratigraphic top is to the top of the picture. 12-18-79-16W5, 2127.9 metres. 2) Clay filled stylolite (yellow arrow) surrounding open pore space. 11-34-79-16W5, 2093.9 metres. 3) High amplitude stylolite cutting across stromatoporoid fragment; hydrocarbons (HC) "filling" the stylolite. 5-23-80-16W5, 6849.5 feet. 4) Relatively late-diagenetic calcite cement (Cc) filling void. 8-25-79-16W5, 2044.5 metres 5) Calcite dogtooth spar filling void space; note iron-rich spar (FeCc). 5-19-79-16W5, 1979.1 metres. 6) Late-stage cementing filling dissolved shell fragment; note cement 'feeder' system (*f*). 9-24-80-16W5, 1995.8 metres.

dissolve at point contacts to produce sutured and concavo-convex contacts (Tucker and Wright, 1990). Chemical compaction generates predominately stylolites and non-sutured dissolution seams. Stylolites are irregular, commonly discontinuous surfaces that cut limestones and have a cross section resembling the trace of a stylus on a chart recorder (Wanless, 1981). Dissolution seams are smooth, anastomosing seams of fine, relatively insoluble, particles (clays, micas, organic matter, and sulphides) that deflect around and between grains (Wanless, 1981; Tucker and Wright, 1990). Pressure solution is a continuous burial process (Qing and Mountjoy, 1994), however, it may begin to develop at depth of as little as 300 metres in limestones, but more commonly at depths greater than 600 to 900 metres (Lind, 1993). Pressure solution causes a significant loss of porosity (up to 30% of original pore volume) and thinning of beds (Boggs, 1992).

At Dawson, stylolites and dissolution seams are common in all facies of the Slave Point Formation. Furthermore, stylolites are ubiquitous in facies that have been pervasively dolomitized. Stylolitization occurred before late calcite cementation (Plate I/2). Stylolites are commonly filled with relatively insoluble clay residue, organic matter, and hydrocarbons, and range in amplitude from a few millimetres to a few centimetres (Plate I/3).

4.2.4 Cementation

Cements precipitate in carbonate sediments when pore-fluids are supersaturated with respect to the cement phase (e.g., calcite, dolomite etc.) and when there are no kinetic factors inhibiting precipitation (Tucker and Wright, 1990). Cementation can be an important process in deep burial regimes, however, the conditions that control

cementation at depth are poorly understood. Factors that have been cited to be involved in carbonate cementation at depth include: 1) unstable mineralogy (i.e., the presence of aragonite and/or high-magnesian calcite), 2) pore waters highly over saturated with respect to calcium carbonate, 3) high porosity and permeability, 4) increase in temperature and, 5) decrease in carbon dioxide partial pressure (Boggs, 1992). Extensive cementation of limestones with carbonate cements requires an efficient fluid flow mechanism because of the relatively low solubility of the carbonate minerals. The source of $CaCO_3$ varies with the diagenetic environment: in the marine realm it is seawater; in the meteoric and burial environments it is mostly dissolution of metastable $CaCO_3$ from the sediment itself (Tucker and Wright, 1990).

At Dawson, calcite cementation spans the entire diagenetic history of the Slave Point Formation. Early marine calcite cements commonly occlude primary porosity in stromatoporoids (Plate H/3), whereas late-stage calcite cement fills voids and fractures that had formed after burial dissolution (Plate I/4 to 6).

4.2.5 Recrystallization

Recrystallization is a common process in carbonates. Grains and skeletal material tends to dissolve and reprecipitate with time and burial, thereby changing the textures and chemical compositions of the original sedimentary constituents.

The term recrystallization has been problematic in carbonate research. The term 'neomorphism' was originally introduced by Folk (1965) as a substitute term for 'recrystallization' in limestones. However, very few dolomite researchers use the term 'neomorphism' even though it is well and strictly defined (Machel, 1997). Folk (1965)

defined neomorphism to embrace the following processes where gross composition remains constant: 1) inversion (aragonite to calcite, i.e., change from one carbonate polymorph to another), recrystallization (calcite to calcite), and strain-recrystallization (strained calcite to unstrained calcite). Gregg and Sibley (1984) and Sibley and Gregg (1987) applied the term neomorhpism also to dolomites "to include the transformation of poorly ordered and/or non-stoichiometric dolomite to ordered and stoichiometric dolomite". They did not use the term recrystallization for this process because they considered the transformation to be a change in mineralogy.

Machel (1997) combined the previous definitions of neomorphism and recrystallization with conventions that are engrained in sedimentary, igneous, and metamorphic petrology, and with the properties that are known to change via recrystallization and can be measured. Machel (1997) recommended abandonment of the term neomorphism and redefined the term recrystallization to encompass the following:

1) textural changes, i.e., increases in crystal size via Ostwald ripening, and changes in crystal shapes, such as from non-planar to planar;
2) structural changes, i.e., changes in ordering and in strain;
3) compositional changes, i.e., changes in stoichiometry, trace elements, changes in isotopic composition, changes in fluid inclusion properties;
4) changes in the paleomagnetic properties.

Additionally, Machel (1997) introduced the term 'significant recrystallization'. This is a modification via recrystallization of the original texture, ordering, chemical composition, or magnetic properties that is larger then the original range during mineral formation. Significant recrystallization is recognized if recrystallization modified at least

one of the above listed properties to a range larger than the original (Figure 4.2a).

Conversely, any carbonate, limestones or dolostones, whose changes via recrystallization in texture, structure, composition, and/or paleomagnetic properties are so small that the total data range after recrystallization is a large as when the carbonate first formed, is defined as 'insignificant recrystallization' (Figure 4.2b; Machel, 1997).

4.3 Dolomitization

Dolomitization is a diagenetic process whereby sediments or limestones consisting of aragonite and/or calcite are replaced by dolomite. Dolomitization is important for the development of hydrocarbon reservoirs because it can retain, enhance (common), or destroy (rare) porosity and permeability (Machel, 1990). Dolomite formation is governed by thermodynamic and kinetic constraints, which can interact with, and to an extent, counteract each other, and commonly takes place via heterogeneous nucleation on a $CaCO_3$ substrate (Sibley and Gregg, 1987).

Chemically, dolomitization is favoured by the following constraints: 1) low Ca^{2+}/Mg^{2+} ratios, 2) low Ca^{2+}/CO_3^{2-} ratios, 3) high temperature; and, 4) salinity above saturation with respect to dolomite (Machel and Mountjoy, 1986). Based on these constraints, Machel and Mountjoy (1986) suggested the following natural environments as being chemically conducive to dolomite formation, noting that this alone does not imply that large amounts of dolomite are necessarily formed:

1) environments with any salinity above dolomite saturation, including fresh water/sea water mixing-zones and normal marine to hypersaline subtidal environments;

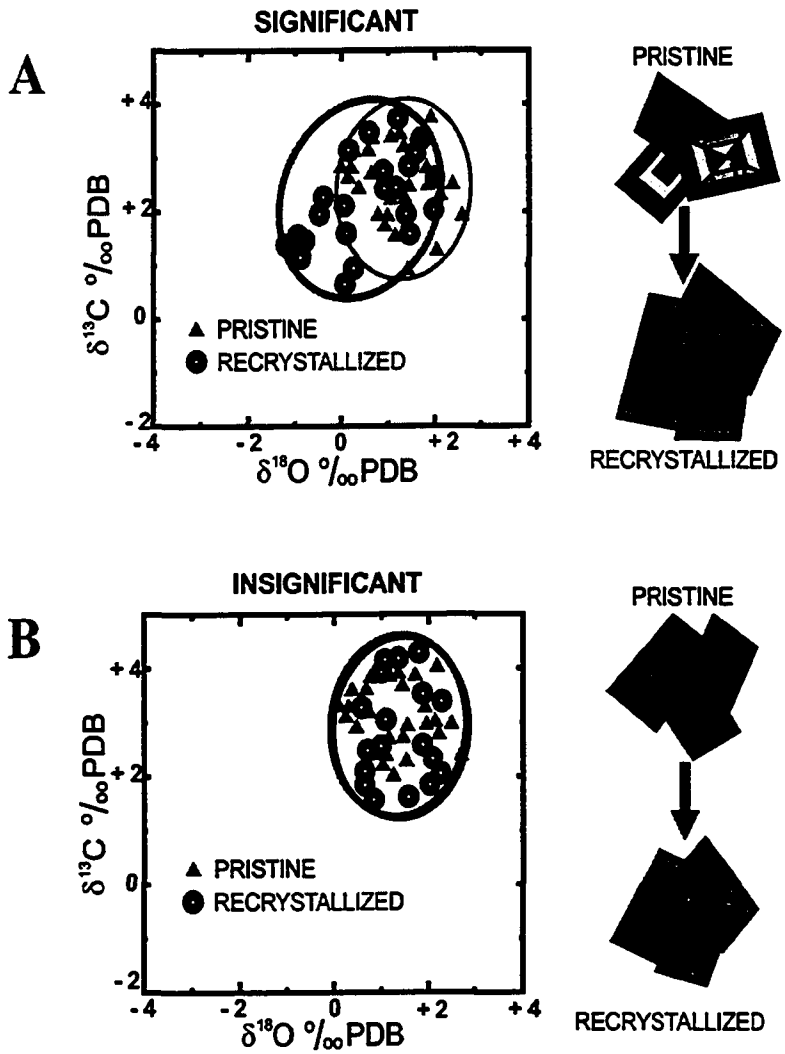

Figure 4.2 A) Schematic illustration of significant recrystallization. For the properties shown, i.e., $\delta^{13}C$ and $\delta^{18}O$ values, crystal sizes and luminescence,the pristine and recrystallized samples are different. At least some isotope values of the recrystallized samples fall outside the range of the pristine sample. The crystals have increased in size and lost their zoning. However, not at all these properties have to change during significant recrystallization. B) Schematic illustration of insignificant recrystallization. For the properties shown, i.e.,$\delta^{13}C$ and $\delta^{18}O$ values, crystal size and luminescence, the pristine and recrystallized are identical (modified from Machel, 1997).

2) alkaline environments, for example, those under the influence of bacterial reduction and/or fermentation process;

3) subsurface environments with temperatures greater than about 50^0C.

Dolomitization is the most significant diagenetic process that affected the Slave Point Formation at Dawson. Regionally, dolomitization of the Slave Point Formation around the PRA has resulted in a "halo" of dolostones that extends about 38 kilometres from the zero edge of the Slave Point Formation to the north and east of the Arch (Craig, 1987). The best oil producing fields are located within this dolomite "halo", including Dawson, Golden, Seal, and Slave (Figure 1.4). In the Dawson field proper, the majority of reservoir porosity is in the dolostones. Therefore, understanding the paragenesis, genetic mechanisms, types, and distribution of dolomite is essential for successful exploration for hydrocarbons.

Two main textural types of dolomite have been identified petrographically at Dawson: 1) matrix dolomite, and 2) saddle dolomite. Textural classification follows Sibley and Gregg's (1987) classification of dolomites.

4.3.1 Matrix Dolomite

Matrix dolomite is the fine-grained (up to 0.5 mm) replacement phase of the original limestone matrix. Matrix dolomite is volumetrically important, accounting up to 70% of the total rock volume at Dawson. Based on petrographic evidence, matrix dolomite is an intermediate burial diagenetic product and formed prior to chemical

compaction. This is evidenced by dissolution seams that are deflected around individual crystals of matrix dolomite, and matrix dolomite crystals are truncated by stylolites (Plate I/5). Matrix dolomites generally range from non-planar-a to planar-e (Plate J/1 and 2). An average of 5-10% of the replacive dolomites display small crystal overgrowths/zoning with a cloudy core and clear rim (Plate J/3; see Sibley, 1990; Budd, 1997; Machel, 2004). The implication of this texture is discussed later.

4.3.2 Saddle Dolomite

Saddle dolomite is characterized by non-planar, coarse-grained, curved crystals, and displays sweeping extinction in cross polarized light. Saddle dolomite commonly precipitates in open pore spaces at temperatures ranging from $80^0C - 150^0C$ at least three ways: 1) from advection, 2) from local redistribution of older dolomite during stylolitization; and, 3) as a by-product of thermochemical sulphate reduction (TSR) in a closed system (Radke and Mathis, 1980; Machel, 1987; Machel and Lonnee, 2002). Davies (2002) concluded that hydrothermal fluids are solely responsible for the precipitation of saddle dolomite. This notion, however, is incorrect: while saddle dolomite formed from rapidly ascending fluids in fracture systems may be hydrothermal, saddle dolomite formed via local redistribution during stylolitization is geothermal, forming in equilibrium with the surrounding strata (Machel and Lonnee, 2002), and saddle dolomite formed as a by-product of TSR commonly is hydrofrigid.

At Dawson, saddle dolomite is volumetrically unimportant and comprises less than 1% of the total rock volume. Saddle dolomite occurs primarily as a fracture or vug-filling cement (Plate J/4). Petrographically, a distinct boundary can be seen between

PLATE J

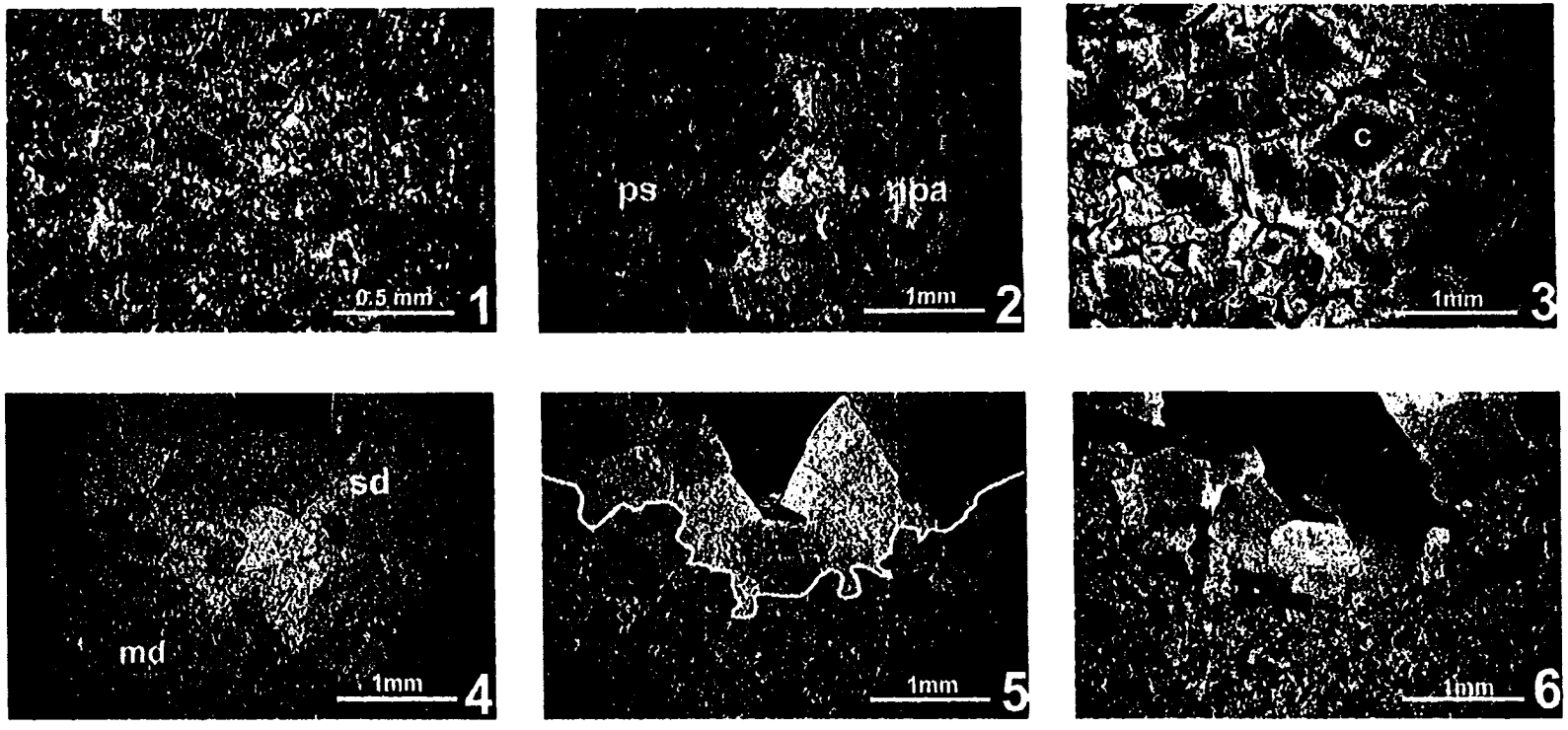

1) Photomicrograph of planar-c dolomite; disseminated pyrite scattered throughout (black). 16-25-79-16W5, 2060 metres. 2) Contact between planar-s (ps) and non-planar-a (npa) matrix dolomite. 1-21-80-71W5, 2121.8 metres. 3) Zoned matrix dolomite crystals; note cloudy core (c) and clear rim (r). 15-15-80-16W5, 2082.4 metres. 4) Saddle dolomite (sd) filling void (blue epoxy); note coarse-crystal size and curved faces of saddle dolomite. 16-25-79-16W5, 2060 metres. 5) Contact between saddle dolomite (sd) and matrix dolomite (md) outlined in yellow; note stylolite (red arrows) cross-cutting the matrix dolomite but not saddle dolomite, suggesting matrix dolomite formation before stylolitization and saddle dolomite formation after stylolitization. Also, the irregular (yellow) interface between the two dolomite types suggest a phase of dissolution of matrix dolomite before the saddle dolomite formed. 4-35-79-16W5, 2091.2 metres. 6) Cross polarized light photomicrograph of (5); note the sweeping extinction of saddle dolomite, and the distinct contact between saddle and matrix dolomite 4-35-79-16W5, 2091.2 metres.

saddle dolomite and the associated matrix dolomite (Plate J/4 and 5), suggesting these phases were likely precipitated from different diagenetic fluids. Saddle dolomite formed relatively late in the sequence, as it is not cut by stylolites and is commonly the last void filling cement (Plate J/5).

Figure 4.3 illustrates the relationship between depositional channels of Granite Wash and areas of dolomitization in the Slave Point. Importantly, areas at Dawson, which have no underlying Granite Wash are not affected by dolomitization. Thus, fluid flow through the Granite Wash was responsible for dolomitization of the Slave Point at Dawson (for further discussion see Chapter 6).

4.4 Evaporite minerals

Anhydrite and/or gypsum exhibiting massive and bladed habits occur as minor vug filling minerals in primary pores of the Slave Point Formation at Dawson. These minerals were precipitated relatively late in the diagenetic history of Dawson. They are commonly found in association with sulphide minerals (Plate K/1).

4.5 Porosity

Diagenetic processes largely controlled porosity development in the Slave Point Formation at Dawson, although, sedimentology and facies were also significant factors. In particular, lithofacies types with a primarily highly porous and permeable matrix were more affected by late diagenetic processes, particularly fluid flow causing dolomitization, than those with a more muddy and much less permeable matrix.

Figure 4.3 Schematic diagram of relationship between dolomitization (pink) and Granite Wash channeling (yellow)at Dawson drawn using the seismic information that is the base for Figure 3.6. The blue area represents an area at Dawson which was not dolomitized and is not associated with a Granite Wash channel.

PLATE K

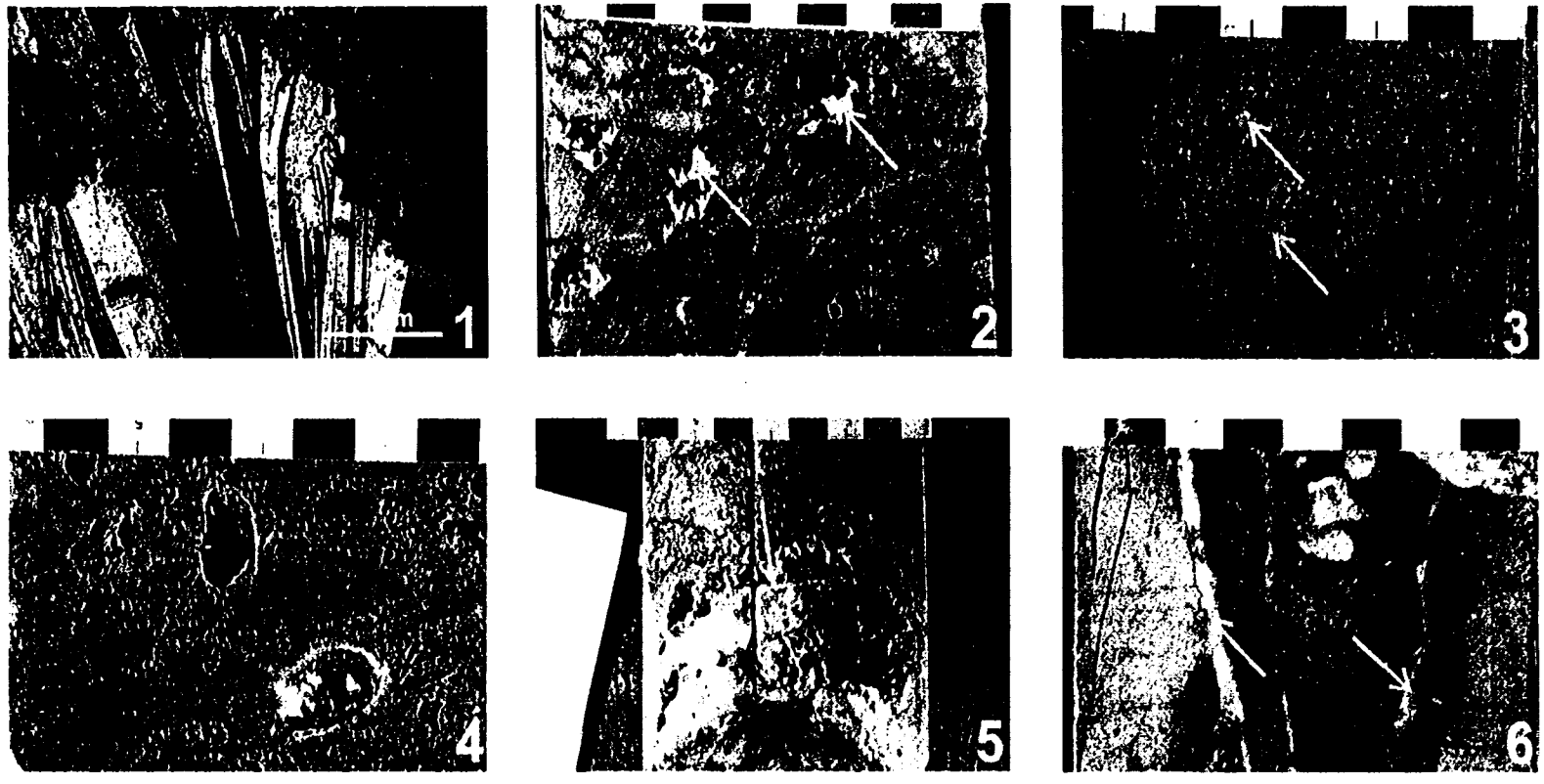

1) Photomicrograph of anhydrite cement filling void; note pyrite (black) rimming void. 4-13-80-16W5, 2042 metres. 2) Core photograph of saddle dolomite cement (white; yellow arrows) filling interparticle pores between fossils constituents. 4-13-80-16W5, 2048 metres. 3) Core photograph of stromatoporoid with intraparticle porosity partially filled with calcite cement (yellow arrows). 4-35-79-16W5, 2081.1 metres. 4) Vuggy and moldic porosity development; vugs range in size from <0.5mm to 1cm. 4-36-79-16W5, 2053.1 metres. 5) Large vug partially filled with late-diagenetic calcite cement (arrow). 1-29-80-17W5, 2020 metres. 6) Fractures filled with calcite cement (arrows). 12-18-79-16W5, 2141.8 metres. Core photograph scale divisions are in centimetres at stratigraphic tops.

Generally, primary porosities in carbonate sediments range from 44 to 75% (Moore, 1989). Primary porosities at Dawson likely were in the same range. Mechanical compaction significantly reduced primary interparticle porosity, especially in mud-supported facies during shallow burial. Shinn and Robin (1983) artificially compacted modern carbonate sediments to about 50% of their original porosity at pressures equivalent to a mere 300 metres of burial. Therefore, during progressive burial of Dawson Slave Point carbonates, most interparticle porosity probably was reduced or lost from mud-supported facies at shallow burial.

Porosities of oil-producing facies at Dawson range from 7-10%, paired with permeabilities ranging from about 50 to 200 millidarcies (mD); these values were derived from well log analysis and core analysis. Porosity in dolomitized facies is extensive at Dawson (>95% of all wells) and displays a good interconnection of biomoldic and intercrystalline pores (Figure 4.4). In contrast, where oil is produced from limestones reservoirs, oil production is from inter- and intra-particle pores. Limestone reservoir make up only a small fraction of all wells (Figure 4.4), as further discussed in Chapter 6.

4.5.1 Primary porosity

Moore (1989) defined primary porosity as any porosity present in a sediment or rock at the end of depositional processes. Interparticle, intraparticle, and fenestral porosity are the common types of fabric selective, primary porosity.

At Dawson, inter- and intra-particle porosity are most common. However, most primary pores are either partially or completely filled by early-diagenetic calcite dogtooth

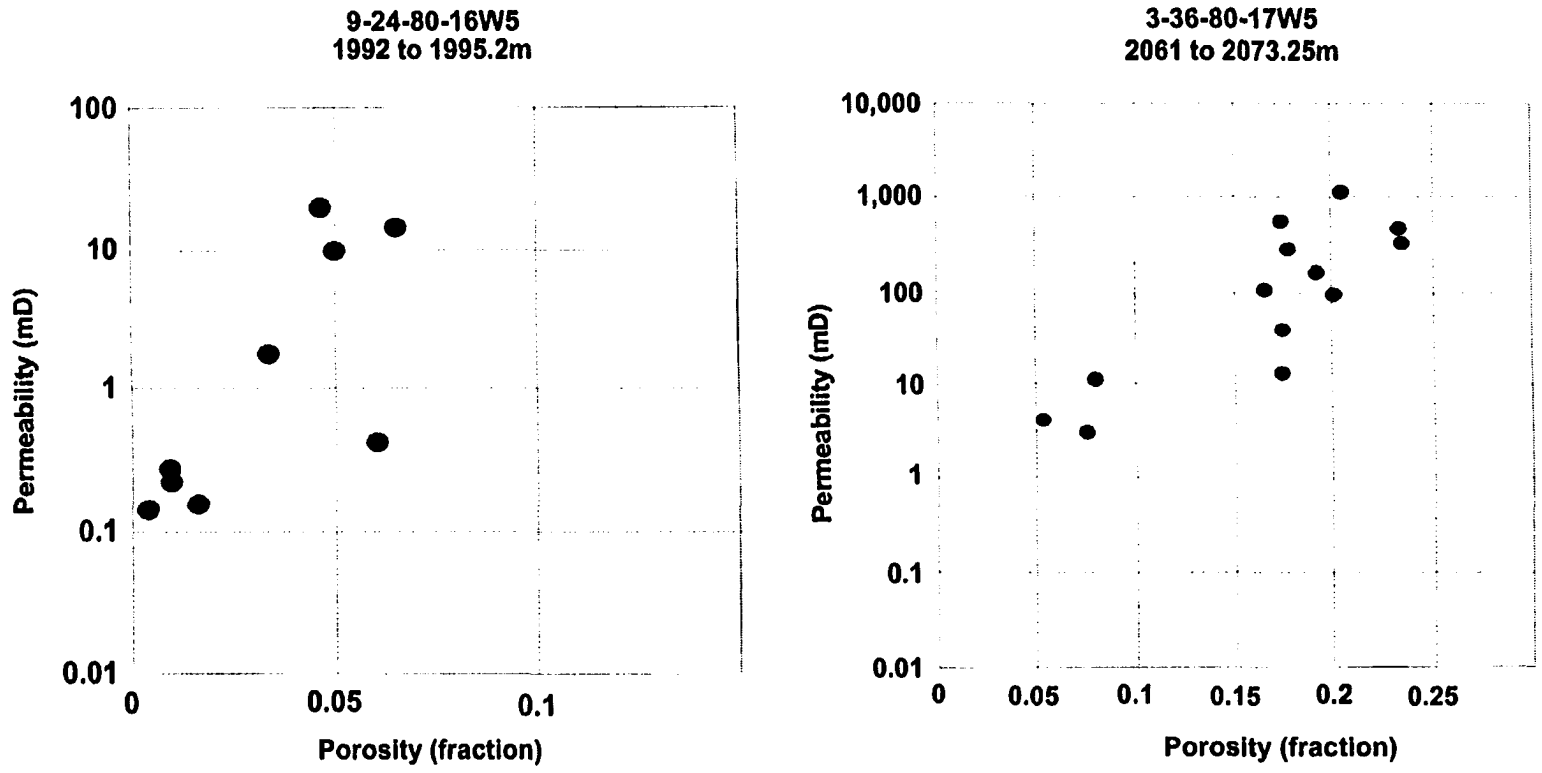

Figure 4.4 Porosity vs. permeability plots. Core 9-24-80-16W5 is a limestone, whereas core 3-36-80-17W5 contains both limestone (red) and dolomite (blue). Higher porosity and permeability are associated with the dolomitized sections. Data is representative of all cored wells (n=32) with analysis at Dawson. The two selected wells chosen best represent the relationship between dolomitization and the resulting increase in porosity and permeability (for further discussion see section 4.5). Data from core analysis provided on AccuMap and AccuLogs.

spar (Plate C/3). Most interparticle pores at Dawson are occluded by sparry calcite cement and/or mechanical compaction (Plate K/2). Intraparticle pores are common in stromatoporoids at Dawson. Intraparticle porosity was reduced by internal sedimentation or calcite cementation (Plate K/3).

4.5.2 Secondary porosity

Though primary depositional porosity is lost during burial, porosity generating processes may increase the total pore volume of the evolving limestone. Secondary porosity may develop anytime after final deposition, and the time elapsed in the generation of secondary porosity may be enormous (Moore, 1989; Choquette and Pray, 1970). Secondary porosity is mainly of two types: 1) porosity generation by dissolution of metastable bioclasts or allochems, 2) porosity as a result of dolomitization; and 3) fractures and karst.

At Dawson, vuggy/moldic porosity formed relatively late in the burial history of the Slave Point after metastable carbonate mineral stabilization. Vuggy porosity developed during or after dolomitization, whereby individual vugs range in size from a few centimetres to a few decimetres in diameter (Plate K/4). Smaller vugs are commonly filled with calcite cement, whereas larger vugs are partially occluded by saddle dolomite or late-stage calcite cement (Plate K/5).

4.5.3 Fracture porosity

Fracture porosity is non-fabric selective and cuts across the fabric of the rock (Tucker and Wright, 1990). In addition, fracturing is effective and common in carbonate

reservoirs because of the brittle nature of carbonate rocks (Moore, 1989). At Dawson, fractures range in size from <0.5 to 3mm in thickness and up to 10 cm's in length. Most fractures are filled with calcite spar, saddle dolomite, or rarely sulphide minerals (Plate K/6) and do not significantly enhance permeability of the Slave Point carbonates. Overall, fractures are rare, comprising only a small portion of the total rock volume (<1-5%), and they occur mainly in mudstone/wackestone facies (Plate K/6).

4.6 Granite Wash

The Granite Wash is dominated by quartz and feldspar (microcline) grains ranging in size from 0.5mm to 3mm (Plate L/1 and 2). Large clasts (>1.5 mm) of quartz and feldspar suggest proximity to Precambrian highs or monadnocks from which these sediments were weathered.

Porosity is well developed in this lithofacies. However, late-diagenetic blocky calcite cement occludes some porosity (Plate L/3). Nevertheless, it is likely that the porous and permeable sands of the Granite Wash acted as a conduit for dolomitizing fluids (discussed in chapter 6). One indication for this assertion is that the Granite Wash is commonly oil-stained (Plate G/4).

4.7 Paragenetic sequence of diagenetic events

The diagenetic phases described in the pervious section comprise a paragenetic sequence of event (Figure 4.5). Four of the 13 distinct diagenetic phases that have been recognized at Dawson generated porosity and, hence, enhance the reservoir potential.

PLATE L

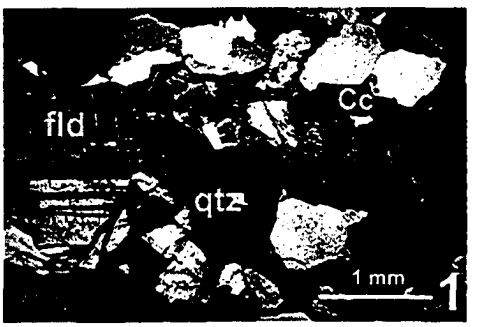

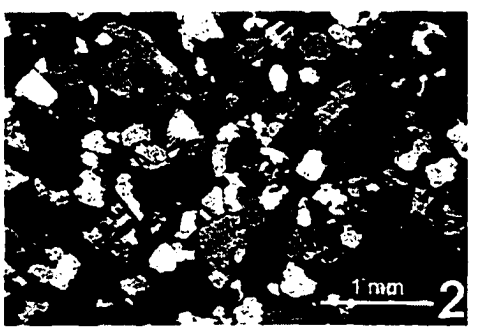

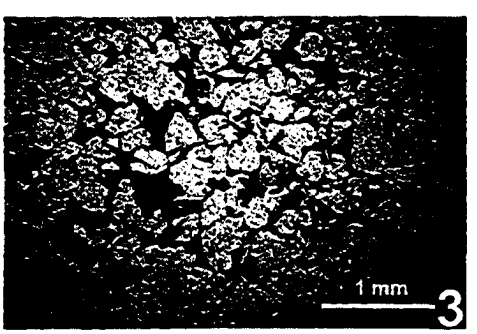

1) Photomicrograph of Granite Wash; note quartz (qtz) and feldspar (fld) grains and calcite (Cc) cement. 13-16-80-16W5, 2089.2 metres, cross polarized light. 2) Subangular to subrounded Granite Wash quartz and feldspar. 2-32-80-17W5, 2117.2 metres, cross polarized light. 3) Porosity (blue epoxy) in the Granite Wash; note sulphides occuring as black specs. 2-32-80-17W5, 2117.2 metres, plane light.

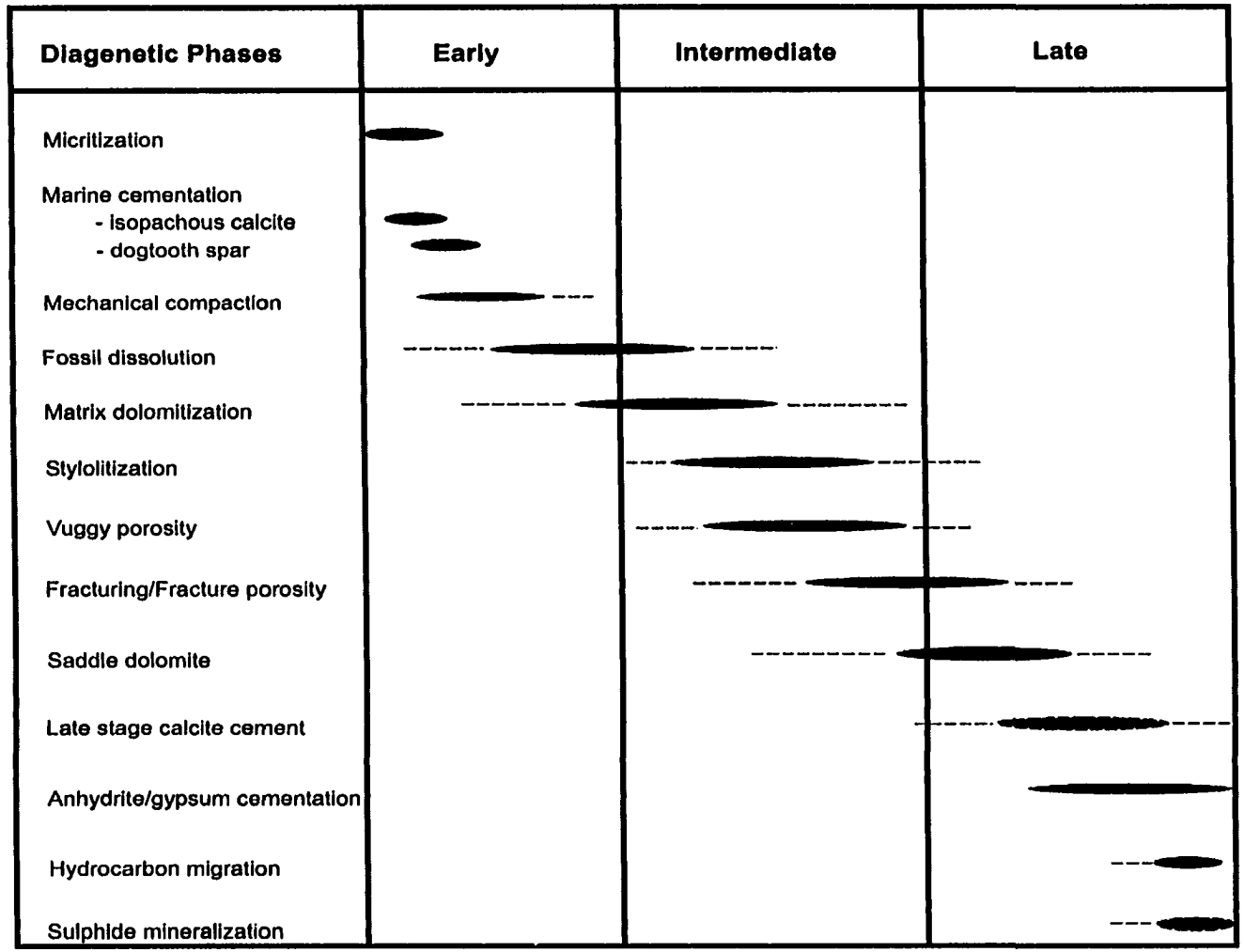

Figure 4.4 Paragenetic sequence. Uncertainty in the range of an event or mineral phase is indicated by dashed lines. Red colour indicates porosity generating diagenetic phases.

CHAPTER FIVE

5 ISOTOPE GEOCHEMISTRY

5.1 Introduction

Carbonates of the Slave Point Formation have been analyzed for both: stable and radiogenic isotopes. The purpose of this part of the investigation is to place controls on fluid composition, fluid source(s), and timing of the various dolomite phases. Interpretation and discussion of isotope data will be presented in chapter 6.

5.2 Stable Isotopes – theoretical concepts

Isotopes are atoms whose nuclei contain the same number of protons but a different number of neutrons. For example, oxygen has isotopes of ^{18}O, ^{17}O, and ^{16}O. As a result of this difference in neutrons, isotopes of the same element have differences in mass that cause certain differences in physical and chemical behaviour. Specifically, the mass difference results in isotopic exchange or isotopic fractionation during phase transformations, mineral precipitation, and diagenetic reactions. Isotopic fractionation refers to the partial separation of isotopes, which can occur during physical or chemical processes (e.g., Anderson and Arthur, 1983). Isotope fractionation can originate from both kinetic and equilibrium effects. Kinetic effects happen because a lighter isotope will diffuse or react faster than a heavier isotope. Equilibrium effects are the result of differences in the thermodynamic properties of isotopically-substituted species.

The fractionation factor (•) is used to determine the amount of partial separation of isotopes during physical or chemical processes that take place for a given reaction between two phases. The fractionation factor is defined as:

$$\bullet = R_A/R_B$$

where R_A is the ratio of the heavy to the light isotope of the molecule or phase A, and R_B is the same in phase B. The fractionation factor for any given system is temperature-dependent and approaches zero with increasing temperatures (Faure, 1986). Because isotope fractionation depends on temperature, it is interpretable in terms of environment temperatures, i.e., the temperatures at which phases A and/or B formed. The fractionation factor is correlated to absolute temperature by:

$$\ln\bullet = AT^{-2} + BT^{-1} + C$$

where *A, B,* and *C* are coefficients determined experimentally, and *T* is the absolute temperature in Kelvin (e.g., Tucker and Wright, 1990).

The isotopic composition of a mineral sample is expressed in per mil (‰) notation relative to a standard of known isotopic ratio. If an element has more than two stable isotopes the two most abundant isotopes are used, for example, ^{18}O and ^{16}O in the case of oxygen. Isotope ratios are expressed in/by the following equation:

$$\delta = [(R_x - R_{std})/R_{std}] * 1000$$

where *R* is the ratio of the abundance of the heavy to light isotope, *x* denotes the sample, and *std* denotes the standard. For carbonates, oxygen and carbon isotope values are reported relative to the Vienna Pee Dee Belemnite standard (VPDB). Conventionally, oxygen is reported SMOW (Standard Mean Ocean Water), which can be converted to VPDB using the following equation (Friedman and O'Neil, 1977):

$$\delta^{18}O \text{ (calcite SMOW)} = 1.03086\ \delta^{18}O \text{ (calcite PDB)} + 30.86$$

5.2.1 Stable isotope application to carbonate diagenesis

The stable isotopes of oxygen and carbon are the most commonly used isotopes in the study of carbonate diagenesis. They are used to determine the isotopic differences between fossil remains of organisms and diagenetic phases (i.e., dolomite, calcite etc), and to make inferences about the physical surroundings of the growth of the organism or crystal phases – especially temperature (Wefer and Berger, 1991). Additionally, the fluids that precipitate calcite and dolomite can be characterized by their isotopic compositions if the temperature of formation is known or can be estimated to a reasonable degree.

5.2.1.1 Oxygen

The following factors control the ratios of oxygen isotopes in carbonates (Brand and Veizer, 1981; Anderson and Arthur, 1983):

1) The isotopic composition of the diagenetic fluids. Meteoric fluids (rainwater), whose source is evaporated seawater, is typically depleted in ^{18}O relative to coeval marine water. This is due to the preferred evaporation of ^{16}O.
2) In the subsurface, under elevated temperature conditions, basinal fluids can exchange oxygen isotopes with carbonate rocks, resulting in the enrichment of ^{18}O in the fluids and commensurate depletion in the carbonates (Clayton et al. 1966).
3) The water/rock ratio. During high water/rock ratios there is a constant supply

of isotopes with the fluids, and the rock composition is isotopically dominated by the fluid composition; whereas, low water/rock ratios involve 'recycling' of isotopes between the fluid and the rock, and the rock composition may be little affected by changes in fluid composition.

4) The fractionation factor, determined primarily by the temperature at which the reaction (precipitation, recrystallization) occurs.

5) Altitude, latitude, and seasonal variations affect the $\delta^{18}O$ composition of meteoric water. Generally, $\delta^{18}O$ decreases with increasing altitude and latitude (Figure 5.1).

6) Secular variations in seawater isotopic composition. Generally, the oxygen isotopic compositions of marine carbonates become progressively more depleted in ^{18}O with increasing age of the rocks (Given and Wilkinson, 1987). Though the validity of this data is not disputed, many disagree with the implications. Veizer (1999) listed the implications as one or all of the following:

   i) seawater $\delta^{18}O$ changed in the course of the Phanerozoic;

   ii) the early oceans was much warmer than today, up to ~70^0C; and/or:

   iii) early oceans were stratified, with deep waters being generated by sinking of salty brines from extensive evaporation at low latitudes.

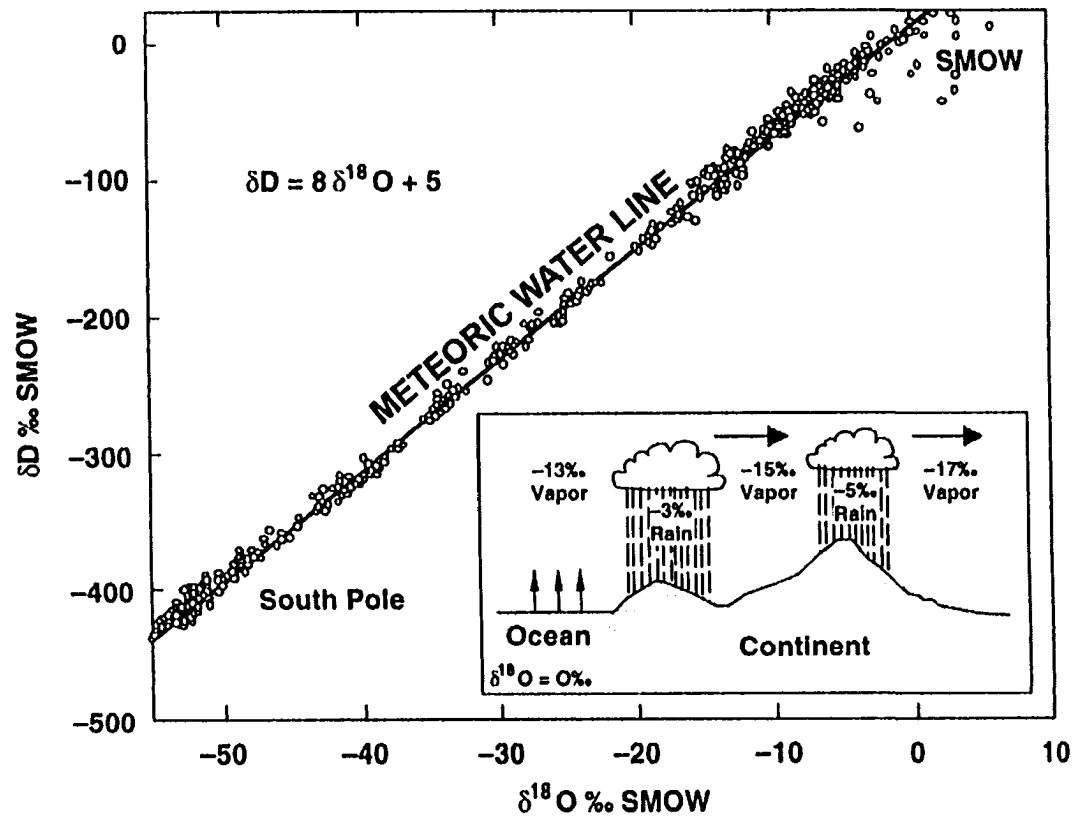

Figure 5.1 Waters of meteoric origin are easily identified using stable isotopes because of the high degree of correlation between oxygen and hydrogen isoptopes in meteoric waters worldwide. During evaporation of seawater, molecules of water containing a smaller proportion of ^{18}O and deuterium (D) than seawater are selectively evaporated from the ocean. Water vapour rising over the oceans cools until dew point is reached. During the outraining of clouds, the rain is enriched in ^{18}O and D and the remaining moisture in the cloud is further depleted in ^{18}O and D (inset). As an air mass moves poleward, inland and higher in elevation, and cools, the rain produced becomes increasingly depleted in both of these isotopes, leading to the spread in values observed along the Meteoric Water Line (Hoefs, 1980).

Objections to i) were raised by Muehlenbachs (1998) who claimed that the $\delta^{18}O$ of ocean water is, and has been, buffered at ~0‰ SMOW by water/rock interactions in hydrothermal convection cells at mid-ocean ridges since at least the Proterozoic. For ii), the persistence of essentially the same faunal assemblages and the recurrence of ice ages throughout the Phanerozoic are difficult to reconcile with the advocated warm temperatures (Veizer et al. 1996). For iii), the implied permanent saline stratification would be difficult to sustain and, even if sustainable, it could account for no more than ~1.5‰ ^{18}O depletion in the near-surface oceanic layer (Railsback, 1990; Veizer, 1999)

7) Biological fractionation (or vital effect), as first proposed by Urey et al. (1951). This refers to the 'vital selection' of isotopes during plant or animal metabolism. For example, some organisms, such as crinoids and rugose corals, produce carbonate that is not in isotopic equilibrium with seawater.

Based on a compilation of isotope data from various locations around the world, Carpenter et al. (1991) suggested a $\delta^{18}O$ composition for pristine, unaltered (not recrystallized) Devonian marine calcite of –4 to –6‰ (VPDB). Using the equilibrium $\delta^{18}O$ fractionation (Land, 1980), $^{18}O_{dolomite\text{-}calcite} = 3 \pm 1‰$, the oxygen isotopic composition of "primary" Devonian marine dolomite is expected to be –1 to –3‰ (VPDB; see also section 5.2.1.3).

Urey (1947) was the first to suggest that oxygen isotopes can be used as paleothermometers for ancient oceans, if the isotopic compositions of calcite and the precipitating fluid is known. The oxygen isotopic composition in the calcium carbonate –

water – bicarbonate system was established by Epstein et al. (1953) using calcareous skeletons. The Epstein et al. (1953) equation was later modified by Craig (1965) to:

$$t(^0C) = 16.9 - 4.2(\delta_c - \delta_w) + 0.13\ (\delta_c - \delta_w)^2$$

where δ_c is the $\delta^{18}O$ of CO_2 produced by reaction of $CaCO_3$ in phosphoric acid at 25^0C, and δ_w is the $\delta^{18}O$ of CO_2 in equilibrium with water at 25^0C (SMOW). Dolomite has a different fractionation factor then calcite, therefore the following equation is used to calculate temperature of dolomite formation (Irwin, 1980):

$$t(^0C) = 31.9 - 5.55(\delta_d - \delta_w) + 0.17\ (\delta_d - \delta_w)^2$$

where δ_d and δ_w represent the oxygen isotopic compositions of dolomite and water, respectively. Conversely, the composition of the fluid can be determined if T and $\delta_c(\delta_d)$ are known.

5.2.1.2 Carbon

Because equilibrium fractionation of ^{13}C between calcite and dolomite is negligible, both minerals would have nearly identical $\delta^{13}C$ values of $+1.5 \pm 1‰$ for the Middle Devonian (Meyers and Lohmann, 1985). These values will be used as marine baseline values further below.

The $\delta^{13}C$ of dolomite is strongly influenced by that of the precursor $CaCO_3$ as a result of the relative insolubility of CO_2 in water (Land, 1980). Hence, the $\delta^{13}C$ value of calcium carbonate being dolomitized is commonly retained by the dolomite (Tucker and Wright, 1990), and additionally, there is little isotopic fractionation between $^{13}C/^{12}C$ with temperature. As a result, the $\delta^{13}C$ values of dolomite, like those of limestone/calcites, primarily provide information on the source of carbon in the carbonate. Values between 0

and +4‰ are typical marine signatures throughout the Phanerozoic. It is not uncommon, however, to have more extreme values of $\delta^{13}C$ in diagenetic carbonates: 1) very negative values, down to - 20‰, indicate that C was derived from organic matter with a range of $\delta^{13}C$ of –30 to –20 ‰; and 2) very positive values, up to +15‰, can result from the fermentation of organic matter, where methanogenesis results in very ^{13}C-enriched CO_2 (Figure 5.2; Irwin et al. 1977).

5.2.1.3 Dolomite

An important consideration in this study, and in many other geochemical studies of carbonates, is the 'dolomite problem'. Though stable isotope data are extensively used in the interpretation of dolomites to help elucidate their origin, there are numerous problems interpreting dolomite formation from geochemical data. The main problem is that the relationship between temperature, $\delta^{18}O_{water}$, and $\delta^{18}O_{dolomite}$ is imprecisely known (Tucker and Wright, 1990). Experimental work, mainly on dolomites at high temperature, has resulted in the following fractionation equations (T=^{0}K):

$$10^3 \ln\alpha_{\text{dolomite-water}} = 3.2 \times 10^6 T^{-2} - 1.50$$

(300-510^{0}C, Northrop and Clayton, 1966)

$$10^3 \ln\alpha_{\text{dolomite-water}} = 3.34 \times 10^6 T^{-2} - 3.34$$

(305-400^{0}C, O'Neil and Epstein, 1966)

$$10^3 \ln\alpha_{\text{dolomite-water}} = 2.78 \times 10^6 T^{-2} + 0.11$$

(25-79^{0}C, Fritz and Smith, 1970)

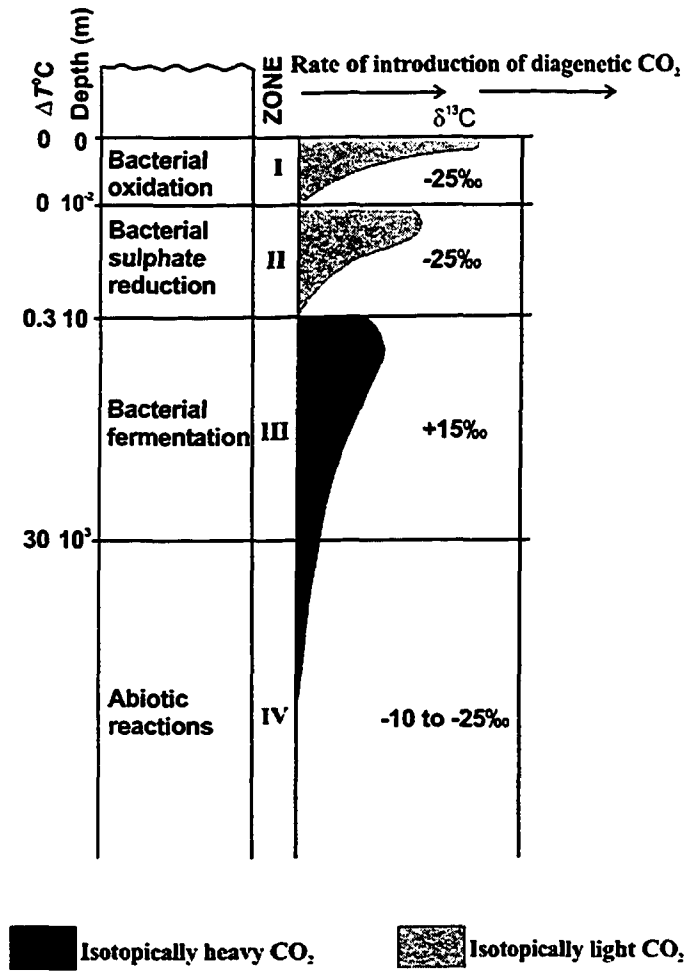

Figure 5.2 Introduction of diagenetic CO_2 within different diagenetic zones. Model for depth zonation with reference to the generation of carbon dioxide. Zones I, II, and II are dominated by bacterial process. The zone I and II boundary is determined by the downward diffusion of dissolved molecular oxygen from overlying waters; the lower limit of zone II is defined by downward diffusion of sulphate. Fermentation, zone III, starts as soon as sulphate reduction stops and continues until prevented by either high temperatures or exhaustion of suitable organic substrate. Zone IV, however, is less clearly defined with respect to depth or process (modified from Irwin et al. 1977).

However, the most commonly used fractionation equation for dolomite-water equilibrium is that of Land (1983):

$$10^3 \ln\alpha_{\text{dolomite-water}} = 3.14 \times 10^6 T^{-2} - 2$$

The dolomitizing fluids can be influenced by the isotopic composition of the carbonate minerals being replaced, i.e., by the water-rock ratio during cementation, replacement, or recrystallization. Since pore-fluids have abundant oxygen, generally the precursor minerals have an effect on $\delta^{18}O_D$only in low water/rock ratio or closed diagenetic systems

5.2.2 Analytical Methods

A total of 56 samples were analyzed for carbon and oxygen isotopes. Four mineral/diagenetic phases of interest were investigated: 1) calcite fossil constituents, i.e., brachiopods, crinoids, and stromatoporoids; 2) replacive matrix dolomite; 3) saddle dolomite cement; and, 4) late-diagenetic calcite cement.

These phases were extracted with a dental drill as a fine powder. Average sample size was about 15 mg, which were processed and isotopically analyzed in the University of Alberta stable isotope research laboratory. The samples were digested in 100% pure phosphoric acid. The samples were left in a water at 25^{0}C for a minimum of 4 hours in the case of calcite samples, or at 50^{0}C for a minimum of 3 hours in the case of dolomite samples. There were no mixed calcite-dolomite samples, hence, selective acid digestion was not necessary. Al-Aasm et al. (1990) determined that for fine-fraction calcite (<200 mesh) as much as 95% theoretical yield CO_2 was achieved after 4 hours (Figure 5.3a). Additionally, Al-Aasm et al. (1990) determined that dolomite submerged in a water bath

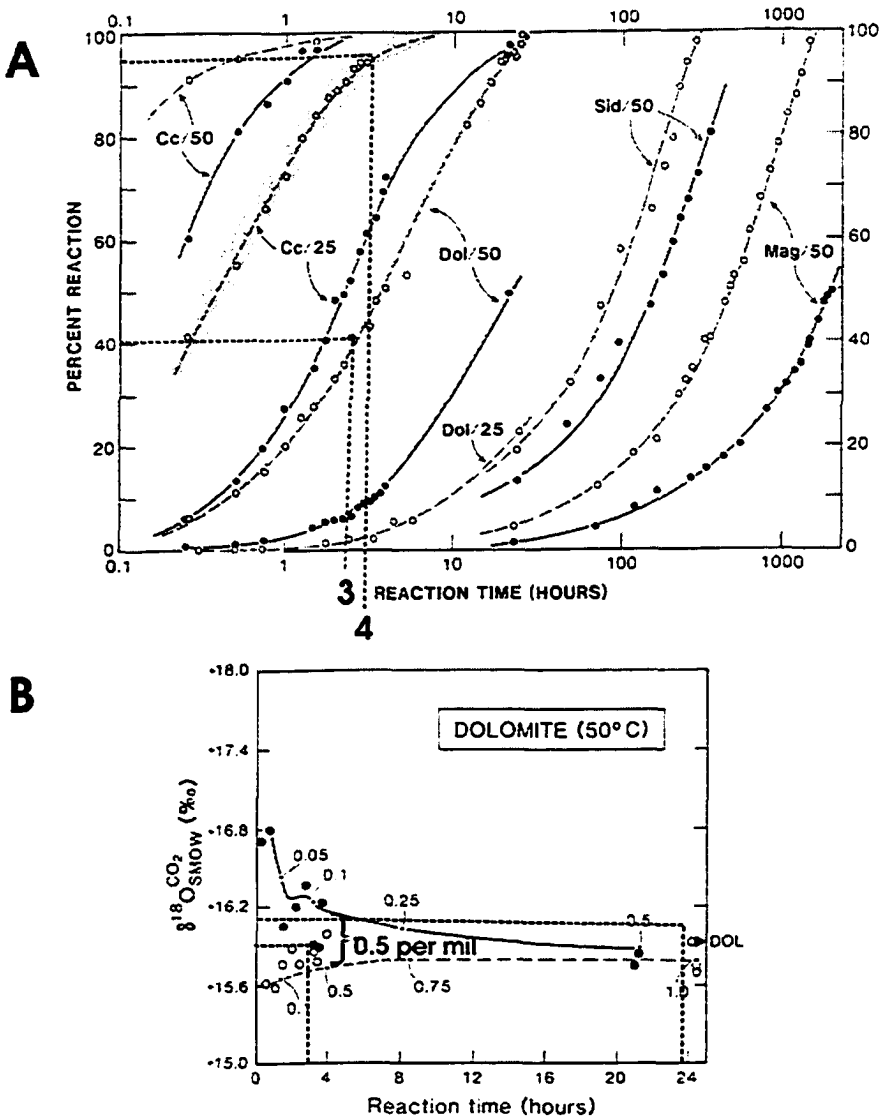

Figure 5.3 Reaction rates for calcite and dolomite respectively. Cc = calcite; Dol = dolomite Sid =siderite; Mag = magnesite, Number beside each phases indicate the temperature the reaction was equilibrated at. A) Reaction rates for fine fraction calcite (<200 mesh) outlined in red (open circles), after 4 hours the reaction is at 95% completion. The fine dolomite fraction in blue (open circles) at 50°C, after 3 hours the reaction is at about 40% completion. B described the detail of the dolomite reaction. B) Plot of dolomite equilibrium at 50°C, after 3 hours the reaction has on ly a 0.5 per mil difference then that which was reacted for 24 hours; therefore, extracting the gas after 3 hours is feasible.

at 50^{0}C for at least 3 hours produced less then 0.5 per mil difference, than if the same reaction goes to equilibrium for 24 hours (Figure 5.3b) Based on these conclusions, the dolomite samples of this study were left to equilibrate for 3 hours before gas extraction.

CO_2 gas was extracted on a vacuum line, and any water in the samples was removed using a mixture of dry ice and ethanol. The CO_2 gas was collected in a separate vessel further down the line that was submerged in liquid nitrogen, which traps CO_2. The CO_2 gas was then thawed and collected for analysis on a Finnigan MAT 252 gas-source mass spectrometer. Stable isotope results where corrected for acid fractionation with a correction factor of 1.0125 (Muehlenbachs, pers. comm.).

5.2.3 Carbon and Oxygen Isotope Results

The following is a summary of the carbon and oxygen isotopic composition of the Slave Point carbonates. All raw data are tabulated in Appendix A.

1. Brachiopods: Isotopic analysis of brachiopod shells (n=3) yield $\delta^{18}O$ values ranging from –10.7 to –5.9‰ VPDB and $\delta^{13}C$ values ranging from +0.9 to +2.7‰ VPDB (Figure 5.4a).
2. Crinoids: Isotope analysis of undolomitized crinoid fragments (n=2) have $\delta^{18}O$ values of –6.6 and –6.4‰ VPDB and $\delta^{13}C$ values of –0.06 and +0.6‰ VPDB. (Figure 5.4a).
3. Stromatoporoids: Massive and bulbous stromatoporoids (n=10) have $\delta^{18}O$ values ranging from –11.2 to –6.6‰ VPDB and $\delta^{13}C$ values ranging from +2.2 to +3.6‰ VPDB (Figure 5.4a).

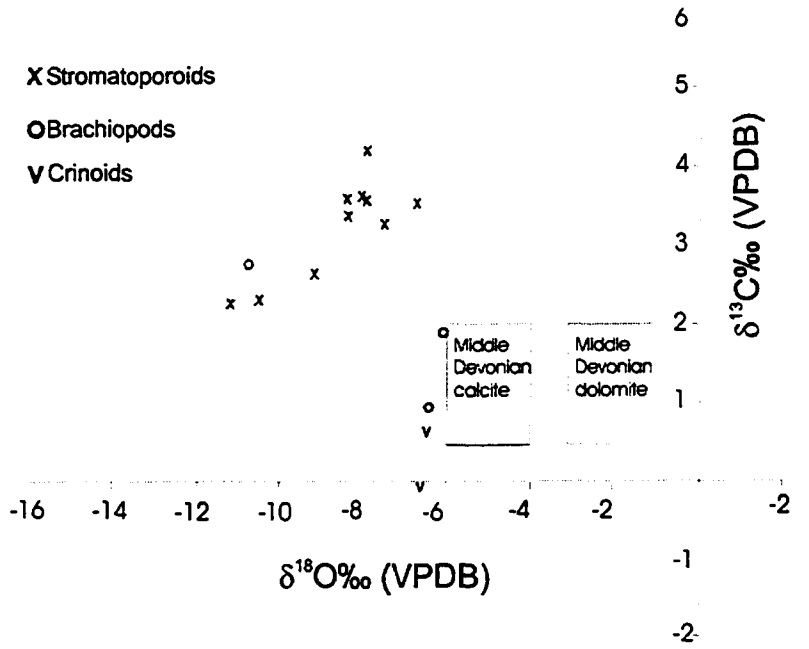

Figure 5.4a Isotope cross plot of carbon and oxygen values for fossil constituents (brachiopods, crinoids, and stromatoporoids). Middle Devonian marine calcite and hypothetical Middle Devonian marine dolomite boxes from Carpenter et al. (1991), Meyers and Lohmann (1985), and Land (1980).

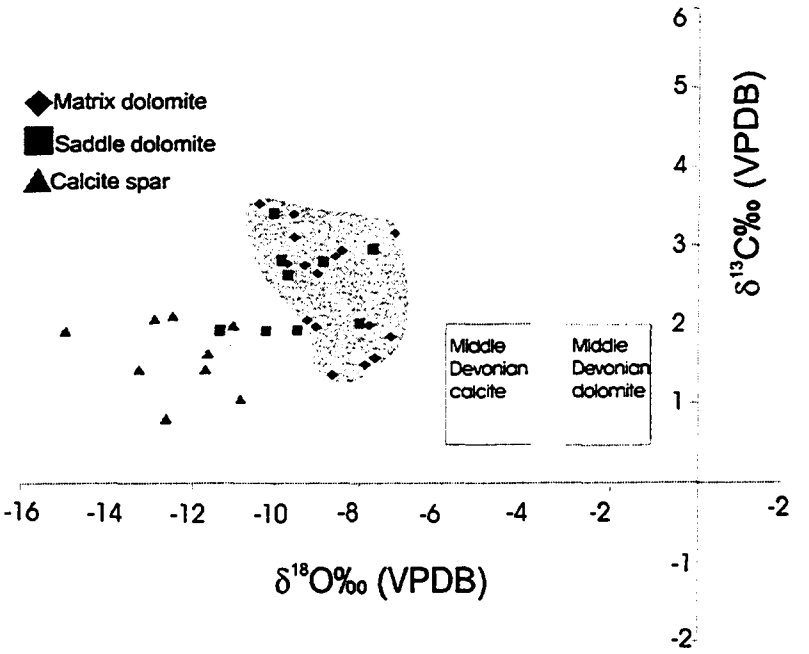

Figure 5.4b Isotope cross plot of carbon and oxygen values for matrix dolomite, saddle dolomite, and late-diagenetic calcite spar. Middle Devonian marine calcite and hypothetical Middle Devonian marine dolomite boxes from Carpenter et al. (1991), Meyers and Lohmann (1985), and Land (1980).

4. Matrix dolomite: Matrix dolomites (n=18) yield $\delta^{18}O$ values ranging from –10.4 to –7.1‰ VPDB and $\delta^{13}C$ values from +1.3to +3.9‰ VPDB (Figure 5.4b)
5. Saddle dolomite (n=9) have $\delta^{18}O$ values ranging from –11.4 to –7.6‰ VPDB and $\delta^{13}C$ values ranging from +1.7 to +3.4‰ VPDB (Figure 5.4b).
6. Calcite spar (n=13) yields $\delta^{18}O$ values ranging from –14.9 to –10.5‰ VPDB and $\delta^{13}C$ values ranging from +0.8 to +2.9‰ VPDB (Figure 5.4b).

The interpretations of these results are discussed in Chapter 6.

5.3 Radiogenic (Sr) isotopes – theoretical concepts

Strontium has four naturally occurring stable isotopes: ^{88}Sr, ^{87}Sr, ^{86}Sr, and ^{84}Sr. ^{88}Sr, ^{86}Sr, and ^{84}Sr are not radiogenic, whereas ^{87}Sr occurs is generated through the decay of ^{87}Rb. The Sr isotopic composition of a rock or mineral depends on its Rb/Sr ratio and age, which is the basis of the Rb-Sr method of radiometric dating (Tucker and Wright, 1990). The negligible Rb content of most carbonates precludes the application of the conventional Rb-Sr dating method to marine carbonate rocks (Dickin, 2000). Furthermore, there is but an insignificantly small fractionation during mineral precipitation and recrystallization. Hence, carbonate minerals directly record fluid $^{87}Sr/^{86}Sr$ isotope compositions (Banner, 1995).

Several workers (Brass, 1976; Veizer and Compston, 1974; Burke et al. 1982; Veizer et al. 1999) have constructed seawater $^{87}Sr/^{86}Sr$ curves reflecting the strontium isotopic composition of seawater through geologic time. A $^{87}Sr/^{86}Sr$ range of 0.7078 to

0.7082 has been suggested for Middle Devonian seawater (Figure 5.5; Veizer et al. 1999).

During diagenesis, carbonates minerals acquire strontium from the diagenetic fluids, which may significantly alter the marine 87Sr/86Sr – signature in the case of recrystallization. Enriched ^{87}Sr values are obtained by interaction with Rb-rich minerals such as clays and feldspars, which are abundant in clastic sediments. Banner (1995) suggested that fluids that have interacted with sandstones, or brines that have passed through a shale sequence, are common ways of generating diagenetic fluids with elevated $^{87}Sr/^{86}Sr$ ratios. Basinal fluids from the Western Canadian Sedimentary Basin generally have more radiogenic Sr ratios than the marine carbonates in the basin (Mountjoy et al. 1992), and some of the ratios in the carbonates may be the result of interaction with extra-formational fluids during burial.

Additionally, Machel and Cavell (1999) introduced the term *MASIRBAS* (**MA**ximum **S**r **I**sotope **R**atio of **BA**sinal **S**hales). The term is used to define the regional background strontium isotope values of basinal shales under normal subsurface diagenetic conditions (Machel and Cavell, 1999). In the Alberta Basin, *MASIRBAS* is defined by a $^{87}Sr/^{86}Sr$-ratio of 0.7120. Consequently, any carbonate cement with a $^{87}Sr/^{86}Sr$-ratio >0.7120 are likely to have been formed from formation waters with a metamorphic and extra-basinal component. Whereas, carbonate cements with a $^{87}Sr/^{86}Sr$-ratio <0.7120 are likely to have been formed from fluids that has acquired their Sr isotopes intrabasinally with interaction with metamorphics (Figure 5.6). Comparison with literature data (Connolly et al. 1990a, 1990b; Armstrong et al. 1998) shows that the

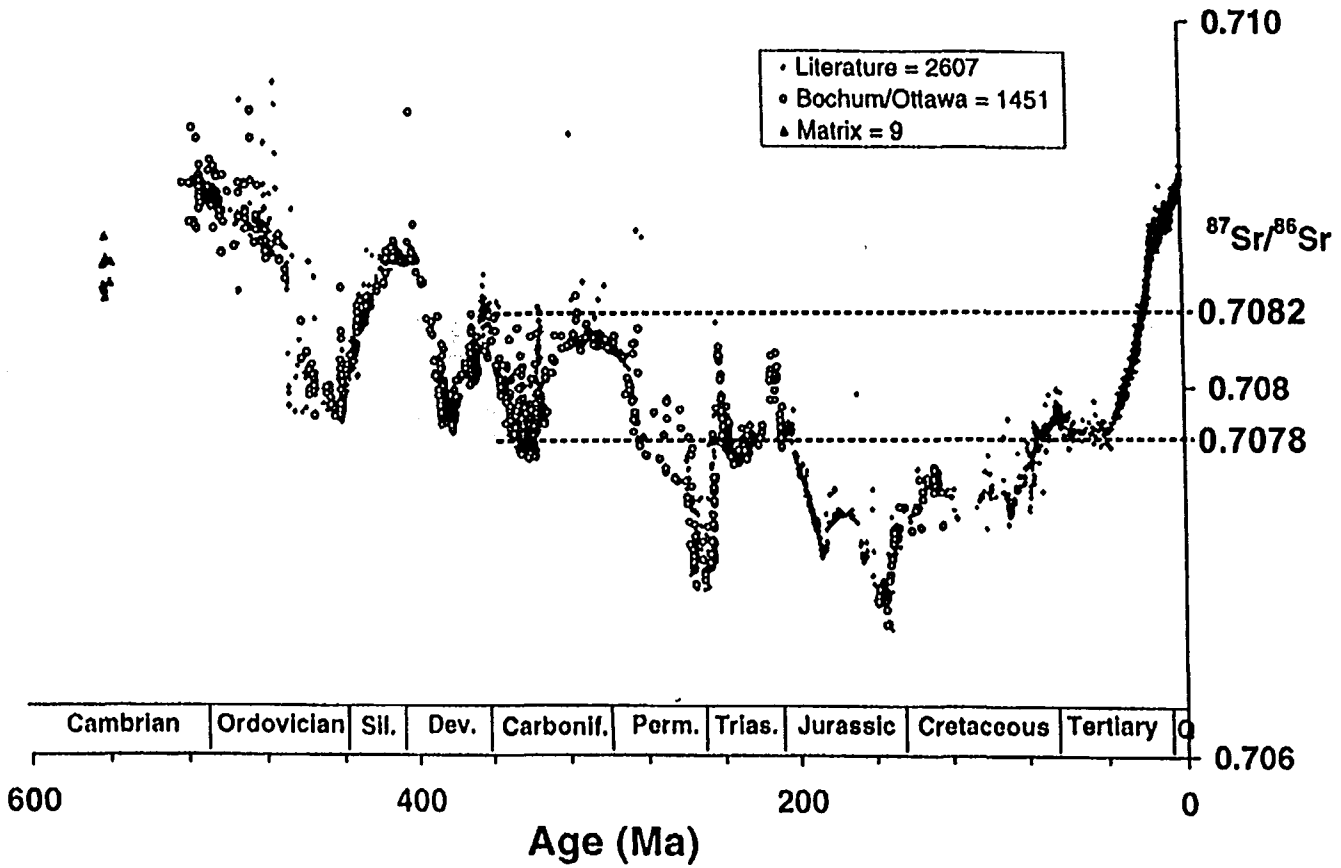

Figure 5.5 $^{87}Sr/^{86}Sr$ variations for the Phanerozoic based on 4055 samples of brachiopods, belemnites and conodonts, normalized to NBS 987 of 0.7102 (from Veizer et al., 1999). Blue box represents Sr range of Middle Devonian seawater.

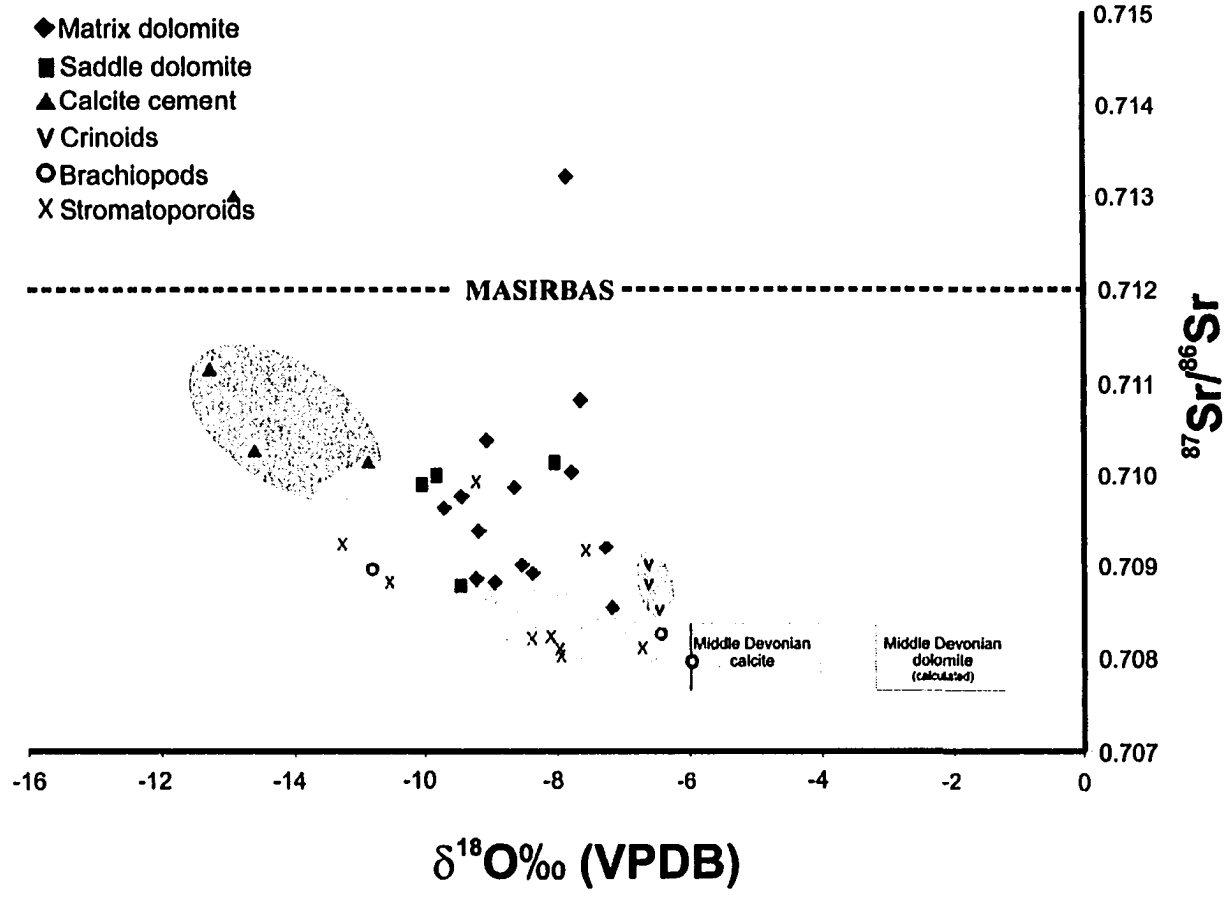

Figure 5.6 Radiogenic isotope plot of carbonate phases at Dawson. Middle Devonian marine calcite and hypothetical Middle Devonian marine dolomite boxes from Veizer et al. (1999) and Hurley and Lohmann (1989). Highly ^{87}Sr-enriched matrix dolomite (~0.713) and calcite cement (~0.713)data points are included in the data set although they are not reliable results. Purple = calcite cement; blue bubble = saddle and matrix dolomite;green bubble = crinoids; red bubble = brachiopods; yellow bubble = stromatoporoids. MASIRBAS (MAximum Sr Isotope Ratio of Basinal Shale), see text for discussion

Alberta Basin *MASIRBAS* is valid for the entire stratigraphic section from the Pleistocene glacial till to at least the Middle Devonian (Machel and Cavell, 1999).

5.3.1 Radiogenic Isotope Methods

Strontium (Sr) was extracted from calcite and dolomite powder sample (~10-20mg) at the University of Alberta's radiogenic isotope geochemistry laboratory. All samples were processed on a VG 354 multi-collector Thermal Ionization Mass Spectrometer (TIMS). The samples were loaded as a phosho-tantalate gel on a single Re ribbon bead assembly. Values for $^{87}Sr/^{86}Sr$ were corrected to NBS SRM-987 for which repeated analytical runs during the course of this study gave a value of 0.7102. Analytical precision on individual runs was better then 0.000024 (2σ).

5.3.2 Strontium Isotope Results

Figure 5.6 is a plot of $^{87}Sr/^{86}Sr$ ratios plotted vs. $\delta^{18}O$ (VPDB) for all phases from the Slave Point Formation at Dawson (n=37). The raw data are tabulated in Appendix A. Fossil constituents, namely crinoids and brachiopods, show slightly enriched values of 0.7085 to 0.7094 and 0.7080 to 0.7089, respectively, compared to Middle Devonian seawater. Stromatoporoids have values ranging from 0.7081 to 0.7099, slightly more enriched then the brachiopod and crinoid constituents. All diagenetic carbonate phases/cements (i.e., calcite and dolomite) have enriched $^{87}Sr/^{86}Sr$ ratios relative to Middle Devonian seawater. Fine-crystalline matrix dolomite has values ranging from 0.7085 to 0.7108 and coarse-grained, pore-filling saddle dolomite has values ranging

from 0.7087 to 0.7101. The most radiogenic phase, late-diagenetic calcite spar, has values ranging from 0.7101 to 0.7212.

CHAPTER SIX

6 DISCUSSION AND INTERPRETATION OF DIAGENESIS

6.1 Introduction

This chapter provides an interpretation of the diagenetic history of the Slave Point carbonates at Dawson. Based on the preceding stratigraphic, petrographic, and geochemical results. The timing and products of diagenetic events are summarized in the paragenetic sequence in Figure 6.1. In addition, a diagenetic evolution summarizing all aspects of diagenesis at Dawson will be presented at the end of this chapter.

6.2 Cementation

Cementation, most notably by calcite and/or anhydrite and gypsum, is an important aspect of the diagenetic history of the Slave Point carbonates. Cementation initially occurred in marine environments, and reoccurred in deep burial environments (section 4.2.4), and exerted some control on later diagenetic events. Important consequences of cementation are early lithification and occlusion of porosity.

6.2.1 Early marine cementation

Radial fibrous cement - composed of elongate, isopachous crystals - is the only generation of pre-burial cement recognizable in thin section within the Slave Point and denotes a marine origin (Tucker and Wright, 1990). Radial fibrous cement predates

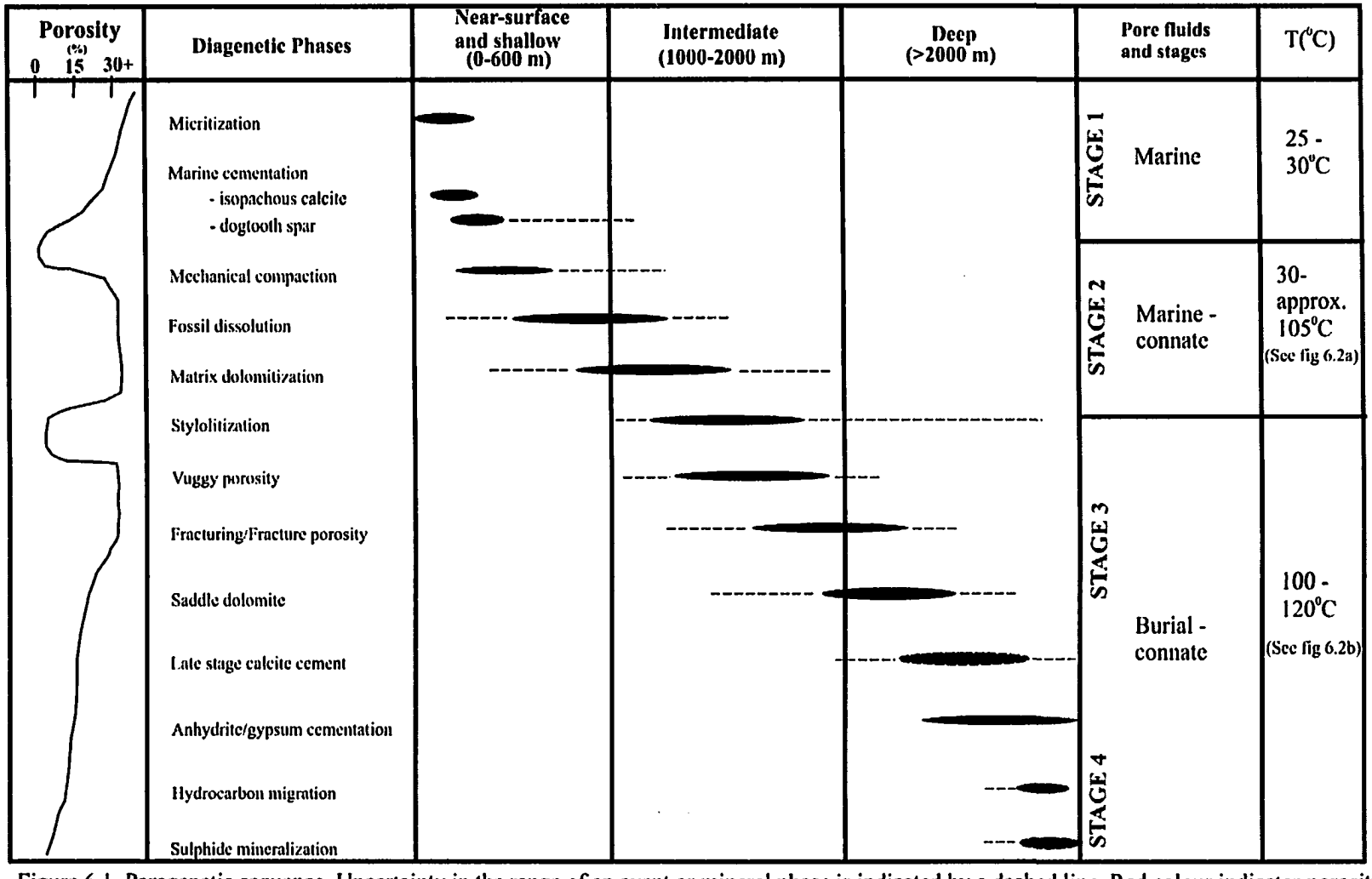

Figure 6.1 Paragenetic sequence. Uncertainty in the range of an event or mineral phase is indicated by a dashed line. Red colour indicates porosity generating diagenetic phases. A porosity trend is shown to relate porosity generating diagenetic phases to porosity trend in the subsurface.

compaction, which is indicated by cross-cutting relationships with compaction features (see section 4.2.3). Early marine cementation also occluded primary interparticle porosity of stromatoporoids (Plate H/3).

6.2.2 Dogtooth calcite spar cement

Tucker and Wright (1990) suggested that dogtooth calcite spar cements (Plate H/3 and 6) can form in either meteoric or burial settings. Samples for geochemical analysis were not collected from dogtooth calcite spar, therefore, the paragenetic and diagenetic history of this calcite spar is based solely on petrography.

At Dawson, evidence for precipitation of dogtooth calcite spar in an early burial environment includes precipitation after micritization of grains and the occurrence of calcite spar filling primary porosity of micritized stromatoporoids (Plate H/3 and 6; Plate I/5; and Plate K/3). Therefore, dogtooth calcite spar precipitated after mechanical compaction and fossil dissolution in a near surface to shallow burial environment. The stage is intermediate between the preceding early marine cementation and late-stage calcite cementation of the Slave Point at Dawson.

6.2.3 Late-stage calcite cement

Late-stage coarse calcite cement, which fills voids, and in some cases fractures (Plate I/4 to 6; and Plate K/6), is the final calcite cementing stage within the Slave Point at Dawson.

The diagenetic timing of this cement is also evidenced geochemically. The oxygen isotopic composition of this cement ($\delta^{18}O$ to -14.92‰ to -7.88; Figure 5.3b) is

consistent with precipitation from a warmer and/or diagenetically altered fluid with respect to $\delta^{18}O$.The $\delta^{13}C$ compositions (+0.81 to +2.97‰), however, reflect an internal source for carbon. The strontium isotope ratios for this late-stage cement (0.7101 to 0.7213) are significantly more radiogenic than Middle Devonian marine values (0.7078 to 0.7082; Figure 5.5), indicating that the fluid that precipitated this late stage cement was enriched in radiogenic strontium compared to other phases at Dawson. The source of the highly radiogenic fluids will be discussed in a latter section of this chapter.

6.2.4 Anhydrite cementation

Anhydrite cementation is minor and occurs as a vug filling mineral in primary pores of the Slave Point Formation at Dawson. Based on petrographic evidence, anhydrite was precipitated late in the diagenetic history and is commonly found in association with sulphide minerals (Figure 6.1; Plate K/1).

6.3 Dolomitization

6.3.1 Models of Dolomitization

Any model used to explain dolomitization requires a supply of Mg^{2+} ions as well as a mechanism to deliver the Mg^{2+} and export the Ca^{2+} (Morrow, 1982; Land, 1985; Machel and Mountjoy, 1987). Many models have invoked for replacive dolomitization, including: 1) hypersaline/reflux model, 2) meteoric/marine mixing model, 3) burial compaction model, 4) seawater (Kohout) convection model, 5) tectonic hydrothermal model and 6) dolomitization from normal seawater. The successful application of any one

of these models requires detailed knowledge of paleogeography, petrography, geochemistry, facies, and dolomite distribution. There is overlap between some models, and several models could apply to one setting. Dolomites formed in different settings may not be chemically and petrographically distinct from another (Tucker and Wright, 1990), and recrystallization and/or multiple dolomitizing events must also be considered. For a review and critique of the major models see Hardie (1987), Morrow (1990), Budd (1997), Warren (2000), and Machel (2004).

Additionally, Machel (2004) noted that dolomitization often begins as a selective replacement of the matrix as a result of three interacting and reinforcing factors: (a) the matrix contains or consists of thermodynamically metastable carbonates, which have higher solubilities than low-Mg-calcite; (b) the matrix has much smaller grain sizes and, thus, a higher surface area per grain than the larger biochems, allochems or cement crystals formed prior to dolomitization; and, (c) the matrix has a higher permeability than the larger, more massive particles or cements. Lime muds have a greater surface area than coarser grained components and are thus preferentially dolomitized due to the abundance of nucleation sites, a common and well-know phenomenon (Murry and Lucia, 1967).

6.3.2 Matrix dolomitization at Dawson

At Dawson, all facies of the Slave Point Formation have been dolomitized to varying degrees. Facies exerted a minor control on dolomite distribution. For example, matrix dolomite is confined to facies with a precursor mud matrix.

Any process or mechanism invoked to explain the origin of matrix dolomite must account for its formation during relatively early diagenetic stages of the Slave Point

Formation. This is indicated petrographically, i.e., matrix dolomite penetrates the edges of some fossils grains, suggesting formation during mechanical compaction (Plate I/2). Additionally, matrix dolomite precipitation occurred before the onset of chemical compaction because dissolution seams deflect around individual dolomite crystals, and dolomite rhombs are truncated along stylolites (Plate J/5). As chemical compaction (i.e., stylolitization and dissolution seams) begins between 300 and 600 m (Lind, 1983), matrix dolomitization at Dawson happened during shallow burial.

Circumstantial evidence such as facies and petrographic analysis would thus suggest that the dolomitizing fluid was essentially seawater. However, isotopically, original marine compositions are not found in the matrix dolomite. Figure 5.3b illustrates $\delta^{18}O$ values are depleted in ^{18}O relative to those calculated for Middle Devonian dolomite. This depletion in ^{18}O is the likely result of resetting of oxygen isotopes during recrystallization (Packard et al. 1990; Machel, 1997). In addition, radiogenic $^{87}Sr/^{86}Sr$ values for matrix dolomite at Dawson deviate significantly from the estimated Middle Devonian seawater value (Figure 5.5). Hence, the dolomitizing fluid cannot be deduced from the stable and radiogenic isotopes in terms of original composition. What can be said is that the dolomitizing fluid probably was originally marine but that the matrix dolomite must have recrystallized at greater depths, thereby resetting the $\delta^{18}O$ and $^{87}Sr/^{86}Sr$ composition.

Based on $\delta^{18}O$ values of -10.4 to -7.1‰VPDB, the formation of matrix dolomite occurred at a temperature range of 80 to 105^{0}C, assuming that the diagenetic fluid from which matrix dolomite formed had near Middle Devonian seawater isotopic composition (Figure 6.2a, blue dashed arrows). However, if Middle Devonian seawater had an

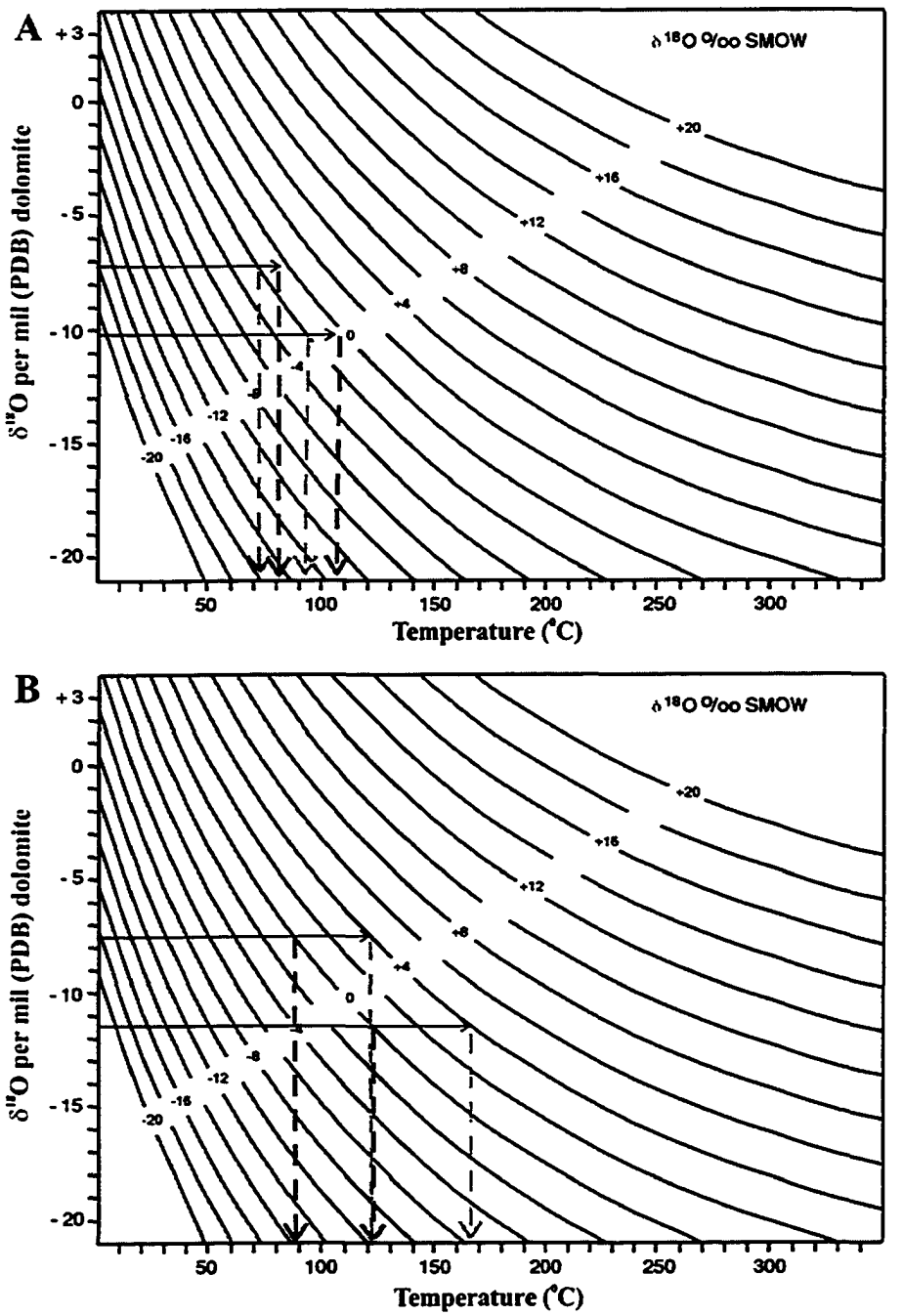

Figure 6.2 Temperature determination plot of dolomite phases at Dawson. A) Based the $\delta^{18}O$ range of matrix dolomite -10.4 to -7.1VPDB, the formation of matrix dolomite occurred at a temperature range of 80 to 105°C (blue arrows) assuming 0 per mil SMOW; whereas green arrows assume -2 per mil SMOW in which matrix dolomite would have formed at a temperature range of 70-90°C. See text section 6.3.2 for further discussion. B) Based the $\delta^{18}O$ range of saddle dolomite -11.4 to -7.6 VPDB, the formation of saddle dolomite occurred at a temperature range of 90 to 125°C (blue arrows) assuming 0 per mil SMOW whereas green arrows assume +4 per mil SMOW in which saddle dolomite would have formed at a temperature range of 120-165°C. See text section 6.3.3 for further discussion.

oxygen isotope value closer to 2‰ SMOW, suggested by some authors (Veizer, 1990), the Dawson matrix dolomites would have formed at 70-90^{0}C (Figure 6.2a, green dashed arrow). $^{87}Sr/^{86}Sr$ values for matrix dolomites indicate that they were formed from formation waters that were "intra-basinal" because they plot below MASIRBAS (Figure 5.5). See section 6.3.4 for a more detailed interpretation.

Matrix dolomitzation at Dawson is here interpreted to be a one-stage process, i.e., limestone replacement from one fluid that may have evolved slightly through time. This process may form texturally and geochemically homogeneous dolomites and/or zoned dolomites, as observed in some Dawson sample (Plate J/3). If so, the dolomitizing fluid had to remain supersaturated with respect to dolomite after all the matrix was replaced, thereby forming clear overgrowths (cements) around some parts of the replacement dolomites (cloudy cores). A similar explanation for these textures was provided by Sibley (1982) and Budd (1997). The possibility of two-stage dolomitization, whereby the clear overgrowths represent cementation by another fluid after a significant hiatus, is considered highly unlikely. In this case, the zonation should be pervasive, and samples with overgrowths should have a significantly different composition (isotopes, trace elements) from samples without overgrowths. This, however, is not the case at Dawson.

The source(s) of the fluids are unknown. During burial, faults associated with tectonic events (i.e., block-faulting of the Peace River Arch) may have funneled fluids into the Slave Point Formation and caused dolomitization. In the Western Canada Sedimentary Basin, large scale fluid movement has occurred twice since the deposition of the Slave Point Formation: 1) between the Late Devonian and Early Mississippian (Antler Orogeny), and 2) between the Late Jurassic and Early Tertiary

(Columbian/Laramide Orogeny). Either of these events would be sufficient to cause the amount of fluid flow required to precipitate saddle dolomite.

6.3.3 Saddle Dolomite

Characteristics of saddle dolomite at Dawson, both petrographic and geochemical, include: 1) occurrence in open voids, 2) coarse grain size, 3) late diagenetic timing, 4) depleted $\delta^{18}O$ values, and 5) slightly enriched $^{87}Sr/^{86}Sr$ relative to matrix dolomite. With these lines of evidence taken together, the saddle dolomite is interpreted to have formed during later diagenetic stages.

The oxygen isotopic composition of Slave Point saddle dolomite at Dawson ($\delta^{18}O$ = -11.49 to -7.69‰ VPDB) is consistent with precipitation from relatively warm or hot fluids, the $\delta^{13}C$ composition (+1.80 to +3.41‰ VPDB) reflects an internal source for carbon. These isotopic compositions are consistent saddle dolomites elsewhere in the WCSB, which have been interpreted to have precipitated from fluids of "burial origin" (e.g., Mattes and Mountjoy, 1980; Qing and Mountjoy, 1989). The strontium isotope ratios for saddle dolomite at Dawson (0.7088 to 0.7102) are significantly more radiogenic than Middle Devonian marine values (0.7078 to 0.7082), thus indicating that marine carbonates and/or evaporates are not the source for radiogenic ^{87}Sr.

Though no fluid inclusion data were available for saddle dolomites, it is hypothesized –based on $\delta^{18}O$ of the saddle dolomites – that warm, possibly saline fluids were responsible for precipitating saddle dolomite within the Slave Point Formation. Based on $\delta^{18}O$ values of -11.5 to -7.6‰ VPDB, the formation of saddle dolomite occurred at a temperature range of 90 to 125^{0}C, assuming that the diagenetic fluid from

which saddle dolomite formed had near Middle Devonian seawater isotopic composition (Figure 6.2b, blue arrows). However, if the assumption of SMOW is ~ +4‰, as suggested by some authors for some Devonian subsurface brines in the WCSB (Buschkuele, 2003) for the range of $\delta^{18}O$ values (-10.4 to -7.1‰) at Dawson, saddle dolomite would have formed at 120-165^{0}C (Figure 6.2b, green dashed arrow). Using the temperature range obtained from Figure 6.2b, saddle dolomite would have formed at depths greater than 3000 m (assuming a geothermal gradient of 30°C/km).

$\delta^{18}O$ and $^{87}Sr/^{86}Sr$ ranges for saddle and matrix dolomite are very similar (Figure 6.2 suggesting that the fluid that recrystallized the matrix dolomite also formed the saddle dolomite, this can happen in two different ways: 1) fluid flow up from faults, which has been documented by Packard (1990) in the Tangent field, and/or, 2) locally redistributed matrix dolomite along stylolite seams, which precipitated in open voids and formed saddle dolomite. This situation needs no fluid conduit to transport dolomitizing fluids, however, petrographic evidence (marine textures and cements, etc) suggest buried marine waters, which were reset with respect ^{18}O, were responsible for the matrix recystallization and high $^{87}Sr/^{86}Sr$ values suggest interaction with a source enriched in radiogenic strontium (section 6.3.4).

6.3.4 Conduit for dolomitizing fluids

With respect to matrix dolomite, the dolomitizing fluid is interpreted to be seawater that had incorporated ^{87}Sr from migration through the Granite Wash, with subsequent recrystallization that changed the $\delta^{18}O$ of the matrix dolomite (Figure 5.5) but not the $\delta^{13}C$ (Figure 5.3b) and its $^{87}Sr/^{86}Sr$ ratio.

Saddle dolomite formation probably was also the product of fluids interacting with the Granite Wash and incorporating ^{87}Sr though its migration in this lithozone. However, petrographic evidence suggests saddle dolomite post-dates the formation of matrix dolomite (Section 4.3.2; Plate J/4 and 5).

Though a definitive source of dolomitizing fluids is difficult to determine, the available data, as well as circumstantial evidence, suggest that the dolomitizing fluid was seawater that traveled through the porous sands and gravels of the underlying Granite Wash lithozone. This fluid migration pathway is consistent with the regional hydrostratigraphy; the aquifers for fluid flow being the Granite Wash lithozone, Gilwood, Slave Point, and Swan Hills Formations, and the aquitards represented by the Waterways, Keg River, Muskeg, and Fort Vermillion Formations (Figure 6.3). Therefore, fluid flow from the Granite Wash aquifer into the overlying Slave Point was likely, as evidenced by the enriched $^{87}Sr/^{86}Sr$ ratios of the dolomites at Dawson: the result of exchange with the highly radiogenic rich sediments (e.g., feldspars) of the Granite Wash.

Taking all lines of evidence together, it appears that the Granite Wash channels acted as conduits for marine seawater that dolomitized the Slave Point. This fluid was subsequently enriched in ^{87}Sr, which is the most direct line of physical evidence for unequivocally stating that the fluid(s) migration through the Granite Wash. As for the current dolomite models, none of them quite applies. Seawater migration through underlying clastics is a highly unusual mode of fluid transport for dolomitization, and thus so far unique in the WCSB.

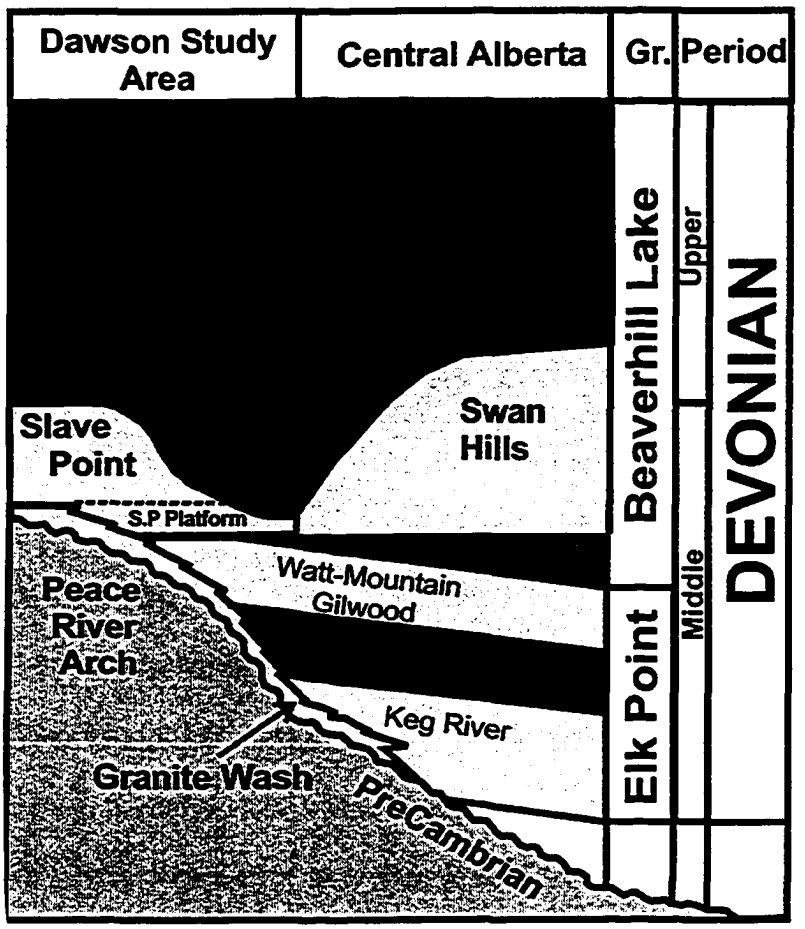

Figure 6.3 Modified stratigraphic column showing Formations (yellow), which acted as aquifers and/or are porous and permeable regionally, and at Dawson, and Formations which acted as aquitards (green). The porous and permeable sands and gravels of the Granite Wash acted as a conduit for dolomitizing fluids, which dolomitized the Slave Point at Dawson. Buried seawater was enriched in $^{87}Sr/^{86}Sr$ as a result of passing through the Granite Wash, which accounts for high radiogenic Sr values in the dolomites at Dawson. Seawater migration through underlying clastics is a highly unusual mode of fluid transport for dolomitization, and thus so far unique in the WCSB. This figure gives evidence that seawater migration a likely form of fluid transport through the underlying Granite Wash (modified from Gosselin et al. 1989).

6.4 Dissolution

Porosity development was related to the processes of dolomitization, tectonics (via fracturing), and dissolution (vuggy/moldic porosity), where the removal of significant amounts of calcium carbonate is necessary for the development of porosity in carbonates. This was accomplished at Dawson by two different processes: 1) $CaCO_3$ removed by dissolution unrelated to dolomitization (e.g. dissolution by meteoric fluids), and 2) the removal of calcium carbonate associated with the dolomitization process

Dissolution took place several times during the diagenetic history of the Slave Point Formation resulting in secondary porosity generation by 4 separate phases of dissolution, which offset the overall porosity decrease with depth at certain depth and time intervals (Figure 6.1).

1) A first phase removed fossil grains relatively early, within the first 0-600 metres of burial. This early dissolution may have been caused by the infiltration of meteoric water, or in a shallow burial, marine-phreatic environment, and the voids were occluded by calcite spar, which has been shown to be an early and shallow burial precipitate.

2) A second phase of porosity development via dissolution was matrix dolomitization. This matrix dolomite is the fine-grained replacement of the original limestone matrix of carbonates. Matrix dolomitization is important at Dawson because it dolomitized facies with a precursor mud matrix, essentially transforming a non-reservoir quality rock into a potential reservoir with excellent intercrystalline porosity. This process of porosity develop is extremely important at Dawson.

Matrix dolomitization begins as a selective replacement of the matrix, probably as the result of three interacting factors: (a) the matrix contains or consists of thermodynamically metastable carbonates (aragonite and/or high-Mg calcite), which have higher solubilities than low-Mg calcite; (b) the matrix has much smaller grain size and therefore a higher surface area per grain than the larger biochems, allochems or cement crystals formed prior to dolomitization; and (c) the matrix has a higher permeability than the larger, more massive particles or cements (Machel, 2004).

3) A third phase of secondary porosity is the development of vuggy porosity, which developed sometime after matrix dolomitization (Figure 6.1) at intermediate burial depths after carbonate mineralization. This carbonate mineralization, or calcite cement filling voids left by fossil dissolution, was then dissolved by burial/connate water, undersaturated with respect to $CaCO_3$, produced individual vugs ranging in size from a few centimetres to a few decimetres.

The development of vuggy porosity in dolomites has been interpreted to result from dissolution that took place in a completely matrix-dolomitized rock, whereby dissolution started in the unreplaced larger allochems and biochems and then proceeded beyond the margins of the molds into the already dolomitized matrix (Machel, 2004). However, this interpretation requires that the solution has stopped 'making' dolomite and that the solution has attained undersaturation with respect to dolomite. The more plausible explanation, both thermodynamically and kinetically, of vuggy porosity development in dolomites is that the matrix was incompletely replaced before the vugs formed (Machel, 2004).

4) Fracture porosity is the final phase of porosity development at Dawson (Figure 6.1). Fractures, and fracture porosity at Dawson are rare (<1-5% total rock volume), and most fractures are filled with dogtooth calcite spar or saddle dolomite, thus, they do not significantly enhance permeability in the carbonates.

6.5 Porosity evolution during diagenesis

Diagenetic processes were the primary controls on the evolution of porosity in carbonates of the Slave Point Formation. These diagenetic processes created, destroyed and preserved primary or secondary porosity during burial (Figure 6.1).

Primary porosity, and to a lesser extent, secondary porosity, in the Slave Point Formation was also reduced by cementation. At Dawson, early marine cements and dogtooth calcite spar, have partially filled interparticle porosity, and most of the remaining intraparticle porosity. Late-stage calcite cements precipitated within vugs during deep burial, further reduced porosity.

The most important aspect for hydrocarbon reservoir development was reservoir-enhancing porosity generation that is found in dolomitized sections of the Slave Point Formation (Figure 6.4). Apparently, porosity was created during dolomitization of limestones due to mass balance transfer reactions, in which calcite converts to dolomite with a molar volume reduction of 8-13% (Machel and Mountjoy, 1986). Secondary dolomitized intercrystalline porosity and vuggy pores are important reservoir porosities (Plate J/3, I/2 and 4). However, intercrystalline pores, as a product of matrix dolomitization formation, are by far the most important since they significantly increase porosity and permeability.

6.6 Diagenetic evolution of the Slave Point Formation

The diagenetic phases at Dawson can be grouped into four major stages (see Figure 6.1):

NEAR SURFACE: Stage 1: *Initiation of Slave Point deposition occurred during* the Middle Devonian with the deposition of the restricted, muddy marine platform carbonates on top of the previously uplifted and block-faulted Precambrian and/or Granite Wash detritus. During this stage, micritzation and precipitation of early marine radial fibrous cements occurred syndepositionally.

The base of the near-surface phase is defined by the significant decrease in porosity associated with mechanical compaction (stage 2). Also, pore waters of this phase are dominantly marine, which is not the case for stage 2.

SHALLOW BURIAL: Stage 2: The beginning stage 2 is defined by the change from marine pore waters in stage 1 to marine-connate waters of stage 2. Additionally, this stage starts to show an increase in porosity (Figure 6.1, porosity log) through to matrix dolomitization.

Mechanical compaction began to affect non-cemented carbonates and resulted in re-orienting of grains and closer grain packing. Dogtooth calcite spar precipitated within intraparticle pores - such as primary pores in stromatoporoids. Fossil dissolution also occurred late during this stage and produced moldic porosity in the allochems. After precipitation of calcite spar cement, matrix dolomite formed from marine pore fluids,

preferentially replacing carbonate lime mud. It was in this stage that the majority of secondary porosity formed, via dissolution and matrix dolomitization.

INTERMEDIATE BURIAL: Stage 3: The end of stage 2 and beginning of stage 3 is defined by the onset of stylolitization and a general decrease in porosity associated with stylolitization. Porosity, however, increases after stylolitization, and pore waters changed from marine-connate (stage 2) to connate of stage 3.

The vuggy porosity development enhanced reservoir quality of the carbonates at Dawson, which was further enhanced by the connection of vugs to a more porous and permeable matrix.

DEEP BURIAL: Stage 4: There is not a definitive boundary between the beginning of stage 4 and end of stage 3. Pore waters are the same (burial- connate), however, there is an overall decrease in porosity with increased burial depth.

During the Late Devonian and Mississippian, tectonism caused uplift of the Western Canada Sedimentary Basin, which resulted in the fracturing of the Slave Point Formation. Though minor in percent of total rock volume, these fractures provided conduits for ascending formation fluids that precipitated saddle dolomite and some late-stage calcite spar and anhydrite cement. Hydrocarbon migration and sulphide mineralization occurred during this stage in the diagenetic history of Dawson.

CHAPTER SEVEN

7 SUMMARY AND CONCLUSIONS

The following summary and conclusions are based on detailed core examination, petrographic, diagenetic and geochemical analysis of samples obtained from the Slave Point Formation, Dawson field, northwestern Alberta.

1) The Peace River Arch (PRA) has greatly influenced the overall geometry, facies distribution, and reservoir characteristics of the Slave Point Formation at Dawson. Specifically, the locations of Slave Point carbonate buildups are controlled by the pre-depositional topographic relief of the underlying Precambrian.

2) No significant biohermal reef buildups are found at Dawson. Reef plays produce only from a few small, isolated patch reefs. The best developed play type, the backstepping carbonate ramp, is around the 'nose' of the Peace River Arch, where Dawson and several other large pools are located.

3) At Dawson, the Slave Point Formation backsteps onto the antecedent Precambrian topography of the PRA. As sea level continued to rise, which is consistent with the overall sea level rise in the Middle Devonian, the Slave Point stepped farther back onto the Peace River Arch, but without ever completely covering the Arch.

4) Small erosional remnants of the PRA acted as nuclei for localized patch reef growth, commonly referred to as monadnocks. The monadnocks at Dawson are the result of faulting augmented by fluvial erosion, which created a series of relatively small, isolated land masses of the Precambrian arch that the Slave Point covered and mantled.

5) Definition of the bank margin is critical for exploration and defining the overall field geometry. In order to constrain exploration, it is important to identify the bank margin or, in lithologic terms, the boundary between the shales of the Waterways Formation and the porous Slave Point Formation carbonates. Three-dimensional (3D) seismic data provided for detailed definition of the underlying Precambrian highs, allowing the explorationist to avoid the 'bald highs' (i.e., no Slave Point), and focus on exploring their flanks, where reefs are more common. The most useful way of defining the bank margin, however, is utilizing and integrating seismic data and drill core/facies analysis.

6) Within the Slave Point, six major depositional facies can be recognized. They are: the shallow shelf, back reef, reef, forereef, off reef, and basinal facies. Oil production is commonly associated with the back reef, reef, and forereef. In addition, three other formations play an important role in trapping of hydrocarbons, secondary oil production, and the overall geometry of the Dawson field: 1) the Waterways Formation; 2) the Granite Wash; and, 3) the Precambrian basement.

7) Where the Slave Point Formation was exposed to relatively strong current and wave action, its matrix is grainy or porous. However, in areas without pervasive and constant wave action, such as behind a barrier like a monadnock, the matrix is muddier. Generally, the Slave Point is more porous on the eastern sides of monadnocks (windward) compared to the western sides (leeward), which might be a helpful insight when deciding on where to drill.

8) The depositional evolution of the Slave Point was initiated upon previously uplifted and block-faulted Precambrian basement and/or Granite Wash sands and gravels. Continuous sea-level rises forced the Slave Point Formation to colonize higher onto the exposed PRA until the entire Slave Point was covered by marine sediments of the Waterways Formation. Where the Slave Point was not able to cover the highest portion of the Precambrian, a 'bald high' was created.

9) The Slave Point Formation carbonates at Dawson have undergone a complex diagenetic history from early marine diagenesis to deep burial environments, with distinct and varying fluid compositions. There are several types of cement that formed in marine to deep burial environments; they are: radial fibrous (marine), dogtooth calcite spar (shallow burial), and blocky calcite cement (deep burial). These cements can occlude porosity, thus rendering poorer reservoir quality rocks.

10) At Dawson, most facies of the Slave Point Formation have been dolomitized to varying degrees. Facies exerted a minor control on dolomite distribution. Matrix dolomitization formed during a relatively early diagenetic stages and occurred before the onset of chemical compaction.

11) Based on $\delta^{18}O$ values of -10.4 to -7.1‰ VPDB, the formation of matrix dolomite occurred at a temperature range of 80 to 105^{0}C, assuming that the diagenetic fluid from which matrix dolomite formed had near Middle Devonian seawater isotopic composition. However, this temperature range does not denote the original replacement process, rather, the event of burial recrystallization of the bulk of the dolomite. $^{87}Sr/^{86}Sr$ values for matrix dolomite indicate it was formed from formation waters that were intra-

basinal since. The fluid(s) responsible for matrix dolomitization at Dawson is interpreted to be seawater that incorporated ^{87}Sr from migration through the Granite Wash with subsequent recrystallization that changed the $\delta^{18}O$ of the matrix dolomite but not the $\delta^{13}C$ and its $^{87}Sr/^{86}Sr$.

12) The minor amounts of saddle dolomite are interpreted to have formed during later diagenetic stages Saddle dolomite –based on $\delta^{18}O$ values– formed from warm, possibly saline fluids. Based on $\delta^{18}O$ values of –11.5 to -7.6‰VPDB, the precipitation of saddle dolomite occurred at a temperature range of 90 to 125^{0}C, assuming that the diagenetic fluid from which saddle dolomite formed had near Middle Devonian seawater isotopic composition. Saddle dolomite would have formed at depths greater than 3000 m, assuming a geothermal gradient of 30°C/km. As is the case for matrix dolomite, $^{87}Sr/^{86}Sr$ values for saddle dolomite indicate it was formed from formation waters that were intra-basinal.

All evidence taken together suggests that the dolomitizing fluid(s) responsible for the precipitation of both matrix and saddle dolomite, was seawater that traveled through the porous sands and gravels of the underlying Granite Wash lithozone. In addition, areas at Dawson which have no underlying Granite Wash are not affected by dolomitization.

13) Dissolution took place throughout the diagenetic history of the Slave Point Formation resulting in secondary porosity formation during 4 diagenetic phases that offset the overall porosity decrease with depth at certain depth and time intervals : i) A first phase removed fossil grains relatively early. ii) Matrix dolomitization. iii)

Development of vuggy porosity, which developed sometime after matrix dolomitization.

iv) Development of fracture porosity.

The diagenetic processes that affected the carbonates at can be grouped into 4 major stages:

Stage 1 - Near surface: diagenetic conversions (i.e., micritzation) and precipitation of early marine radial fibrous cements occurred syndepositionally. Pore waters of this phase are dominantly marine.

Stage 2 - Shallow burial: fossil and intercystalline dissolution during matrix dolomitization, thus significantly increasing intercrystalline porosity and permeability. Pore waters of this stage are marine-connate.

Stage 3 - Intermediate burial: defined by the onset of stylolitization and associated decrease in porosity. Sometime after stylolitization, vuggy porosity was developed at Dawson, which enhanced reservoir quality of the carbonates at Dawson by connecting vugs to a porous and permeable matrix as a result of matrix dolomitization. Pore waters were connate.

Stage 4 - Deep Burial: there is an overall decrease in porosity with increased burial depth. . Hydrocarbon migration and sulphide mineralization occurred latest in the diagenetic history of Dawson.

14) With all lines of evidence taken together, it is the opinion of the author that further exploration should focus on resolving the bank margin, via facies and well log analysis, to the west of Dawson. Additionally, 3D seismic data should be incorporated in order to delineate Precambrian highs and monadnocks around which these Slave Point carbonates formed. Further exploration should be focused towards the

northwestern and west of Dawson where the Slave Point further backsteps onto the PRA, however, this exploration should take into account the Slave Point pinches out to the northwest against the PRA and forms the Slave Point zero edge.

15) Delineation of Granite Wash channels using core analysis and geophysical techniques is critical to exploration. It is the suggestion of the author that further work should attempt to detail the spatial distribution and geometry of these channels in order to further constrain exploration at Dawson and how they relate to the dolomitization of the Slave Point.

REFERENCES

Al-Aasm, I.S., Taylor, B.E., and South, B., 1990. Stable isotope analysis of multiple carbonate samples using selective acid extraction. Chemical Geology, v.80, p. 199-125.

American Geological Institute, 1999. Illustrated dictionary of Earth Science CD-ROM.

Amthor, J.E., Mountjoy, E.W., and Machel, H.G., 1993. Subsurface dolomites in Upper Devonian Leduc Formation buildups, central part of Rimbey-Meadowbrook reef trend, Alberta, Canada. Bulletin of Canadian Petroleum Geology, v.41, p.164-185.

Anderson, T.F., and Arthur, M.A., 1983. Stable isotopes of oxygen and carbon and their application to sedimentologic and paleoenvironmental problems.

Armstrong, S.C., Struchio, N., and Hendry, N.J., 1998. Strontium isotope evidence on the chemical evolution of pore waters in the Milk River aquifer, Alberta, Canada. Applied Geochemistry, v.13, p. 463-467.

Banner, J.L., 1995. Application of the trace element and isotope geochemistry of strontium to studies of carbonate diagenesis. Sedimentology, v.42, p. 805-824.

Bassett, P.B., and Stout, J.G., 1967. Devonian of western Canada. Proc. International Symposium of the Devonian System, Calgary, v.1, p.717-725.

Belyea, H.R. and Norris, A.W., 1962. Middle Devonian and older Paleozoic formations of southern District of Mackenzie and adjacent areas. Geological Survey of Canada, Paper 62-15.

Boggs, S., 1992. Principles of sedimentology and stratigraphy. Prentice Hall, 2nd edition, 774 pp.

Brand, U., and Veizer, J. 1981. Chemical diagenesis of a mutlicomponent carbonate system –2: stable isotopes. Journal of Sedimentary Petrology, v.51, p.987-998.

Brass, G.W., 1976. The variation of the marine $^{87}Sr/^{86}Sr$ ratio during Phanerozoic time: interpretation using a flux model. Geochimica et Cosmoschimica Acta, v.40, p.721-730.

Budd, D.A., 1997. Cenozoic dolomites of carbonate islands: their attributes and origin. Earth Science Reviews, v.42, p.1-47.

Burke, W.H., Denison, R.E., Hetherington, E.A., Koepnick, R.B., Nelson, H.F., and Otto,

J.B., 1982. Variation of seawater $^{87}Sr/^{86}Sr$ throughout Phanerozoic time. Geology, v.10, p.516-519.

Buschkuehle, M., 2003. Geology, diagenesis, and paleofluid flow in the Devonian Southesk-Cairn carbonate complex in west-central Alberta, Canada. Unpublished PhD thesis, Edmonton, University of Alberta, pp. 320.

Bustin, R.M., Barnes, M.A., and Barnes, W.C., 1985. Diagenesis 10. Quantification and modeling of organic diagenesis. Geoscience Canada 12, p.4-21.

Cameron, E.M., 1968. A geochemical profile of the Swan Hills reef. Canadian Journal of Earth Sciences, v. 5, p. 287-309.

Campbell, C.V., 1992. Beaverhill Lake Megasequence. . In Devonian-Early Mississippian carbonates of the Western Canada Sedimentary Basin: A Sequence Stratigraphic Framework, SEPM Short Course No. 28.Cant, D., and O'Connell, S., 1988. The Peace River Arch: Its Structure and Origin. In Sequences, Stratigraphy, Sedimentology: Surface and Subsurface. D.P. James and D.A. Leckie (eds.). Canadian Society of Petroleum Geologists, Memoir 15, p. 537-542.

Carpenter, S.J., Lohman, K.C., Holden, P., Walter, L.M., Huston, T.J., and Halliday, A.N., 1991. $\delta 18O$, $^{87}Sr/^{86}Sr$ and Sr/Mg ratios of Late Devonian abiotic marine calcite: Implications for the composition of ancient seawater. Geochimica et Cosmochimica Acta, v. 55, p. 1991 – 2010.

Choquette, P.W., and Pray, L.C., 1970. Geologic nomenclature and classification of porosity in sedimentary carbonates. American Association of Petroleum Geologists Bulletin, v. 54, p. 205-250.

Choquette, P.W., and James, N.P., 1987. Diagenesis in limestones – 3. The deep burial environment. Geoscience Canada 14, p.3-35.

Choquette, P.W., and James, N.P., 1990. Limestones – The burial diagenetic environment. *In:* McIlerath, I.E., and Morrow, D.A. (eds.) Diagenesis. Geoscience Canada reprint series 4, p. 72-112.

Clayton, R.N., Friedman, I., Graf, D.L., Mayeda, T.K., Meents, W.F., and Shimp, N.F., 1966. The origin of saline formation waters, I. Isotopic composition. Journal of Geophysical Research, v.71, p. 3869-3882.

Collony, C.A., Walter, L.M., Baadsgaard, H., and Longstaffe, F., 1990a. Origin and evolution of formation waters, Alberta Basin, Western Canada Sedimentary Basin I. Chemistry. Applied Geochemistry, v. 5, p. 375-395

Collony, C.A., Walter, L.M., Baadsgaard, H., and Longstaffe, F., 1990a. Origin and

evolution of formation waters, Alberta Basin, Western Canada Sedimentary Basin II. Isotope systematics and water mixing. Applied Geochemistry, v.5, p.397-413.

Craig, J.H., 1987. Depositional Environments of the Slave Point Formation Beaverhill Lake Group, Peace River Arch. In: Krause, F.F., and Burrowes, O.G. (eds), Devonian Lithofacies and Reservoir styles in Alberta. Canadian Society of Petroleum Geologists, International Symposium of the Devonian System, p.181-199.

Crawford, F.D., 1972. Facies analysis and depositional environments in the Middle Devonian Fort Vermillion and Slave Point Formation of northern Alberta. Unpublished M.Sc. thesis. Calgary, University of Calgary, pp.91.

Davies, G.R., 2002. Thermobaric dolomitization: transient fault-controlled pressure-driven processes and the role of boiling/effervescence. Diamond Jubilee Convention of the Canadian Society of Petroleum Geologist, Calgary, June 3-7, 2002, Program & Abstracts, p. 105.

Dickin, A.P., 2000. Radiogenic Isotope Geology. Cambridge University Press, 1st edition, 490pp.

Dunham, J.B., Crawford, G.A., and Panasiuk, W., 1983. Sedimentology of the Slave Point Formation (Devonian) at Slave Field, Lubicon Lake, Alberta. Society of Economic Paleontologists and Mineralogists, Core Workshop, no.4, 73-111.

Dunham, R.J., 1962. Classification of carbonate rocks. In: Classification of carbonate rocks, a symposium. Edited by W.E. Ham. American Association of Petroleum Geologists, Memoir 1, pp. 108-121. Faure, G., 1986. Principles of Isotope Geology. Smith-Wyllie. John Wiley & Sons, 1st edition, 464pp.

Fischbush, N.R., 1968. Stratigraphy, Devonian Swan Hills reef complexes of central Alberta. Bulletin of Canadian Petroleum Geology, v.16, p. 446-587.

Folk, R.L., 1965. Some aspects of recrystallization in ancient limestones. In: Dolomitization and limestone diagenesis. L.C. Pray and R.C Murray (eds). Society of Economic Paleontologists and Mineralogists Special Publication 12, p.14-18.

Friedman, I., and O'Neil, J.R., 1977. Compilation of stable isotope fractionation factors of geochemical interest. In: Data of geochemistry. US Geol. Surv. Prof. Paper, 440-KK, 1-12.

Fritz, P., and Smith, D.G.W., 1970. The isotopic composition of secondary dolomites. Geochemica et Cosmochimica Acta, v. 34, p.1161-1173.

Galloway, W.E., and Hobday, D.K., 1983. Terrigenous clastic depositional settings-

applications to petroleum, coal, and uranium exploration. Springer, Berlin, Heidelberg, New York.

Given, R.K., and Wilkinson, B.H., 1987. Dolomite abundance and stratigraphic age: constraints on rates and mechanisms of Phanerozoic dolostone formation. Journal of Sedimentary Petrology, v.57, p. 1068-1078.

Gosselin, E.G., 1990. Geology of the Slave Point Formation, northwestern Alberta, Canada. Unpublished M.Sc thesis. Kingston, Queen's University, pp. 274

Gosselin, E.G., Smith, L., and Mundy, D.J.C., 1989. The Golden and Evi Reef Complexes, Middle Devonian, Slave Point Formation, Northwestern Alberta. In Reefs, Canada and Adjacent Area. H.H.J. Geldsetzer, N.P. James, and G.E. Tebbutt (eds.). Canadian Society of Petroleum Geologists, Memoir 13, 1989, p. 440-447.

Gregg, J.M., and Sibley, D.F., 1984. Epigenetic dolomitization and the origin of xenotopic dolomite texture. Journal of Sedimentary Petrology, v.54, p. 908-931.

Hardie, L.A., 1987. Perspectives-Dolomitization: a critical view of some current views/ Journal of Sedimentary Petrology, v.57, p.166-183.

Harris, P.M., Kendall, C., G., St., C., and Lerche, I. 1985. Carbonate cementation – a brief overview. In: Carbonate Cements, N. Schniedermann and P.M. Harris, Society of Economic Paleontologists and Mineralogists, no. 36, p. 223-239.

Hitchon, B., 1984. Geothermal gradients, hydrodynamics, and hydrocarbon occurrences, Alberta, Canada. American Association of Petroleum Geologists, v.68, p.713-743.

Hoefs, J., 1980. Stable Isotope Geochemistry (2nd ed.). Springer-Verlag, Berlin, 208 p.

Hunt, J.M., 1996. Petroleum Geology and Geochemistry, 2nd edition. W.H Freeman, New York

Hurley, N.F., and Lohmann, K.C., 1989. Diagenesis of Devonian reefal carbonates in the Oscar Range, Canning Basin, western Australia. Journal of Sedimentary Petrology, v. 59, p. 127-145.

Irwin, H., 1980. Early diagenetic carbonate precipitation and pore fluid migration in the Kimmeridge Clay of Dorset, England. Sedimentology, v.27, p. 577-591.

Irwin, H., Curtis, C.D., and Coleman, M., 1977. Isotopic evidence for source of diagenetic carbonates formed during burial of organic-rich sediments. Nature, v.269, p.209-213.

Jenik, A.J., and Lerbekmo, J.F., 1968. Facies and geometry of Swan Hills Reef Member of Beaverhill Lake Formation (Upper Devonian), Goose River, Alberta, Canada. American Association of Petroleum Geologist Bulletin, v.52, p.21-56.

Joachimski, M.M., van Geldern, R., Breisig, S., Buggisch, W., and Day, J., 2004. Oxygen isotope evolution of biogenic calcite and apatite during the Middle and Late Devonian. International Journal of Earth Science, v. 93, p.542-553.

Johnson J.G., Klapper G., Sandberg C.A., 1985. Devonian eustatic fluctuations in Euramerica. Geolological Society of America Bulletin, v.96. p.567-587.

Keith, J.W., 1990. The influence of the Peace River Arch on Beaverhill Lake sedimentation. Bulletin of Canadian Petroleum Geology, v. 38a, p.55-65.

Klovan, J.E., 1964. Facies analysis of the Redwater reef complex, Alberta, Canada. Bulletin of Canadian Petroleum Geology, v. 12, p. 1-100.

Land, L.S., 1980. The isotopic and trace element geochemistry of dolomite: the state of the art. In: D.H. Zenger, J.B Durham, and R.L. Etherington (eds.). Concepts and models of dolomitization. Society of Economic Paleontologists and Mineralogists, Special Publication, No. 28, p. 87-110.

Land, L.S., 1985. The origin of massive dolomite. Journal of Geologic Education, v.33, p.112-125.

Land, L.S., Salem, M.R.I., and Morrow, D.W., 1975. Paleohydrology of ancient dolomites: geochemical evidence. American Association of Petroleum Geologists Bulletin, v.59, p.1602-1625.

Lind, I.L., 1993. Stylolites in chalk from Leg 130, Ontong Java Plateau. In: Berger, W.H., Kroenke, J.W., Mayer, L.A. (eds). Proc Ocean Drilling Program, Scientific results 130, p. 445-451.

Machel, H.G., 1987. Saddle dolomite as a by-product of chemical compaction and thermochemical sulphate reduction. Sedimentary Geology, v.15, p. 936-940.

Machel, H.G., 1990. Dolomitization, reservoir development, and dolostone reservoirs of Western Canada. In: The development of porosity in carbonate reservoirs, Canadian Society of Petroleum Geologists Short Course Notes, p. 3-1 to 3-30.

Machel, H.G., 1997. Recrystallization versus neomorphism, and the concept of 'significant' recrystallization in dolomite research. Sedimentary Geology, v.113, p. 161-168.

Machel, H,G., 1999. Effects of groundwater flow on mineral diagenesis, with emphasis on carbonate aquifers. Hydrogeology Journal, v.7, p.94-107.

Machel, H.G., 2004. Concepts and models of dolomitization - a critical reappraisal. In: C. Braithwaite, G. Rizzi, and G. Darke (eds.). The geometry and petrogenesis of dolomite hydrocarbon reservoirs. Special Publication of the Geological Society of London, in press.

Machel, H.G., and Mountjoy, E.W., 1986. Chemistry and environments of dolomitization – a reappraisal. Earth Science Reviews, v.23, p. 175-222.

Machel, H.G., and Mountjoy, E.W., 1987. Reply to discussion of chemistry and environments of dolomitization – a reappraisal, by R.K. Stoessell. Earth Science Reviews, v.24, p. 213-215.

Machel, H.G., and Hunter I.G., 1994. Facies models for Middle to Late Devonian Shallow-marine Carbonates, with comparisons to Modern Reefs: a Guide for facies Analysis. Facies, v. 30, p.155-176.

Machel, H.G., and Cavell, P.A., 1999. Low-flux, tectonically-induced fluid flow ("hot flash) into the Rocky Mountain Foreland Basin. Bulletin of Canadian Petroleum Geology, v.47, no. 4, p.510-533.

Machel, H.G., and Lonnee, J., 2002. Hydrothermal dolomite – a product of poor definition and imagination. Sedimentary Geology, v.152, p. 163-171.

Mattes, B.W., and Mountjoy, E.W., 1980. Burial dolomitization of the Upper Devonian Miette Buildup, Jasper National Park, Alberta. In: D.H. Zenger, J.B. Dunham, and R.L. Etherington (eds.). Concepts and models of dolomitization. Society of Economic Paleontologists and Mineralogists, Special Publication No. 28: 259-297.

Meyers, W.J., and Lohmann, K., 1985. Isotope Geochemistry of regionally extensive calcite cement zones and marine components in Mississippian limestones, New Mexico. In: Carbonate Cements, N. Schniedermann and P.M. Harris, Society of Economic Paleontologists and Mineralogists, no. 36, p. 223-239.

Moore, C.H., 1989. Carbonate diagenesis and porosity. Developments in Sedimentology 46. Elsevier, Amsterdam, pp.338.

Morrow, D.W., 1982. Diagenesis II. Dolomite-part II: dolomitization models and ancient dolostones. Geoscience Canada, v. 9, p. 95-107.

Morrow, D.W., 1990. Part 2: Dolomitization models and ancient dolostones. In: I.A. McIlreath and D.W. Morrow (eds.), Diagenesis. Geoscience Canada, Series 4: 125-140.

Mossop, G., and Shetsen, I., 1994. Geological Atlas of the Western Canada Sedimentary Basin .G.D. Mossop and I. Shesten (comps.). Calgary, Canadian

Society of Petroleum Geologists and Alberta Research Council

Mountjoy, E.W., Qing, H., and McNutt, R., 1992. Sr isotopic composition of Devonian dolomites, western Canada: significance regarding sources of dolomitizing fluids. Applied Geochemistry, v.7, p.59-75.

Muehlenbachs, K., 1988. The oxygen isotopic composition of the oceans, sediments, and the seafloor. Chemical Geology, v.145, p. 263-273.

Murray, J.W., 1966. An oil producing reef-fringed carbonate bank in the Upper Devonian Swan Hills member, Judy Creek, Albertra. Bulletin of Canadian Petroleum Geology, v.14, p. 1-103.

Murray, A., and Lucia, J.F., 1967. Cause and control of dolomite distribution by rock selectivity. Geological Society of America Bulletin, v.78, p. 21-35.

North American Stratigraphic Code, 1983. American Association of Petroleum Geologists Bulletin, v.67, p. 841-875.

Northrop, D.A., and Clayton, R.N., 1966. Oxygen isotope fractionation in systems containing dolomite. Journal of Geology, v.74, p.174-196.

O'Connell, S.C., Dix, G.R., and Barclay, J.E., 1990. The origin, history, and regional structural development of the Peace River Arch, Western Canada. Bulletin of Canadian Petroleum Geology, v. 38a, p. 4-24.

O'Neil, J.R., and Epstein, S., 1966. Oxygen isotope fractionation in the system dolomite-calcite-carbon dioxide. Science, v.152, p.198-201.

Packard, J.J., Pellegrin, G.J., Al-Aasm, I.S., Samson, I.M., and Gagnon, J., 1990. Diagenesis and dolomitization associated with hydrothermal karst in Famennian upper Wabamun ramp sediments, northwestern Alberta. In: Bloy, G.R., and Hadley, M.G. (Compilers), The development of porosity in carbonate reservoirs; short course notes. Canadian Society of Petroleum Geologists.

Playford, P.E., 1980. Devonian 'Great Barrier Reef' of Canning Basin, Western Australia. Bulletin of American Association of Petroleum Geologists, v. 64, p. 814 – 840.

Qing, H., and Mountjoy, E.W., 1989. Multistage dolomitization in Rainbow buildups, Middle Devonian Keg River Formation, Alberta, Canada. Journal of Sedimentary Petrology, v. 59, p. 114-126.

Qing, H., and Mountjoy, E.W., 1994. Formation of coarsely, hydrothermal dolomite reservoirs in the Presqu'ile Barrier, Western Canada Sedimentary Basin. American Association of Petroleum Geologist Bulletin, v. 78, p. 55-77.

Radke, B.M., and Mathis, R.L., 1980. One the formation and occurrence of saddle dolomite. Journal of Sedimentary Petrology, v.50, p.1149-1168.

Railsback, L.B., 1990. Influence of changing deep ocean circulation on the Phanerozoic oxygen isotopic record. Geochimica Cosmochimica Acta, v.54, p. 1501-1509.

Ricketts, B.D., 1989. Western Canada Sedimentary Basin - A Case History. Canadian Society of Petroleum Geologists, 320 p.

Shinn, E.A., 1973. Recent intertidal and nearshore carbonate sedimentation around Rock Highs, E Qatar, Persian Gulf. *In:* Purser, B.H., (eds), The Persian Gulf, p.193-198.

Sibley, D.F., 1982. The origin of common dolomite fabrics: clues from the Pliocene. Journal of Sedimentary Petrology, v.52, p.739-748.

Sibley, D.F., 1990. Unstable to stable transformations during dolomitization. Journal of Geology, v.98, p.739-748.

Sibley, D.F., and Gregg, J.M., 1987. Classification of dolomite rock textures. Journal of Sedimentary Petrology, v.57, p.967-975.

Stoakes, F., 1987. Evolution of the Upper Devonian of Western Canada. In: Principles and concepts for Exploration and Exploitation of Reefs in the Western Canada Basin. Canadian Reef Inventory Project, Canadian Society of Petroleum Geologists, Calgary, Alberta.

Trotter, R. and Hein, F.J., 1988. Sedimentology and depositional setting of the Granite Wash, northwestern Alberta. In: Sequences, Stratigraphy, Sedimentology: Surface and Subsurface, D.P. James and D.A. Leckie (eds.). Canadian Society of Petroleum Geologists, Memoir 15, p. 475-484.

Tucker, M.E. and Wright, V.P., 1990. Carbonate Sedimentology. Blackwell Scientific Publications, 1st edition, 482 p.

Urey, H.C., Lowenstam, H.A., Epstein, S., and McKinney, C.R., 1951. Measurements of paleotemperatures and temperatures of the Upper Cretaceous of England, Denmark, and the Southeastern United States. Bulletin of Geological Society of America, v.62. p.399-416.

Veizer, J. 1983. Chemical diagenesis of carbonates: theory and application of trace element techniques. In: Stable Isotopes in Sedimentary Geology. Blackwell Scientific Publications, Oxford, 482 pp.

Veizer, J., and Compston, W., 1974. $^{87}Sr/^{86}Sr$ composition of seawater during the

Phanerozoic. Geochemica et Cosmochimica Acta, v.38, p. 1461-1484.

Veizer, J., Fritz, P., and Jones, B., 1986. Geochemistry of brachiopods: oxygen and carbon isotopic records of Paleozoic oceans. Geochemica Cosmochimica Acta, v.50, p. 1679-1696.

Veizer, J., Ala, D., Azmy, K., Bruckschen, P., Buhl, D., Bruhn, F., Carden, G.A.F., Diener, A., Ebneth, S., Godderis, Y., Jasper, T., Korte, C., Pawellek, F., Podlaha, O.G., Strauss, H., 1999. $^{87}Sr/^{86}Sr$, $\delta^{13}C$ and $\delta^{18}O$ evolution of Phanerozoic seawater. Chemical Geology, v. 161, p. 59-88.

Wanless, H.R., 1981. *Limestone response to stress: pressure solution and dolomitization.* In: Diagenesis of carbonate rocks: cement-porosity relationships, SEPM reprint series 10, p.251- 276.

Warren, J., 2000. Dolomite: occurrence, evolution, and economically important associations. Earth Science reviews, v.52, p.1-81.

Wefer, G., and Berger, W.H., 1991. Isotope Paleontology: growth and composition of extant calcareous species. Marine Geology, v.100, p.207-248.

Wendte., J.C., 1992. Overview of the Devonian of the Western Canada Sedimentary Basin. In Devonian-Early Mississippian carbonates of the Western Canada Sedimentary Basin: A Sequence Stratigraphic Framework, SEPM Short Course No. 28.

Wright, G.N., McMechan, M.E., and Potter, D.E.G., 1994. Structure and architecture of Western Canada Sedimentary Basin. In Geological Atlas of the Western Canada Sedimentary Basin. G.D. Mossop and I. Shesten (comps.). Calgary, Canadian Society of Petroleum Geologists and Alberta Research Council, p. 25-40.

APPENDIX A

Well ID	Depth	Phase	$\delta^{18}O$	$\delta^{13}C$	$^{87}Sr/^{86}Sr$	Remarks
14-19-79-15W5	2036.4 m	Matrix dolomite	-9.727	2.764	0.709664	
5-29-79-15W5	2066 m	Stromatoporoid	-9.2	2.626	0.709998	
12-7-81-15W5	1993.5 m	Matrix dolomite	-9.244	2.056	0.708897	
12-7-81-15W5	1993.5 m	Saddle dolomite	-9.473	1.942	0.708779	
8-25-79-16W5	2044.5 m	Calcite cement	-10.86	1.065	0.710133	
8-25-79-16W5	2044.5 m	Matrix dolomite	-8.991	2.646	0.708836	
8-25-79-16W5	2038.5 m	Stromatoporoid	-11.239	2.263	0.709301	
8-25-79-16W5	2038.5 m	Matrix dolomite	-9.214	3.92	0.709405	
4-36-79-16W5	2052.3 m	Stromatoporoid	-6.691	3.515	0.708159	
4-36-79-16W5	2050.8 m	Brachiopod	n/a	n/a	0.708021	No O or C values
4-36-79-16W5	2049.4 m	Crinoid	-6.415	0.615	0.708559	
4-36-79-16W5	2049.4 m	Brachiopod	-5.957	1.851	0.708008	
12-18-79-16W5	2144.8 m	Calcite cement	-14.945	1.927	0.721265	
12-18-79-16W5	2137.6 m	Saddle dolomite	-8.833	2.81	n/a	
12-18-79-16W5	2137.6 m	Calcite cement	-12.485	2.118	n/a	
12-18-79-16W5	2137.6 m	Calcite cement	-12.887	2.087	0.713006	
12-18-79-16W5	2127.9 m	Crinoid	-6.612	-0.062	0.708850	
12-18-79-16W5	2127.9 m	Brachiopod	-6.4	0.942	0.708263	
16-25-79-16W5	2060 m	Matrix dolomite	-9.54	3.108	0.709771	

16-25-79-16W5	2060 m	Saddle dolomite	-9.844	2.824	0.709991	
11-34-79-16W5	2094.6 m	Matrix dolomite	-7.152	3.169	0.708555	
4-35-79-16W5	2091.9 m	Matrix dolomite	-10.419	3.533	n/a	
4-13-80-16W5	2047.9 m	Saddle dolomite	-10.053	3.406	0.709924	
4-13-80-16W5	2047.9 m	Stromatoporoid	-8.065	3.63	0.708280	
4-13-80-16W5	2042 m	Anhydrite	n/a	n/a		
9-24-80-16W5	1995.8 m	Brachiopod	-10.795	2.723	0.708957	
9-24-80-16W5	1994 m	Stromatoporoid	-8.365	3.367	0.708248	
8-36-80-16W5	2022.4 m	Stromatoporoid	-7.523	3.277	0.709235	
5-23-80-16W5	6856.5 ft	Saddle dolomite	-9.716	2.626	n/a	
5-23-80-16W5	6856.5 ft	Calcite cement	-11.616	1.644	n/a	
5-23-80-16W5	6856.5 ft	Calcite cement	-12.6	0.805	0.710258	
5-23-80-16W5	6856.5 ft	Matrix dolomite	-9.035	1.982	0.710411	
5-23-80-16W5	6849.5 ft	Stromatoporoid	-10.561	2.304	0.708912	
5-23-80-16W5	6849.5 ft	Crinoid	n/a	n/a	0.709441	No O or C values
5-23-80-16W5	6849.5 ft	Matrix dolomite	-9.571	3.407	0.711168	
5-23-80-16W5	6847.5 ft	Saddle dolomite	-11.364	1.914	n/a	
5-23-80-16W5	6847.5 ft	Calcite cement	-11.145	2.173	n/a	
5-23-80-16W5	6847.5 ft	Saddle dolomite	-11.493	1.799	n/a	
15-15-80-16W5	2082.4 m	Calcite cement	-7.877	2.974	n/a	
15-15-80-16W5	2082.4 m	Matrix dolomite	-8.405	2.941	0.708961	
15-15-80-16W5	2079.5 m	Calcite cement	-13.234	1.434	0.711119	

15-15-80-16W5	2079.5 m	Matrix dolomite	-8.568	2.877	0.709043	
13-16-80-16W5	2082.8 m	Matrix dolomite	-10.132	2.584	n/a	
13-16-80-16W5	2082.8 m	Calcite cement	-13.317	1.128	n/a	
13-16-80-16W5	2082.2 m	Calcite cement	-11.66	1.449	n/a	
13-16-80-16W5	2082.2 m	Dolomite	-10.261	1.912	n/a	Undifferentiated
13-16-80-16W5	2082.2 m	Matrix dolomite	-9.312	2.748	n/a	
13-16-80-16W5	2082.2 m	Calcite cement	-9.583	2.442	n/a	
13-16-80-16W5	2082.2 m	Calcite cement	-11.031	1.989	n/a	
15-18-80-17W5	2082.4 m	Saddle dolomite	-7.689	2.973	n/a	
14-34-80-17W5	6833 ft	Matrix dolomite	-7.622	1.592	0.710837	
14-34-80-17W5	6825 ft	Matrix dolomite	-7.872	1.491	0.713193	
1-29-80-17W5	2116.5 m	Matrix dolomite	-8.638	1.369	0.709891	
5-18-80-17W5	1981.8 m	Stromatoporoid	-7.931	3.582	0.708208	
5-18-80-17W5	1980.1 m	Stromatoporoid	-8.366	3.585	0.708270	
5-18-80-17W5	1979.1 m	Stromatoporoid	-7.937	4.201	0.708166	
1-21-80-17W5	2124.8 m	Saddle dolomite	-8.006	2.019	0.710148	
1-21-80-17W5	2124.8 m	Matrix dolomite	-7.763	2.001	0.710069	
1-21-80-17W5	2121.8 m	Matrix dolomite	-7.232	1.852	0.709207	